Sudan University of Science and Technology
College of Graduate Studies

Performance Evaluation Of Filtering For Wavelength Division Multiplexing Based Optical Fiber Networks

تقييم أداء المرشحات للشبكات الضوئية المعتمدة على التجميع بتقسيم الطول الموجي

A thesis Submitted in Partial Fulfillment of the Requirement for the Degree of M.Sc. in Electronics Engineering (Communications Engineering)

Prepared By:
Abdalrazag Alnazier Mohammed Hassen

Supervisor:
Dr. Ebtihal Haider Gismalla Yousif

July 2019

الإستهلال

بِسْمِ ٱللَّهِ ٱلرَّحْمَٰنِ ٱلرَّحِيمِ

أَفَرَءَيْتُمُ ٱلنَّارَ ٱلَّتِى تُورُونَ ﴿٧١﴾
ءَأَنتُمْ أَنشَأْتُمْ شَجَرَتَهَآ أَمْ نَحْنُ ٱلْمُنشِـُٔونَ ﴿٧٢﴾

سورة ٱلواقْعة {آيهْ ٧١–٧٢}

Acknowledgments

Foremost, I would like to say my sincere gratitude to my advisor Dr. Ebtihal Haidar Gismalla for the continuous hold up of my Master thesis study and research, for his staying power, inspiration, interest, and enormous knowledge. His guidance helped me in all the time of research and writing of this thesis. I could not have imagined having a better advisor and mentor for my Master thesis study.

Abstract

The transmission distance of any WDM fiber-optic communication system is eventually limited by fiber losses and it was introduced from fiber attenuation, connectors, splices, dispersion, interference and bending causes the power reduction in optical fiber communication. This loss limitation was mostly overcome using tunable optical filters, devices in which the desired channel is to be selected at the receiver with negligible crosstalk and small insertion loss.

In this thesis different kinds of tunable optical filters such as: Fabry-Perot, Machzehnder and Acuosto-Optic filters are implemented to compensate losses. From the obtained results, it will be shown that a WDM optical system with a Machzehnder filter gets the best performance to compensate losses than Fabry-Perot and acuosto-optic filters in terms of Q-factor, BER, eye height and threshold when a fiber length, attenuation coefficient and input power design parameters are changed. Also fabry-perot filter produced better results at all cases than acuosto-optic filter which has a bad performance than others.

المستخلص

يتم تحديد مسافة النقل لأنظمة الشبكات الضوئية المعتمدة على التجميع بتقسيم الطول الموجي في الأغلب من خلال الفقد في تلك الألياف الضوئية الناتج بسبب توهين الألياف الضوئية، الوصلات، التوصيلات، التشتت، التداخل والإنحناء، مما يؤدي إلى إنخفاض طاقة الإشارات المرسلة عبر شبكات إتصالات الألياف الضوئية. ولهذا السبب تم إستخدام تقنيات الترشيح الضوئية القابلة للإنضباط، وهي أجهزة توضع في جانب المستقبل يتم فيها انتقاء الأطوال الموجية أو إختيار القنوات المرغوبة بدقة عالية جداً لموازنة الفقد في المنظومة.

في هذه الأطروحة سيتم تنفيذ ثلاثة أنواع مختلفة من تقنيات الترشيح الضوئية القابلة للإنضباط لتعويض الفقود والخسائر في منظومة شبكات الألياف الضوئية وهم: فابري-برو، ماكزندر و أكوستو-أوبتيك. من النتائج التي تم الحصول عليها، سيتبين أن أنظمة الشبكات الضوئية التي تعتمد على التجميع بتقسيم الطول الموجي وتستخدم مرشح الـ ماكزندر تحصل على أفضل أداء لتعويض الخسائر مقارنة بالمرشحين الآخرين بناءا على المقاييس الآتية: معامل الجودة، معدل الخطأ في البت، إرتفاع العين والعتبة في مخطط العين وذلك عند تغيير أحد معاملات التصميم كطول الليف الضوئي، معامل التوهين وكمية الطاقة الناتجة من المصدر الضوئي. أيضا سيتبين أن تلك الأنظمة التي تستخدم مرشح الـ فابري-برو تحصل على نتائج جيدة في كل الحالات بالمقارنة بالأنظمة التي تستخدم مرشح الـ أكوستو-أوبتيك التي لديها أداء سيئ بالمقارنة بهذه المرشحات.

Table of Contents

List of Figures

List of Tables

List of Abbreviations

AO	Acousto-Optic filter
AOTF	Acousto-Optic Tunable Filters
BER	Bit Error Rate
CDM	Optical Code Division Multiplexing
CFBGs	Chirped Fiber Bragg Gratings reflection
CW	Continuous Wave LASER
DFB	Distributed Feedback laser diode wavelength-scanning
EFPI	Extrinsic Fabry-Perot Interferometer cavity
FP	Fabry–Perot filter
FPI	Fabry-Perot Interferometer
FSR	Free Spectral Range
LHM	Left-Handed Metamaterial
MZ	Mach–Zehnder filter
MZI	Mach-Zehnder Interferometer
NRZ	Non-Return to Zero
OTDM	Optical Time-Division Multiplexing
PRBS	Pseudo Random Bit Sequence generator
Q-factor	Quality factor
RF	Radio Frequency
SCM	Subcarrier Multiplexing
SMF	Single Mode Fiber
TDM	Time Division Multiplexing
WDM	Wavelength-Division Multiplexing

List of Symbols

β	Tilt angles
$P_s v$	Space variation
ΔVL	Free spectral range
n_g	Group index
c	Speed of light
L	Length of fiber
ΔVFP	Filter bandwidth
F	Finesse of the FP filter
R	Mirror reflectivity
$T(v)$	Transmittivity
V	Frequency
τ	Relative delay
λ	Wavelength
Δ_n	TE-TM index difference
Λ_a	Acoustic wavelength
$\frac{\delta P}{\delta z}$	Average optical power change
α	Attenuation coefficient
P_{out}	Output Power
P_{in}	Input Power
SNR	Signal-to-Noise Ratio
BER	Bit Error Rate
η	Quantum efficiency
N_P	Receiver sensitivity
P	Probability of deciding
erfc	Error Function
δ_{eye}	Eye closure
Q	Quality Factor

Chapter one
Introduction

1.1 Introduction

According to a large frequency of optical carrier the high capacity of communication systems will be achieved. To extending the system capacity a multiple optical channels of transmission will be used.Channel multiplexing can be done in the optical-domain through OTDM and WDM, respectively. In WDM multiple optical carriers at different wavelengths are modulated by using independent electrical bit streams and are then transmitted over the same fiber. WDM system consist more components one of them is tunable optical filter. The function of it is to pick a preferred channel at the receiver. It needs a wavelength-selective method and can be subdivided into two categories according on whether optical interference or diffraction is the essential physical mechanism. There are many kinds of optical filters namely Fabry–Perot, Mach–Zehnder, grating-based Michelson and Acousto-Optic filters [1].

1.2 Problem Statement

When an optical signal is transmitted over a long distance, the loss from fiber attenuation, connectors, splices, dispersion, interference and bending causes the power reduction in optical fiber communication. Hence there are many filtering technologies can be used to compensate these losses, and there is a need to evaluate their performance.

1.3 Proposed Solution

The proposed solution is to use tunable optical filters like Fabry–Perot, Mach–Zehnder and acousto-optic filter to enhance the performance in the transmission of Wavelength-Division Multiplexing optical fiber networks, since a tunable filter is a device which filters out one channel at a specific wavelength that can be changed by tuning the pass band of the optical filter.

1.4 Objectives

The aim of this research is to evaluate the performance of filtering (Fabry–Perot, Mach–Zehnder and acousto-optic) for Wavelength-Division Multiplexing based optical fiber networks in terms of Quality-factor,Bit Error Rate,Output power ,eye height , threshold all this parameters in eye diagram.

1.5 Methodology

This thesis will simulate using Opti-System software. The performance of WDM optical networks will be evaluated when the data will be transmitted along the optical fiber transmission line that will be use different types of tunable optical filters with special lengths of fiber cable, attenuation coefficients and input powers of the source. Then system performance with different tunable optical filters will be compared in terms of Quality-factor, Bit Error Rate, Eye height and Threshold to show the best one in the all scenarios.

1.6 Thesis organization

The thesis will be organized as follows: Chapter 2 discusses a literature review of Tunable Optical Filters. Chapter 3 discuss a system model and design approach. Chapter 4 presents the implementation, simulation and experimental results. Finally, chapter 5 presents conclusions and recommendation.

Chapter Two
Background and Literature Review

2.1 Multiplexing techniques

In norm, the capacity of optical fiber systems can surpass high bit rates in terms of Tera bit per second because of a huge frequency related with carrier. But there's a limitation in practice for the bit rates comes from dispersion and the nonlinearities. So to deliver a simple method for increasing the bit rates; multiplexing will be used. Multiplexing techniques can be classified as scheduled multiple-access techniques [fixed assignment] and a random multiple access techniques. Scheduled multiple-access technique is simple in routing of data than the other but their utilization is inefficient. Multiplexing can be represented in optical domain through different techniques such as WDM, OTDM, SCM and CDM [2].

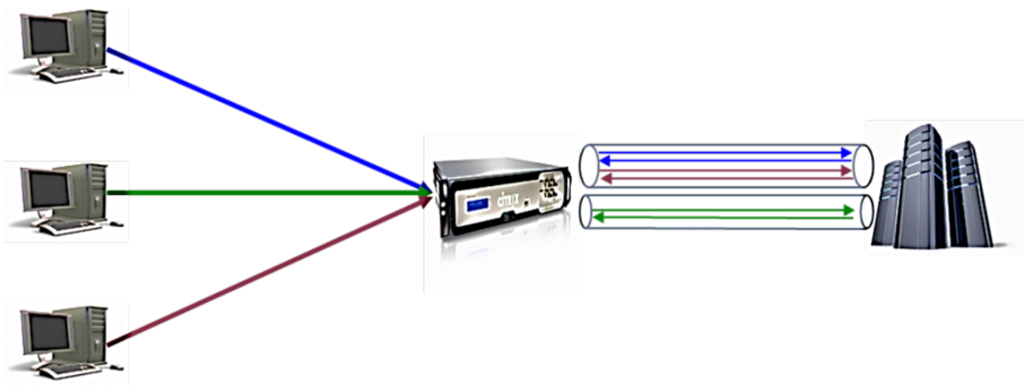

Figure 2.1: Multiplexing process

2.1.1 WDM technique

In WDM technique a large bandwidth (high bit rate) can obtain by a fiber optic because a several carriers modulated by autonomous electrical bits and transmitted over the similar optical fiber then in receiver passes through demultiplexer for separation process. So it used in different Low-loss transmission windows [3].

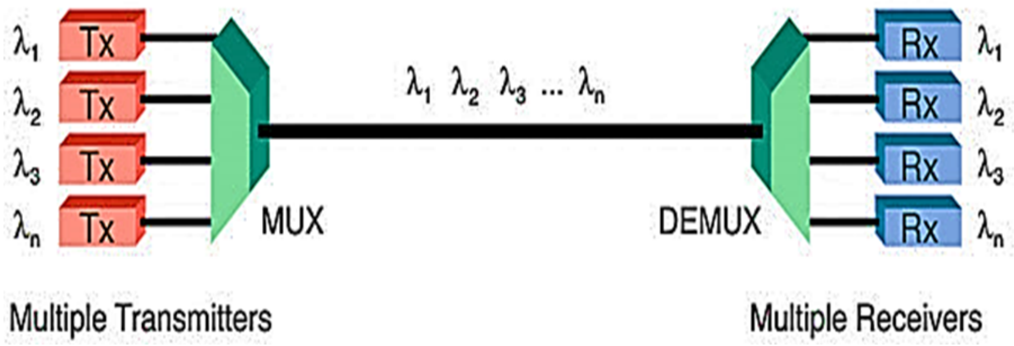

Figure 2.2: Wavelength Division Multiplexing

2.1.2 OTDM technique

In OTDM technique a distinct channel transmit several TDM channels to can increasing the bit rate to higher as possible [4].In additions the OTDM differ from WDM in the usage of line codes and optical sources [5].

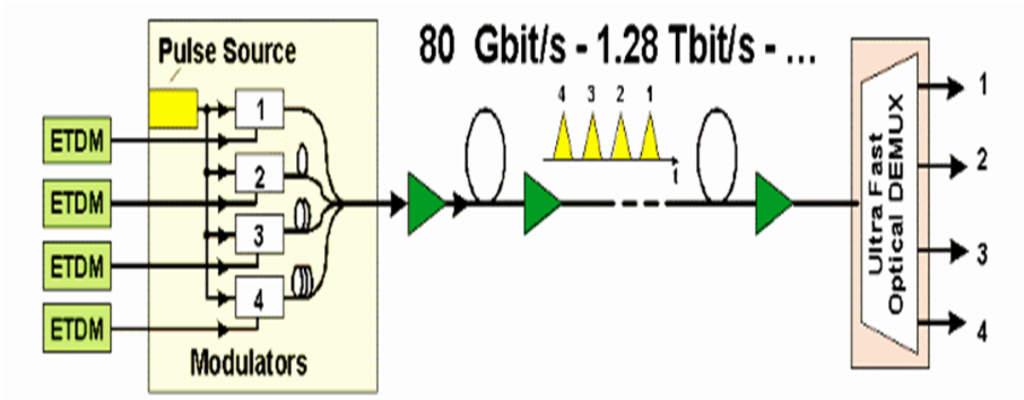

Figure 2.3: Optical Time Division Multiplexing

2.1.3 SCM technique

In SCM a multiple carriers can be used to transmit a multiple channels through a specific medium. In other words a low bit rate per channel but a large number of channels will carried in some different networks applications [6].

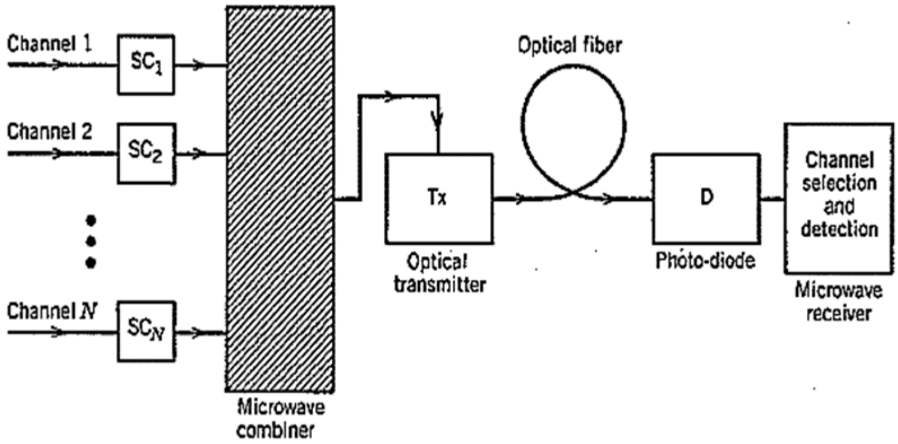

Figure 2.4: Subcarrier Multiplexing.

2.1.4 CDM technique

In CDM spread-spectrum technique will be used for coding every channel over a much broader region than the original signal [7].

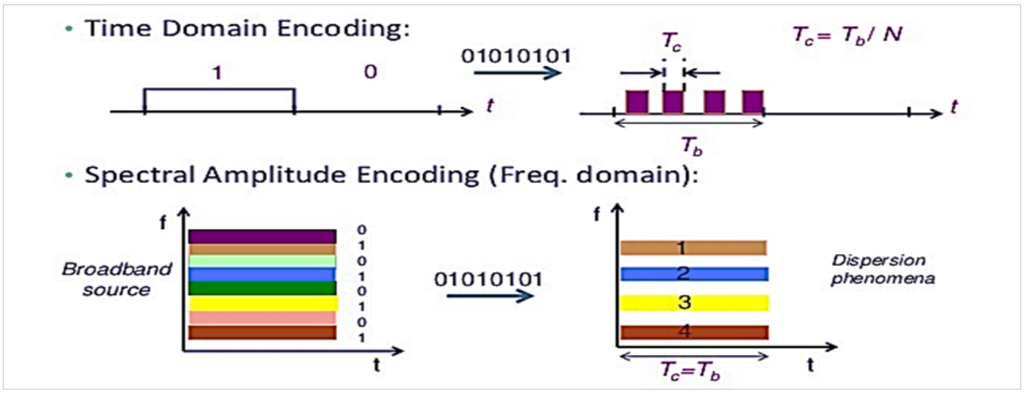

Figure 2.5: Optical Code Division Multiplexing illustrations.

2.2 Tunable Optical Filters

In WDM system, a tunable filter positioned at the receiver is used for channel selection process. According to original physical mechanism Optical filters can be classified into optical interference or diffraction. Based on this classification there are four types of filters shows in the figure below: (a) Fabry–Perot filter; (b) Mach–Zehnder filter; (c) grating-based Michelson filter; (d) Acousto-optic filter. The desirable properties of a tunable optical filter include: (1) wide tuning range to maximize the number of channels that can be selected, (2) negligible crosstalk to avoid interference from adjacent channels, (3) fast tuning speed to minimize the access time, (4) small insertion loss, (5) polarization insensitivity, (6) stability against environmental changes (humidity, temperature, vibrations, etc.), and (7) last but not the least, low cost [8].

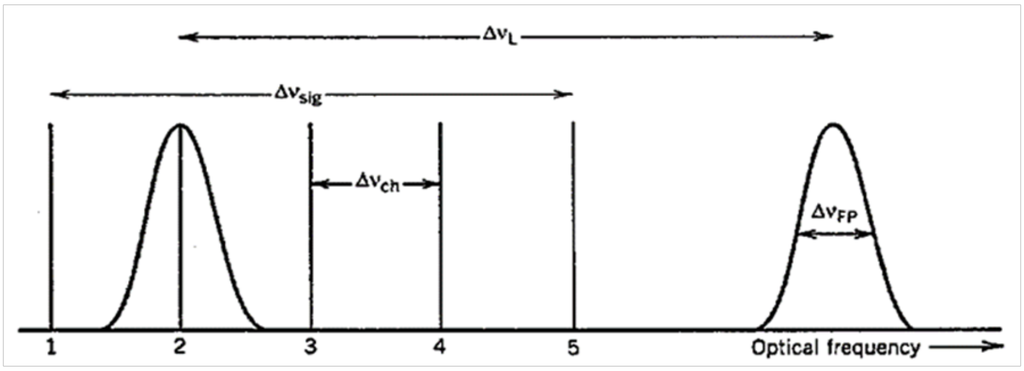

Figure 2.6: Channel selection mechanism.

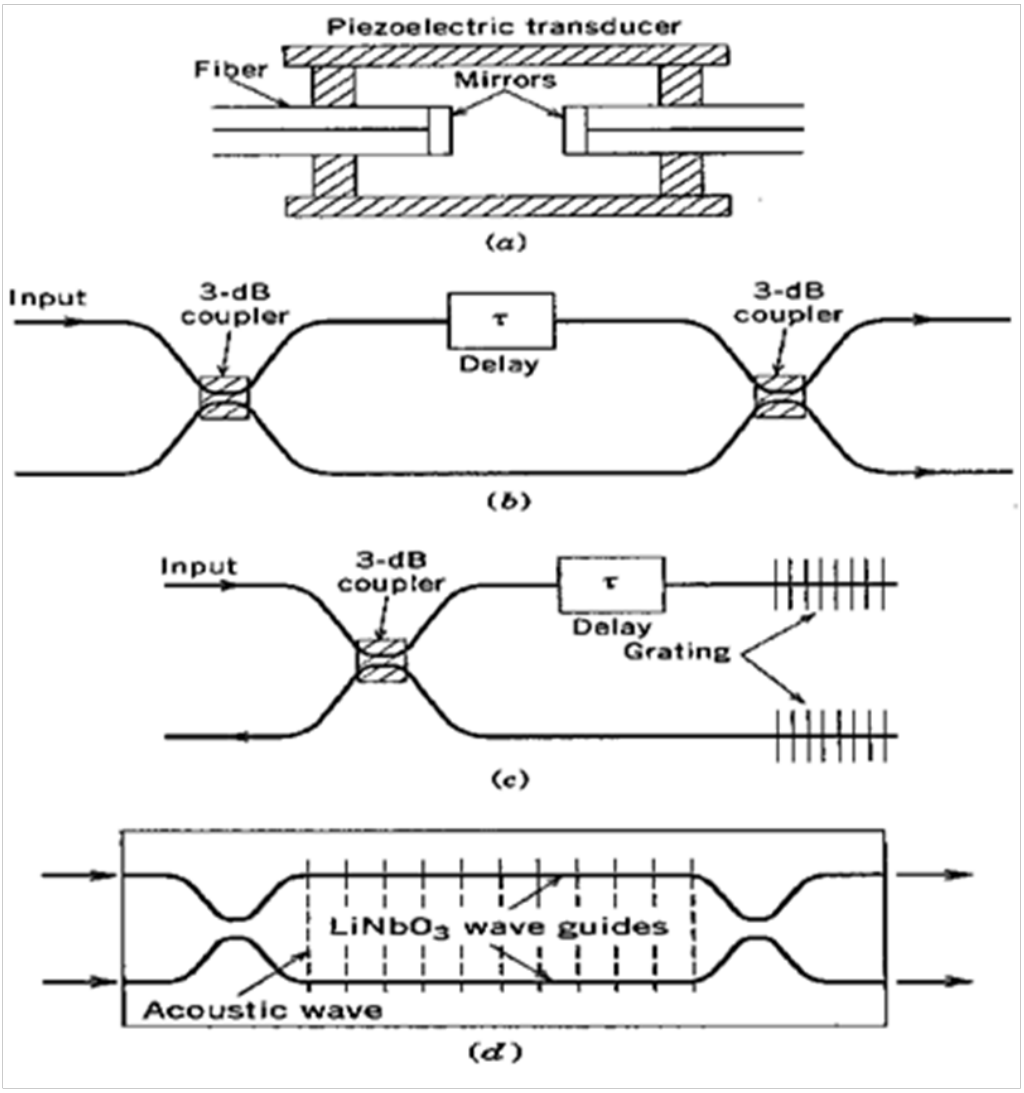

Figure 2.7: Four types of tunable optical filters.

2.2.1 Fabry–Perot Filter

Fabry–Perot interferometer can be tunable if its length is controlled by a piezoelectric transducer electronically [see Fig. 2.7(a)] and the spacing between two sequential peaks, called as the frequency spacing or free spectral range. FP filters uses the air gap between two optical fibers to get a high-reflectivity mirrors [9]. It can be tuned using thermo-optic and Micromechanical tuning [10]- [11].

2.2.2 Mach–Zehnder Filter

Mach–Zehnder interferometers can be formed by connecting the two output ports of a 3-dB coupler to the two input ports of another 3-dB coupler [see

Fig. 2.7(b)] for splitting and interfering process. The first coupler splits the input signal equally into two parts, which acquire different phase shifts (if the arm lengths are made different) before they interfere at the second coupler, also can be made by silica waveguides on a silicon substrate [12].

2.2.3 Grating-based optical Filter

Grating-based optical filter acts as a reflection filter and can be controlled by a grating period in terms of bandwidth and central wavelength. The reflective nature of fiber gratings is often a limitation in practice and requires the use of an optical circulator. Fiber grating filter with an optical circulator can be used for a narrowband transmission [13].

2.2.4 Michelson optical Filter

Michelson interferometer can be formed by using a 3-dB fiber coupler, two fiber gratings and two arms of interferometer [see Fig. 2.7(c)] to realize transmission filters [14]. Most of these schemes can also be implemented in the form of a planar lightwave circuit by forming silica waveguides on a silicon substrate.

2.2.5 Acousto-optic Filter

Acousto-optic filters use acoustic waves to formed grating dynamically and it has tuning range wider as possible to match an applications in optical FDM. The physical mechanism behind the operation of acousto-optic filters is the photoelastic effect through which an acoustic wave propagating through an acousto-optic material creates periodic changes in the refractive index (corresponding to the regions of local compression and rarefaction). [see Fig. 2.7(d)] [15].

2.3 Literature Review

In [16], developed both a mathematical model of Fabry-Perot interferometer (FPI) in s-domain and a relationship between tilt angles (β) with the variation of '$P_s v$' to realize the behavior of extrinsic Fabry-Perot interferometer cavity (EFPI) under tilted condition. In [17], demonstrated a novel absolute strain measurement system by use a Fabry-Perot interferometer (FPI) formed by cascaded high-reflection chirped fiber Bragg gratings (CFBGs) with opposite chirp directions demodulated by a wavelength-scanning distributed feedback (DFB) laser diode. The laser wavelength scanning rate can be improved by increase the frequency and/or the amplitude of the scanning signals.

In [18], proposed and demonstrated a necessary condition for the ultrasonic transducers needed based on microfiber grating for photo acoustic imaging. Results show different characteristics through measure of different mode interference on peak temperature and refractive index sensing. In [19], proposed and demonstrated an optical fiber temperature sensor based on cascaded interferometers. Results achieved the sensitivity is 6 times higher than in single interferometer. Also shows different sensitivity change by a change of optical path difference of Mach-Zehnder interferometer.

In [20], proposed and demonstrated a high gain and high directivity Fabry-Perot resonator antenna with metamaterial lens operating around 14GHz. Results shows the novel left-handed metamaterial (LHM) unit that achieve a greater negative refraction effect with only one-side fabricating on the dielectric board and pen shaped beam is well improved. In [21], demonstrated both athermal and flat-topped transmission in a Mach-Zehnder (MZ) filter. Athermal performance, minimum insertion loss and feature size is measured also the device can be scaled up to multi-channel WDM filters.

In [22], demonstrated both compact low-loss thermo-optic single Mach-Zehnder interferometers (MZIs) and two cascaded MZIs on a silicon nitride-on-insulator platform, which work as tunable filters in the visible range. In [23], demonstrated an acousto-optic tunable filters (AOTFs) optimized for operation in the 2-4 m region. Despite the inherently high RF drive-power requirement at longer wavelengths, practical Acousto Optic Tunable Filters [AOTFs] may be built operating to the transmission window limit of 4.5 m. A further improvement is possible using carefully optimized resonant designs.

In [24], demonstrated a double-filtering method based on two acousto-optic tunable filters for hyper spectral imaging application, the hyper spectral imaging system was built based on two AOTFs. Preliminary results shown that the hyper spectral imaging system based on the two acousto-optic tunable filters is completely doable. In [25], proposed and demonstrated an all-fiber acousto-optic tunable band pass filter based on a coreless optical fiber core mode blocker. Results show an optimization in response with an asymmetric configuration. Also demonstrate a lowest insertion loss when the device is operated as a band pass filter.

Chapter Three
System Model and Design Approach

3.1 Introduction

In this Chapter, we explain the system design of filtering for Wavelength Division Multiplexing based optical fiber networks, then evaluating the effect of limiting factors (fiber length, attenuation coefficient and input power) in terms of quality-factor, bit-error rate, eye height and threshold when we use a Fabry–Perot, Mach-Zehnder and Acousto-Optic tunable filters.

3.2 System Model

In this section we explain the system model of this research. Consider 4 WDM optical fiber networks as shown in the Figure 3.1 . In the transmission side an optical signal modulated with the electrical signal indirectly and multiplexed with the other optical signals then passed through an optical fiber cable and a tunable optical filter until reach the receiver side after demultiplexed operation.

Each transmitter used the Non return to zero modulation format to generate the electrical signal from the output of Pseudo Random Bit Sequence generator. An optical signal can be generated by used continuous wave LASER then both signals externally modulated optically at 12 Gbps with extinction

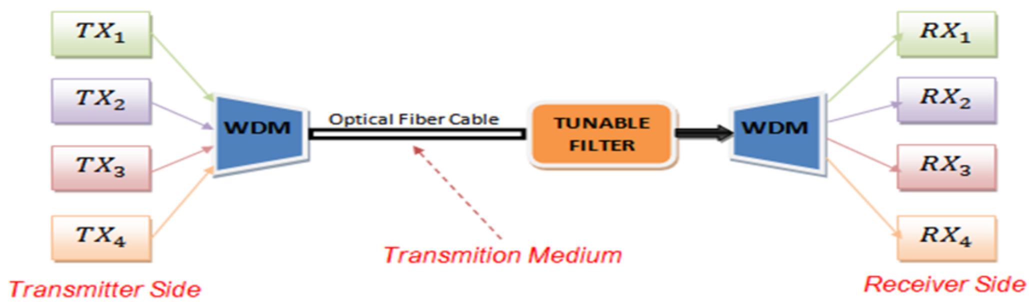

Figure 3.1: 4 WDM optical fiber networks

ratio of 30 dB by using a Mach-Zehnder modulator which is a famous type of optical modulators.

All optical signals with different frequencies (from 193.1 to 193.4 THZ) that generated are multiplexed optically with a (4-to-1) WDM multiplexer and lunched to a single mode fiber with a dispersion of 16.75 ps/nm/km. A tunable filter with different types is connected with a fiber cable to compensate dispersion and nonlinear effects in transmission system. An output signal from a tunable filter is also demultiplexed optically by (1-to-4) WDM demultiplexer, and each signal with specific frequency (from 193.1 to 193.4 THZ) is finally passed to a PIN photo detector to convert the optical signal back into the electrical signal. Overall system performance can be evaluated by using a BER analyzer which is connected at the end of the receiver side.

3.2.1 System model with Fabry–Perot Filter

In this case an optical filter cavity or interferometer is produced by two mirrors with a length between them that controlled electronically by a piezoelectric transducer [8]. The following equation can be used to calculate the FSR between the transmitted peaks

$$\Delta VL = \frac{c}{2n_g L}, \tag{3.1}$$

where n_g is the group index of interactivity material of Fabry–Perot filter, c is the speed of light and L is the length. Also the filter bandwidth, can be given by

$$\Delta VFP = \frac{\Delta VL}{F}, \tag{3.2}$$

where F: finesse of the FP filter. If internal losses are neglected, the finesse is given by

$$F = \frac{\pi\sqrt{R}}{(1-R)}, \tag{3.3}$$

where R is the mirror reflectivity.

3.2.2 System model with Mach-Zehnder Filter

In this case an optical filter interferometer is produced by using a two 3-dB coupler [8]. The following equation can be used to calculate the transmittivity of a chain of m such interferometers

$$T(v) = \prod_{m=1}^{M} \cos^2(\pi V \tau m), \tag{3.4}$$

where V is the frequency and τ is the relative delay in the two arms of the Mach-Zehnder interferometer

3.2.3 System model with Acousto-Optic Filter

In this case an optical filter grating is produced dynamically by using acoustic waves [8]. The following equation can be used to calculate the channel whose wavelength λ satisfies the Bragg condition

$$\lambda = \Delta n \Lambda_a, \tag{3.5}$$

where Δn is the TE-TM index difference and Λ_a is the acoustic wavelength

3.3 Limiting factors for performance of the WDM networks

One of the limiting factors is fiber losses for a reason of power reduction in the receiver side [8]. The following equation shows the Beer's law that govern changes in the average optical power P of a bit stream propagating inside an optical fiber

$$\frac{\delta P}{\delta z} = -\alpha P, \tag{3.6}$$

where α is the attenuation coefficient. The relation between input and output power in terms of attenuation coefficient and fiber length is given by

$$P_{out} = P_{in} \exp(-\alpha L). \tag{3.7}$$

Attenuation coefficient can be expressed in units of dB/km by using the relation

$$\alpha = -\frac{10}{L} \log_{10}\left(\frac{P_{out}}{P_{in}}\right) \approx 3.343\alpha, \tag{3.8}$$

and refer to it as the fiber-loss parameter.

3.4 Performance evaluation of the WDM networks

The system model evaluated its performance in terms of quality factor, bit-error rate, eye height and the threshold.

3.4.1 Quality factor

The Q factor is inversely proportional to the BER [8]; also it's related to SNR by the following equation

$$\text{SNR} = 4Q^2 \approx \eta N_P, \tag{3.9}$$

$$Q = (\eta N_p)^{\frac{1}{2}}, \tag{3.10}$$

where η is the quantum efficiency and N_p is the receiver sensitivity

3.4.2 Bit-error rate

Around an average value a sampled value fluctuates from bit to bit, depending on whether the bit corresponds to 1 or 0 in the bit stream. An error occurs when a sampled value less than a threshold value for bit 1 and vice versa for bit 0, because of receiver noise [8]. The BER is given by

$$\text{BER} = \frac{1}{2}\left[p(0 \mid 1) + p(1 \mid 0)\right], \tag{3.11}$$

where $p(01)$ is the probability of deciding 0 when 1 is received and $p(10)$ is the probability of deciding 1 when 0 is received. Also the BER is given by

$$\text{BER} = \frac{1}{2}\text{erfc}\left(\frac{Q}{2}\right) \tag{3.12}$$

$$=\approx \frac{\exp\ \left(-\frac{Q^2}{2}\right)}{Q\sqrt{2\Pi}} \tag{3.13}$$

$$= \frac{1}{2}\text{erfc}\left(\sqrt{\frac{\eta N_p}{2}}\right) \tag{3.14}$$

3.4.3 Eye height

An optical receiver performance may change with time, for this reason the eye diagram is best suitable in this case; closing of the eye is a measure of degradation in receiver performance and is related with subsequent increase in the BER and vice versa [8]. This observation relates eye closure to the BER and it is quantified (in dB) as

$$\delta_{eye} = -10\log_{10}\left(\frac{\text{eye opening after transmission}}{\text{eye opening before transmission}}\right) \tag{3.15}$$

3.4.4 Threshold Considerations

Simply to get the threshold condition is to detect how the amplitude of an optical mode changes during one round trip in a definite cavity. The decision circuit compares the output from the linear channel to a threshold level, at sampling times determined by the clock-recovery circuit, and decides whether the signal corresponds to bit 1 or bit 0. The greatest sampling time is maximum corresponds to the situation in which the signal level difference between 1 and 0 bits [8].

3.4.5 Eye Diagram

A method which is often used to obtain a qualitative indication of the performance of a regenerative repeater or a PCM system is the examination of the received waveform on an oscilloscope using a sweep rate which is a fraction of the bit rate. The display obtained over two bit intervals duration, which is the result of superimposing all possible pulse sequences, is called an eye diagram or pattern [8]. An illustration of an eye diagram for a binary system with little distortion and no additive noise is shown in Figure (a) 3.2. It may be observed that the diagram has the shape of a human eye which is open and that the decision time corresponds to the center of the opening. To regenerate the pulse sequence without error the eye must be open thereby indicating that a decision area exists, and the decision crosshair (provided by the decision time and the decision threshold) must be within this open area. The effect of practical degradations on the pulses (i.e. intersymbol interference and noise) is to reduce the size of, or close, the eye, as shown in Figure (b) 3.2. Hence for reliable transmission it is essential that the eye is kept open, the margin against an error occurring being the minimum distance between the decision crosshair and the edge of the eye [26].

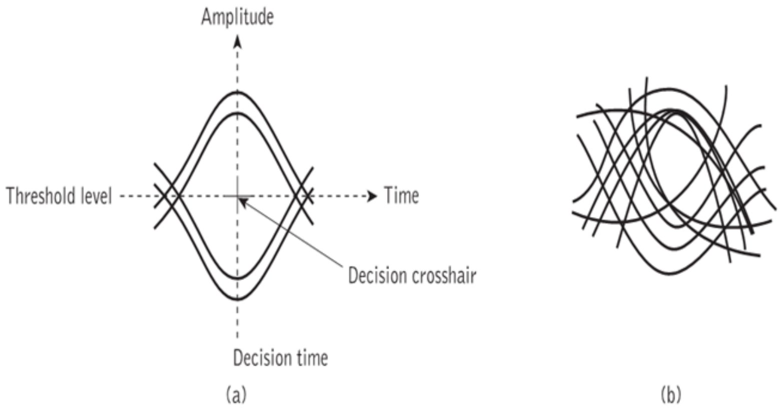

Figure 3.2: Eye Diagrams in binary digital transmission

Chapter Four
Results and Discussion

4.1 Introduction

In this chapter we discuss the performance analysis of filtering for WDM based optical fiber networks is evaluated by OptiSystem simulation. We will discuss the result of the performance analysis for WDM based optical fiber networks for different filtering types and limiting factors and then compared with each other.

4.2 Performance Analysis For Filtering WDM Based Optical Fiber Networks

The initial values of various components in the system as follow:

- CW Input Power: 0 dBm
- CW LASER frequency: (193.1-193.4 THz)
- Fiber length: 40 Km
- Reference wavelength: (1552.7-1551.2 nm)
- Mach-Zehnder modulator extinction ratio: 30 dB
- Attenuation coefficient: 0.1 dB/Km
- Bit rate: 12 Gbps
- PIN photodiode responsitivity: 1 A/W
- PIN photodiode dark current: 10 nA

4.2.1 Performance Analysis With a Fabry–Perot Tunable Filter

The initial Fabry–Perot optical filter properties as follow:

- Frequency: 193.1 THz
- Bandwidth: 5 GHz
- Free spectral range: 5 GHz
- Insertion loss: 0 dB

- Depth: 100 dB

In this case the following limiting factors are taken to see the performance of Fabry–Perot optical filter.

4.2.1.1 Effect Of Fiber Length

In this case the following parameters are taken to see the effect of fiber length.

- Input power: 0 dBm
- Attenuation coefficient: 0.1 dB/Km

Figure 4.2, Figure 4.3, and Figure 4.4, show the system performance parameters when the fiber length is equal to 40 Km. Next, the fiber length is set to 80 Km and the performance is shown in Figure 4.5, Figure 4.6, and Figure 4.7. Next, the fiber length is set to 120 Km and the performance is shown in Figure 4.8, Figure 4.9, and Figure 4.10. Next, the fiber length is set to 160 Km and the performance is shown in Figure 4.11, Figure 4.12, and Figure 4.13. Finally, the fiber length is set to 200 Km and the performance is shown in Figure 4.15, Figure 4.16, and Figure 4.17. The figures are presented in the next pages, which is shown that in the case of fiber length 40 Km (Highest Performance) a clearly output signal and open eye in the diagram also shown maximum Q-factor, Eye Height, Threshold and minimum BER. The performance gradually degraded until reach fiber length 200 Km (Lowest Performance), which is shown that a noisy output signal and closed eye in the diagram also shown minimum Q-factor, Eye Height, Threshold and maximum BER.

The following table, Tables 4.1 concluded the presents a summary of the results obtained from Figure 4.2 to Figure 4.17

Table 4.1: FP,Evaluation(L=40 to 200Km,α=0.1dB/Km,P_in=0dBm)

Length (Km)	Max .Q-Factor	Min. BER	Eye Height	Threshold
40	12	9e-032	3e-004	5e-005
80	11	5e-030	10e-005	5e-005
120	6.7	9e-012	3e-005	2.9e-005
160	2.9	2e-003	-6e-007	1e-005
200	0	1	0	0

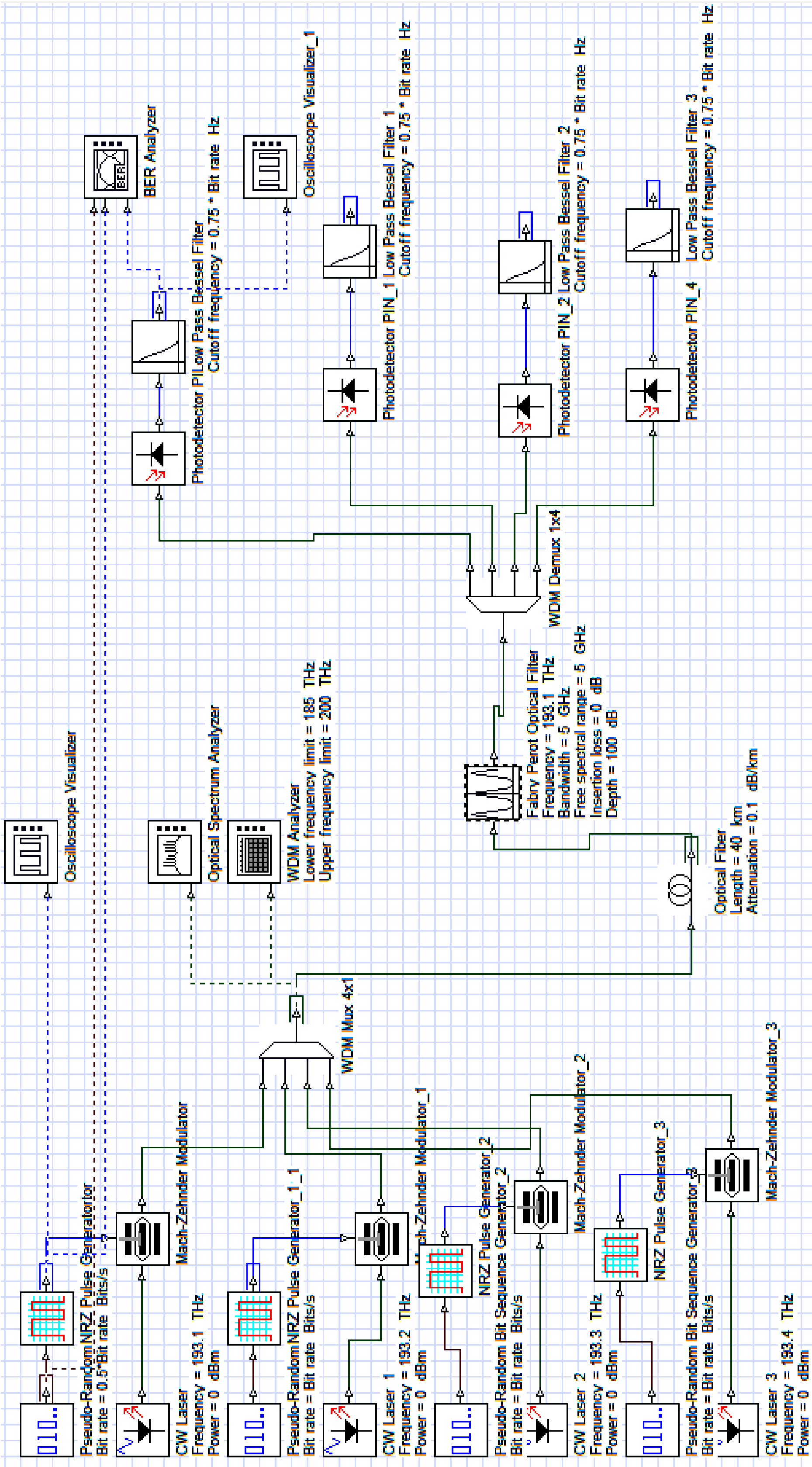

Figure 4.1: The system with FP filter and Length=40Km

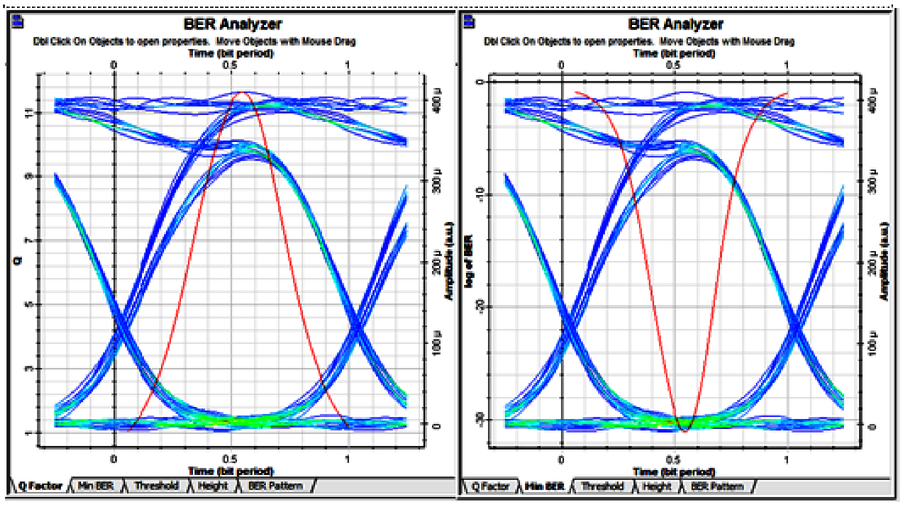

Figure 4.2: FP,Q-factor and BER(L=40Km,α=0.1dB/Km,P_in=0dBm)

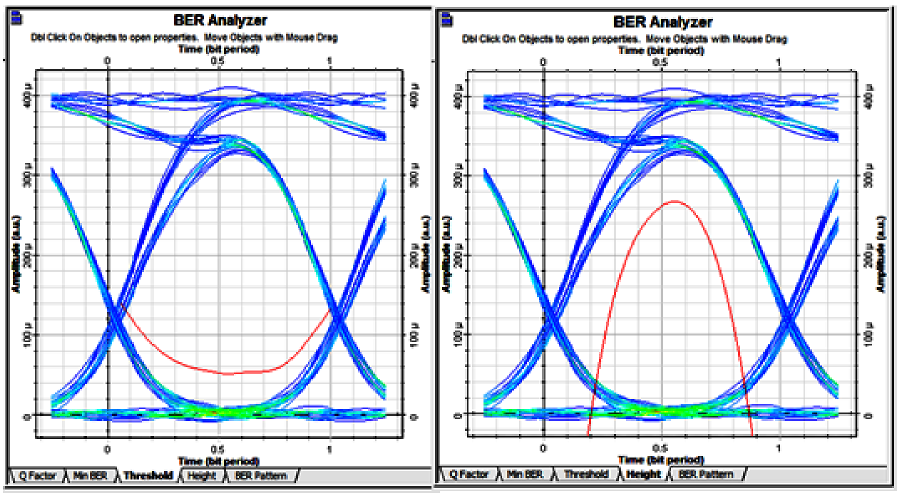

Figure 4.3: FP,Threshold and eye height(L=40Km,α=0.1dB/Km,P_in=0dBm)

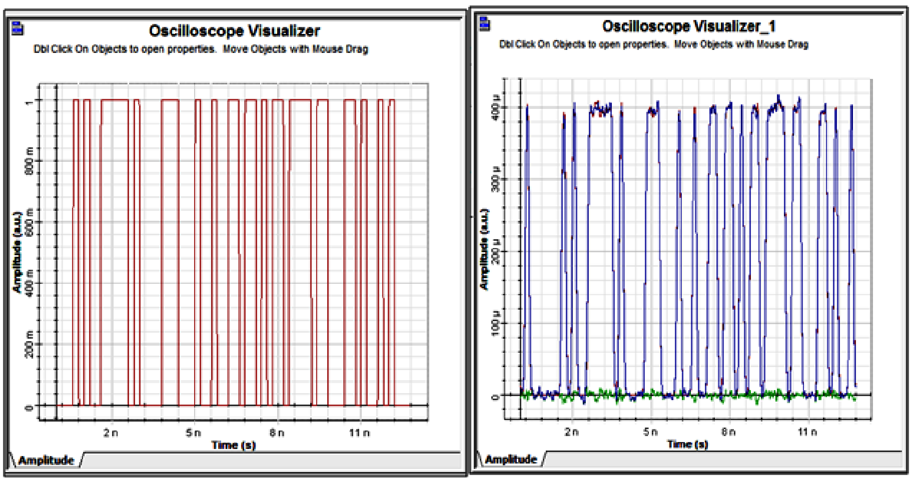

Figure 4.4: FP,Input and output signals(L=40Km,α=0.1dB/Km,P_in=0dBm)

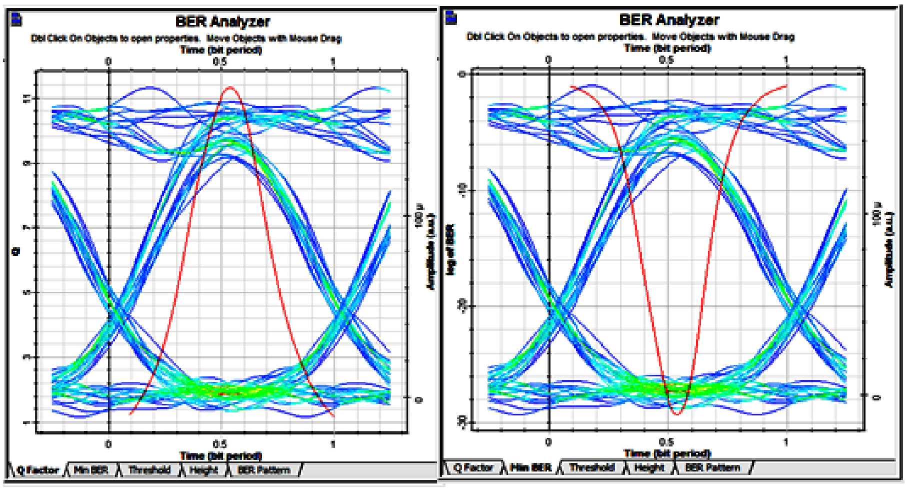

Figure 4.5: FP,Q-factor and BER(L=80Km,α=0.1dB/Km,P_in=0dBm)

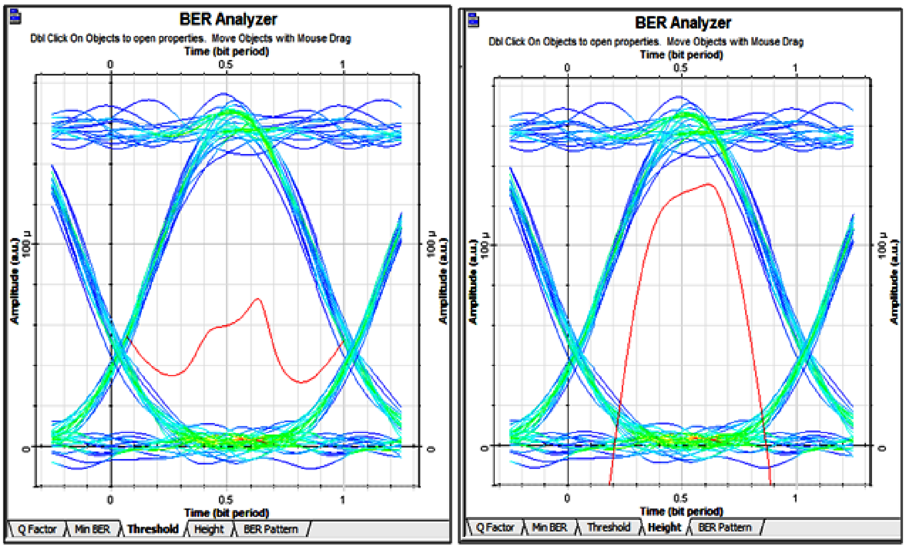

Figure 4.6: FP,Threshold and eye height(L=80Km,α=0.1dB/Km,P_in=0dBm)

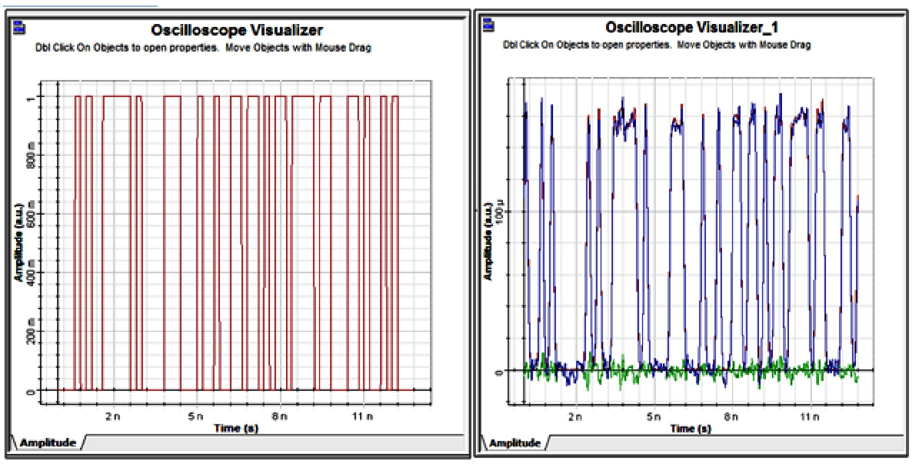

Figure 4.7: FP,Input and output signals(L=80Km,α=0.1dB/Km,P_in=0dBm)

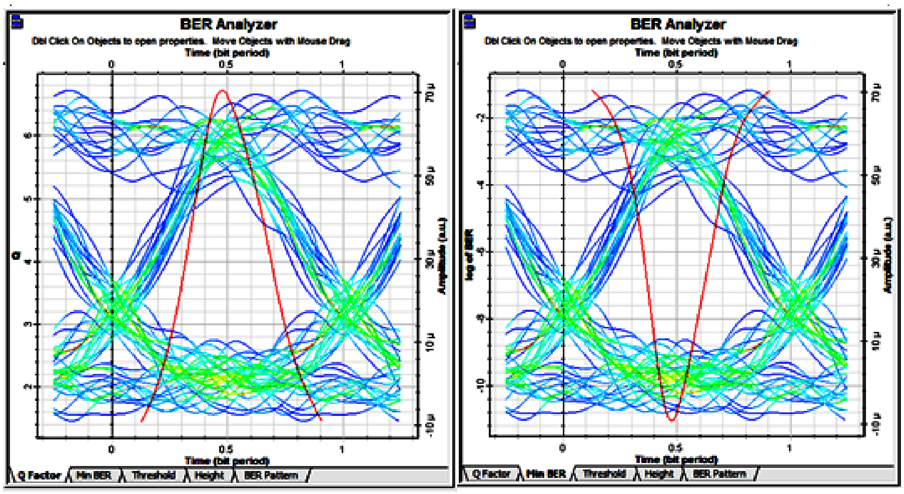

Figure 4.8: FP,Q-factor and BER(L=120Km,α=0.1dB/Km,P_in=0dBm)

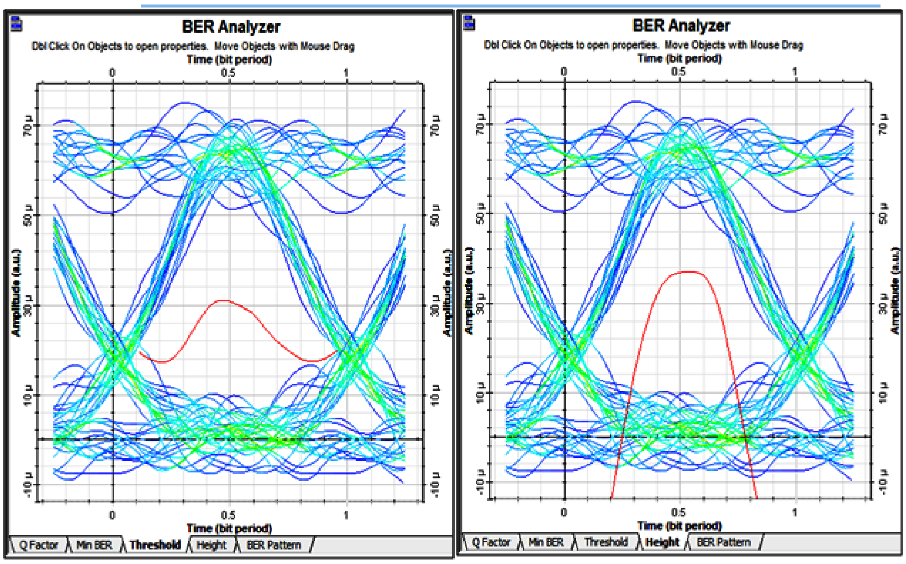

Figure 4.9: FP,Threshold and eye height(L=120Km,α=0.1dB/Km,P_in=0dBm)

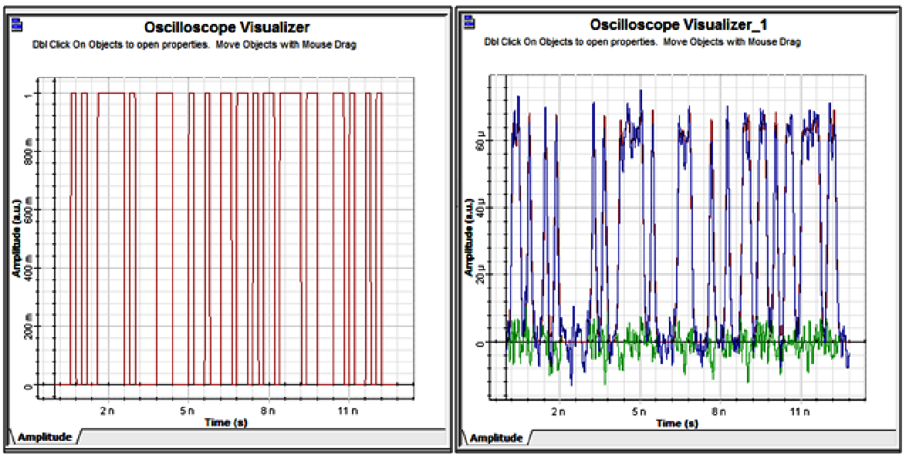

Figure 4.10: FP,Input and output signals(L=120Km,α=0.1dB/Km,P_in=0dBm)

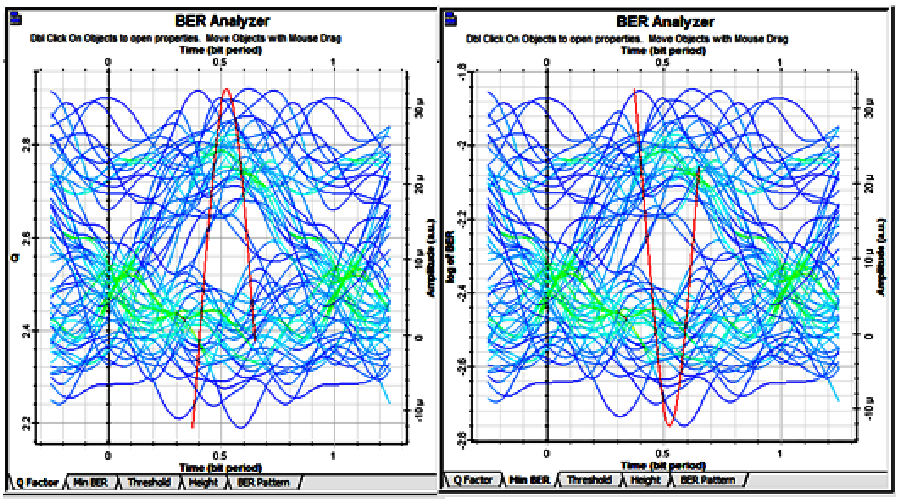

Figure 4.11: FP,Q-factor and BER(L=160Km,α=0.1dB/Km,P_in=0dBm)

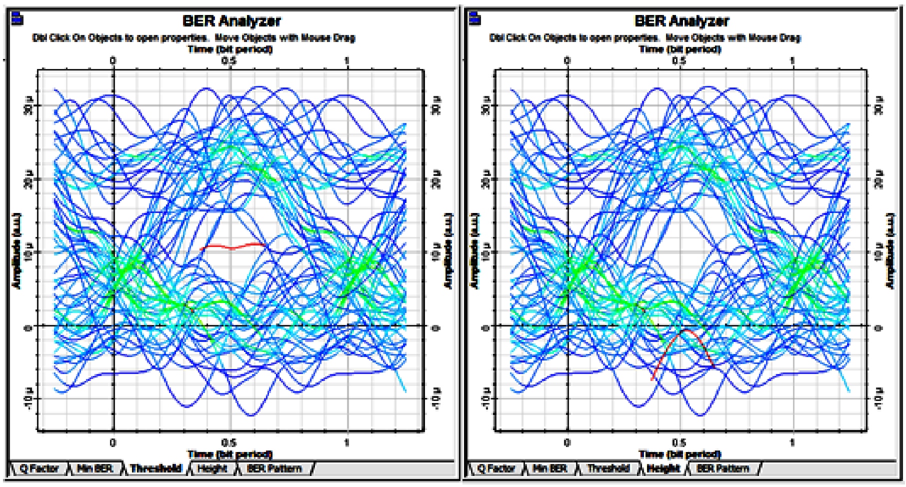

Figure 4.12: FP,Threshold and eye height(L=160Km,α=0.1dB/Km,P_in=0dBm)

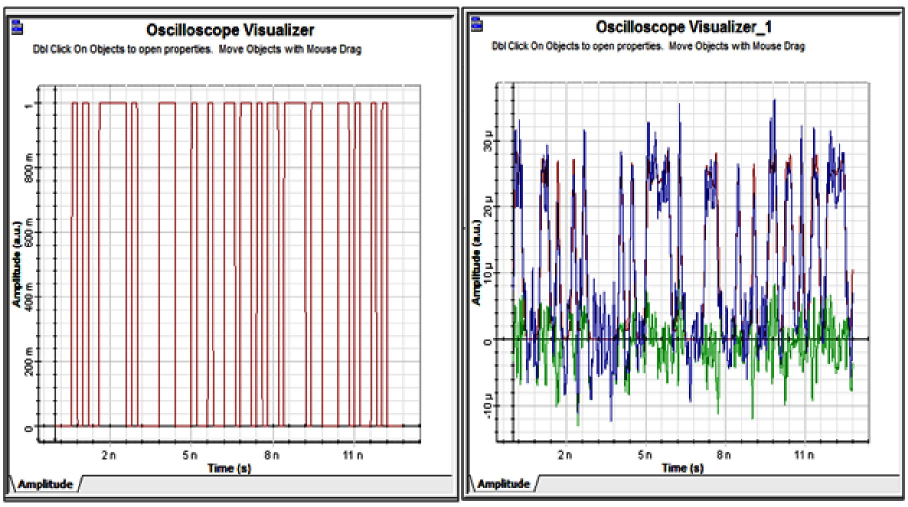

Figure 4.13: FP,Input and output signals(L=160Km,α=0.1dB/Km,P_in=0dBm)

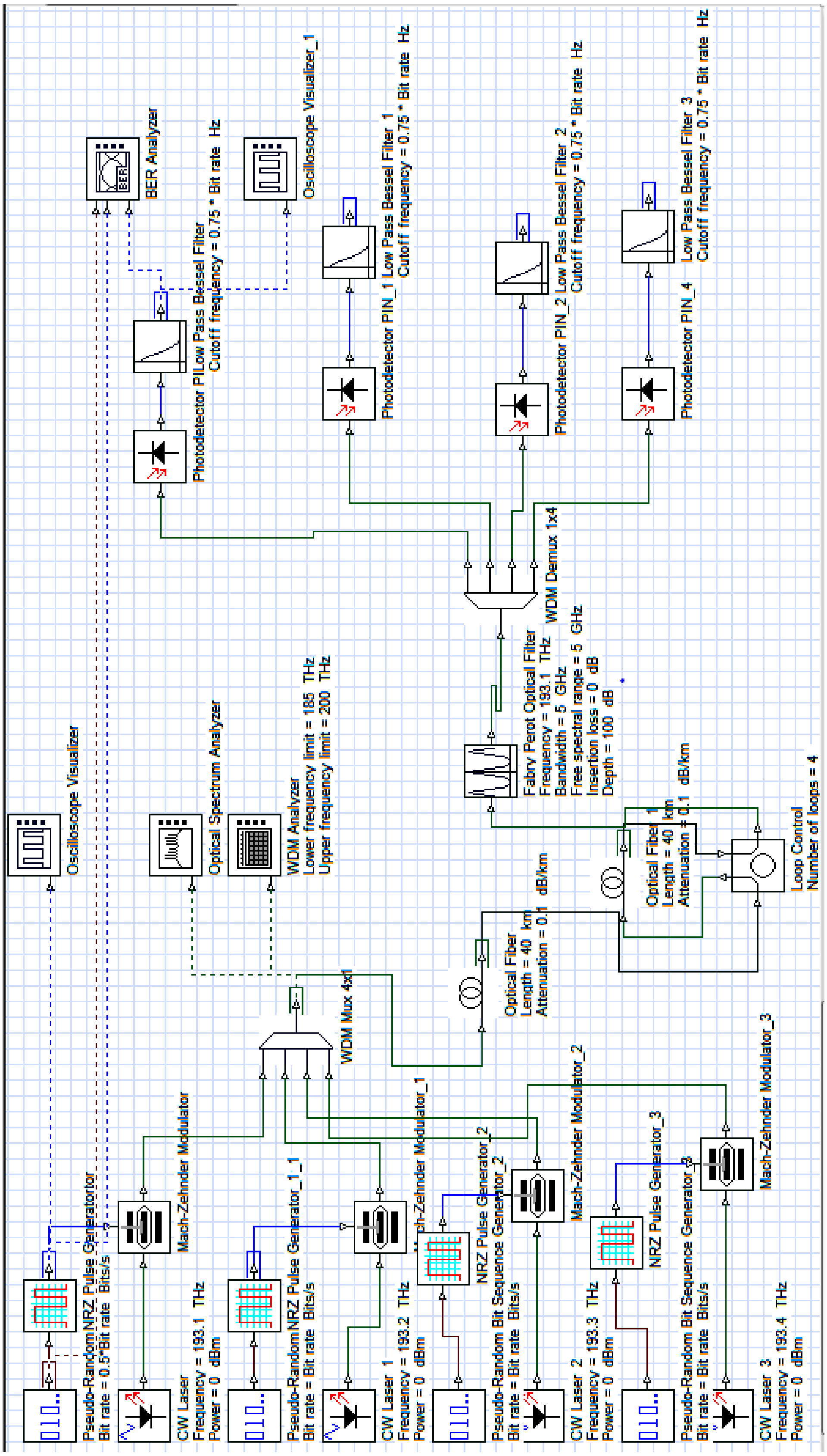

Figure 4.14: The system with FP filter and Length=200Km

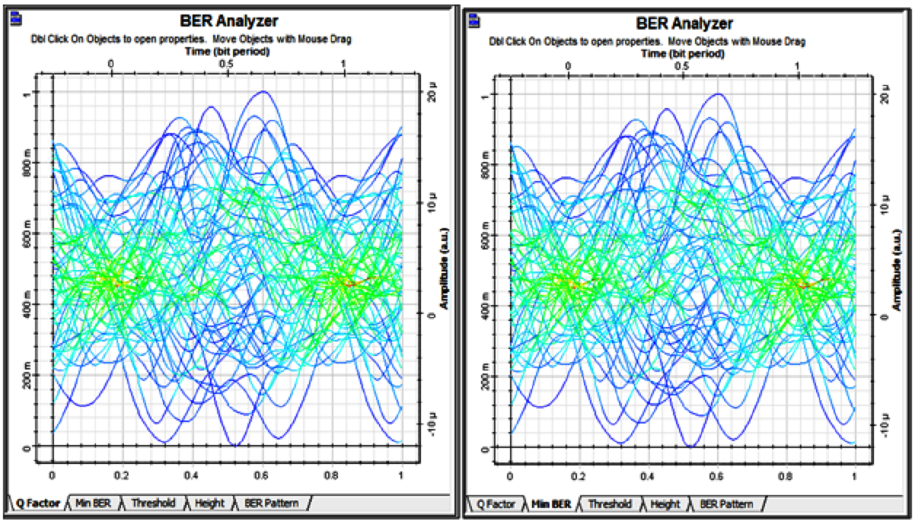

Figure 4.15: FP,Q-factor and BER(L=200Km,α=0.1dB/Km,P_in=0dBm)

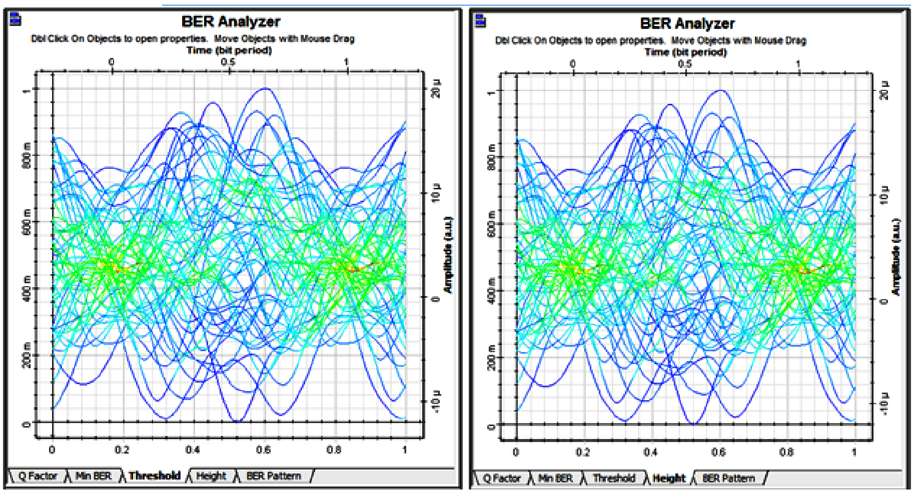

Figure 4.16: FP,Threshold and eye height(L=200Km,α=0.1dB/Km,P_in=0dBm)

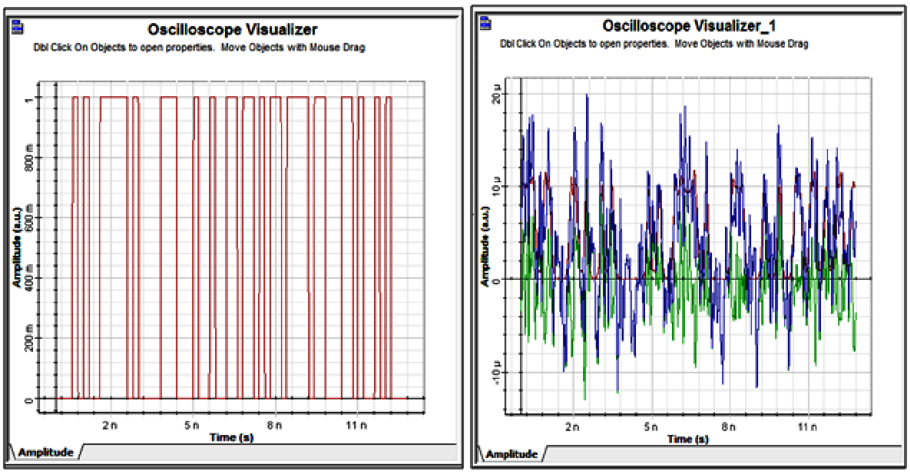

Figure 4.17: FP,Input and output signals(L=200Km,α =0.1dB/Km,P_in=0dBm)

4.2.1.2 Effect Of Attenuation Coefficient

In this case the following parameters are taken to see the effect of fiber attenuation coefficient.

- Input power: 0 dBm
- Fiber length: 40 Km

Figure 4.19, Figure 4.20, and Figure 4.21, show the system performance parameters when the fiber attenuation coefficient is equal to 0.1 dB/Km. Next, the attenuation is set to 0.2 dB/Km and the performance is shown in Figure 4.22, Figure 4.23, and Figure 4.24. Next, the attenuation is set to 0.3 dB/Km and the performance is shown in Figure 4.25, Figure 4.26, and Figure 4.27. Next, the attenuation is set to 0.4 dB/Km and the performance is shown in Figure 4.28, Figure 4.29, and Figure 4.30. Finally, the attenuation is set to 0.5 dB/Km and the performance is shown in Figure 4.31, Figure 4.32, and Figure 4.33. The figures are presented in the next pages, which is shown that in the case of an attenuation 0.1 dB/Km (Highest Performance) a clearly output signal and open eye in the diagram also shown maximum Q-factor, Eye Height, Threshold and minimum BER. The performance gradually degraded until reach an attenuation 0.5 dB/Km (Lowest Performance), which is shown that a noisy output signal and closed eye in the diagram also shown minimum Q-factor, Eye Height, Threshold and maximum BER.

The following table, Tables 4.2 concluded the presents a summary of the results obtained from Figure 4.19 to Figure 4.33

Table 4.2: FP,Evaluation(L=40Km,α=0.1 to 0.5dB/Km,P_in=0dBm)

Attenuation (dB/Km)	Max .Q-Factor	Min. BER	Eye Height	Threshold
0.1	12	9e-032	3e-004	5e-005
0.2	9	2e-019	9.6e-005	4e-005
0.3	5	6e-008	2.5e-005	2e-005
0.4	2.6	41e-004	-3e-006	8e-006
0.5	0	1	0	0

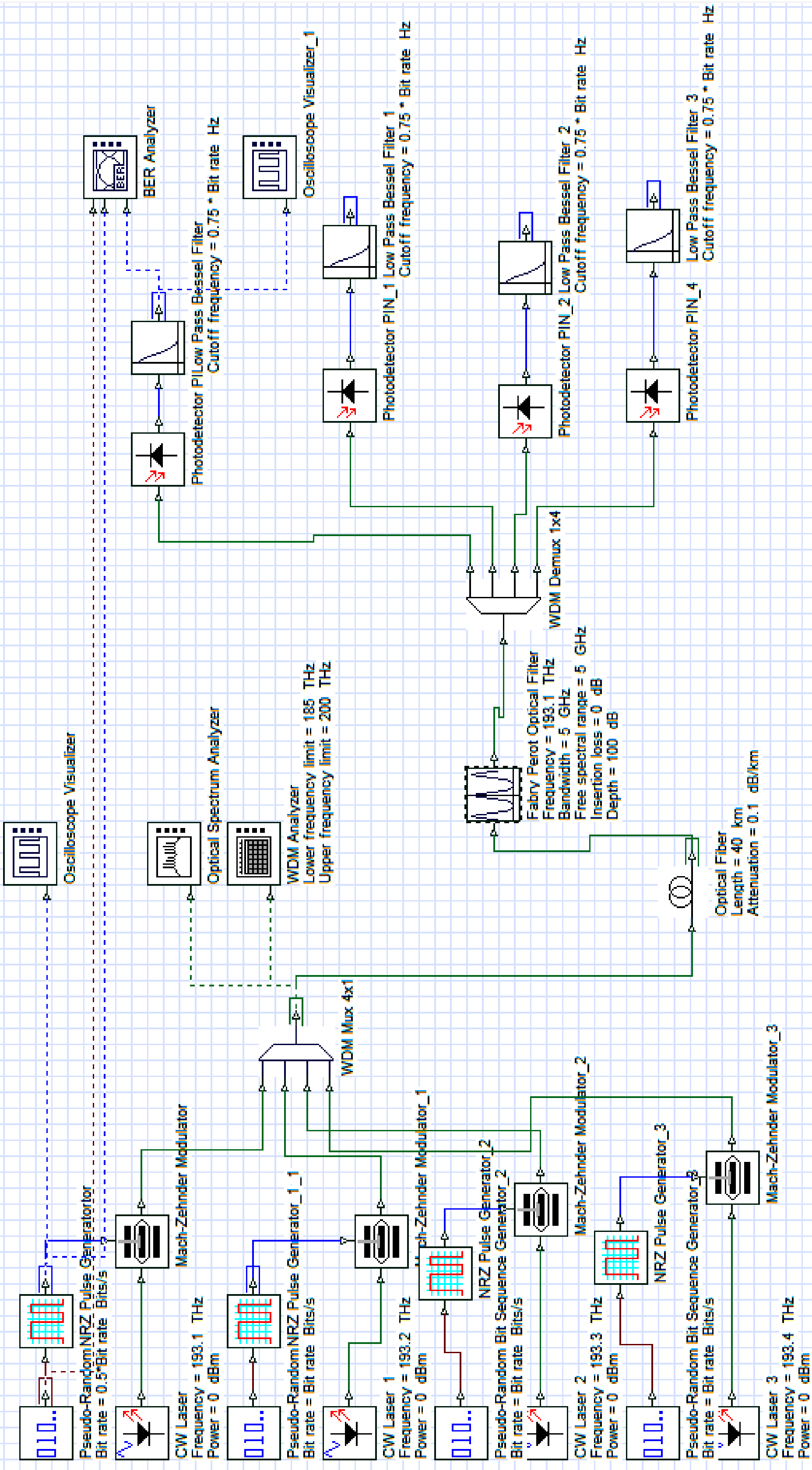

Figure 4.18: The system with FP filter and Attenuation=0.1dB/Km

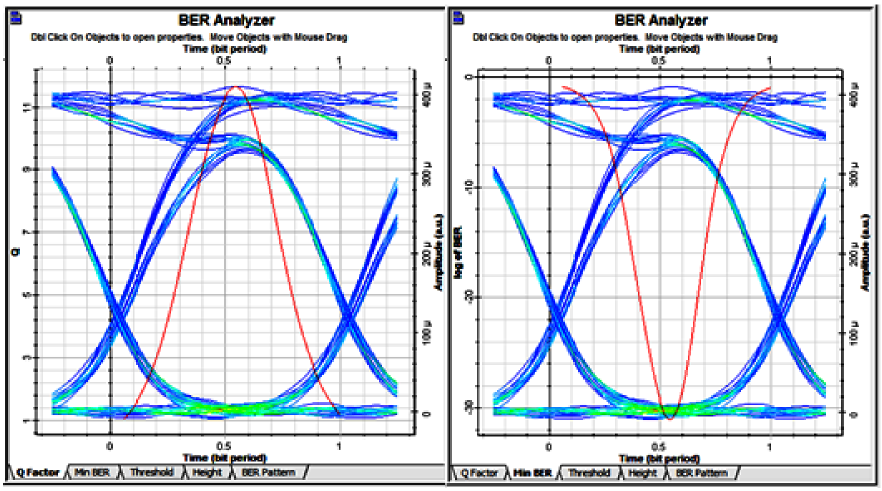

Figure 4.19: FP,Q-factor and BER(L=40Km,α=0.1dB/Km,P_in=0dBm)

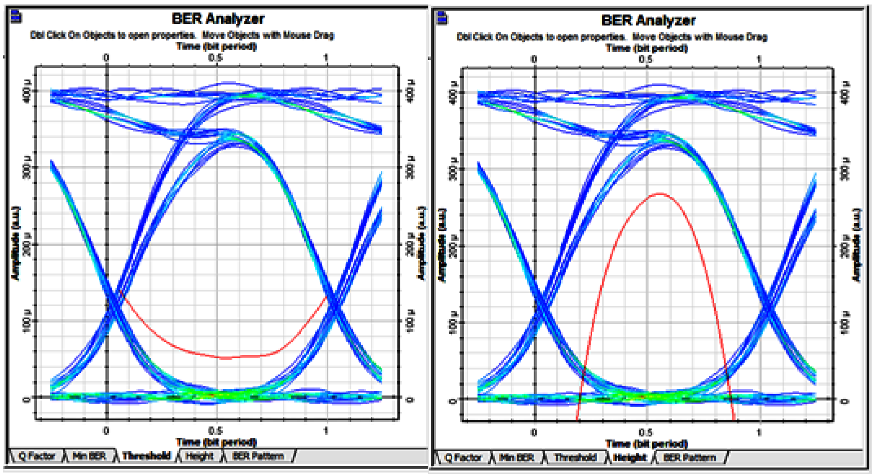

Figure 4.20: FP,Threshold and eye height(L=40Km,α=0.1dB/Km,P_in=0dBm)

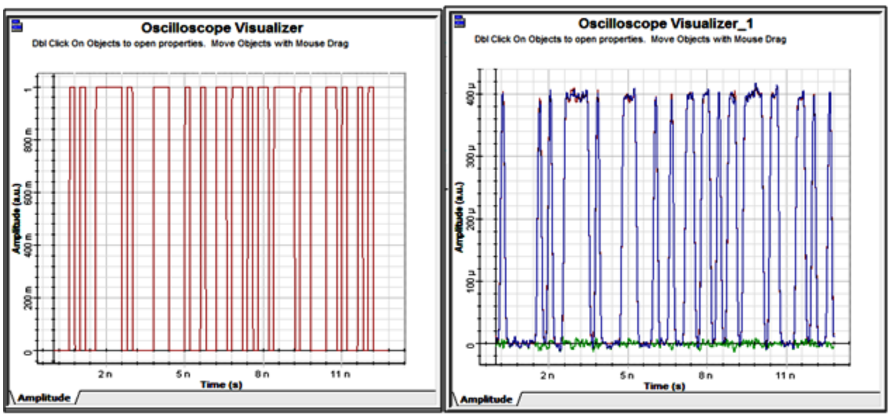

Figure 4.21: FP,Input and output signals(L=40Km,α=0.1dB/Km,P_in=0dBm)

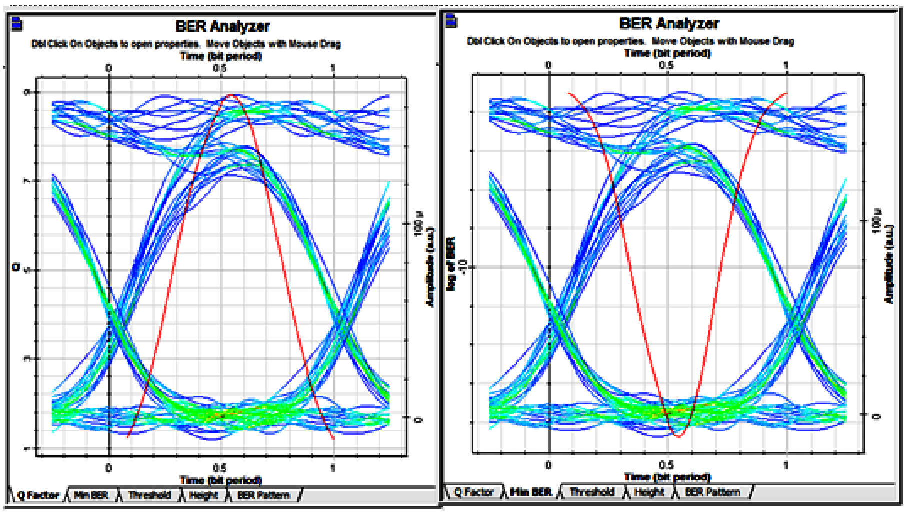

Figure 4.22: FP,Q-factor and BER(L=40Km,α=0.2dB/Km,P_in=0dBm)

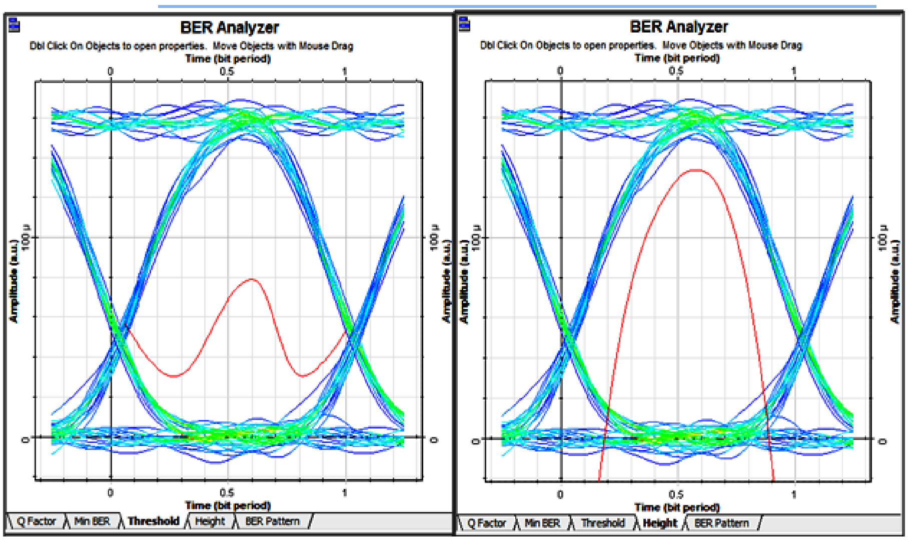

Figure 4.23: FP,Threshold and eye height(L=40Km,α=0.2dB/Km,P_in=0dBm)

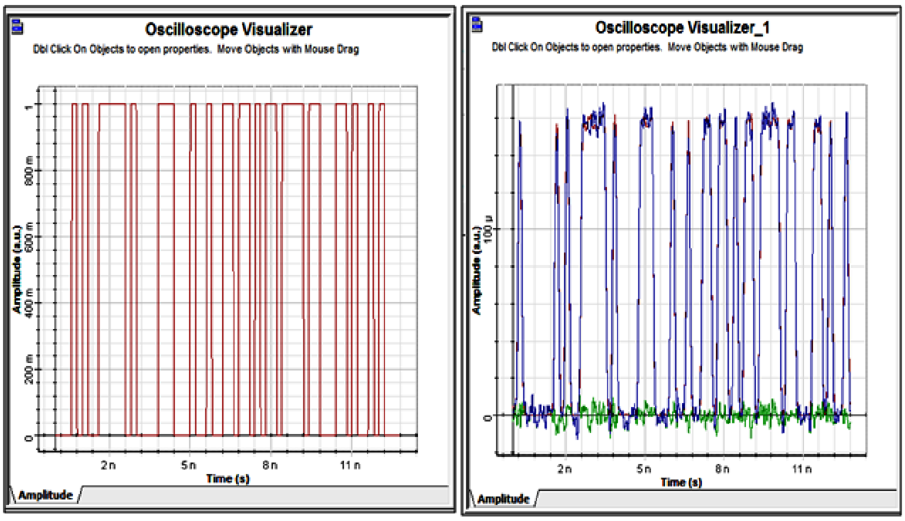

Figure 4.24: FP,Input and output signals(L=40Km,α=0.2dB/Km,P_in=0dBm)

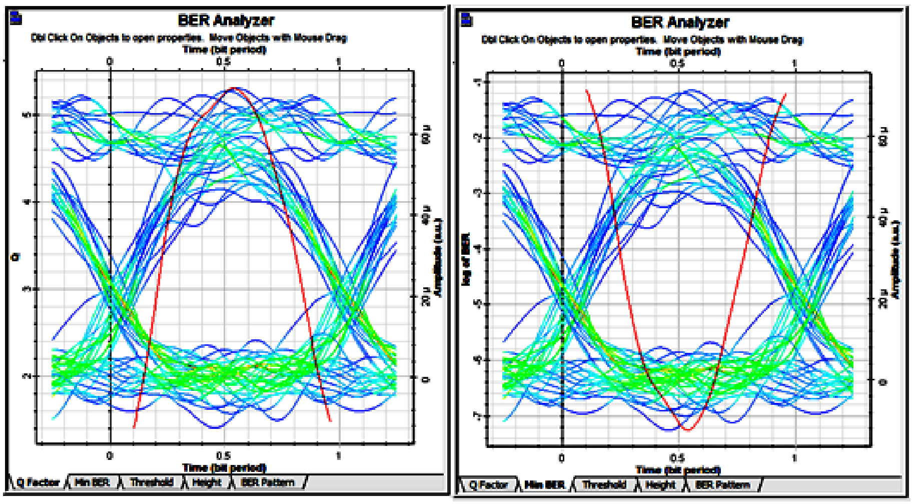

Figure 4.25: FP,Q-factor and BER(L=40Km,α=0.3dB/Km,P_in=0dBm)

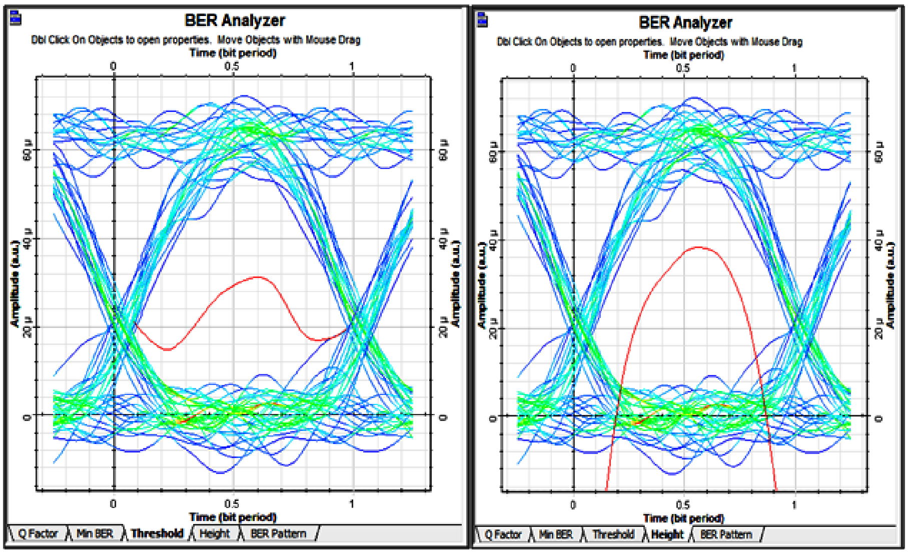

Figure 4.26: FP,Threshold and eye height(L=40Km,α=0.3dB/Km,P_in=0dBm)

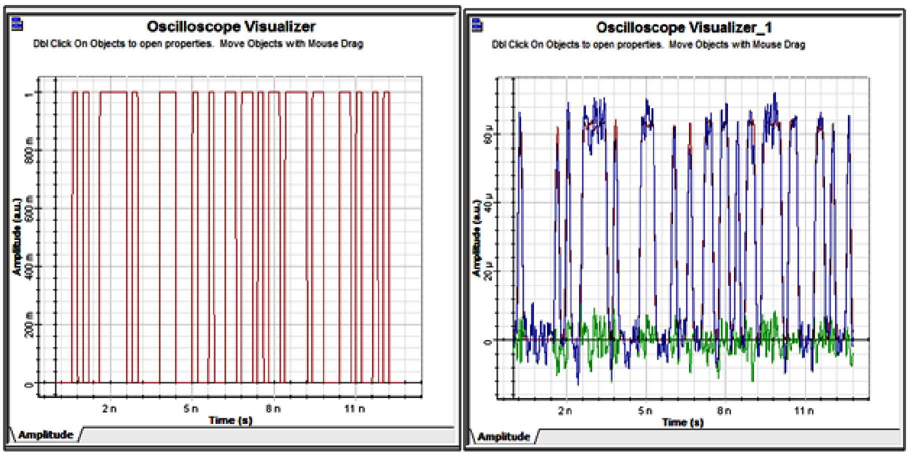

Figure 4.27: FP,Input and output signals(L=40Km,α=0.3dB/Km,P_in=0dBm)

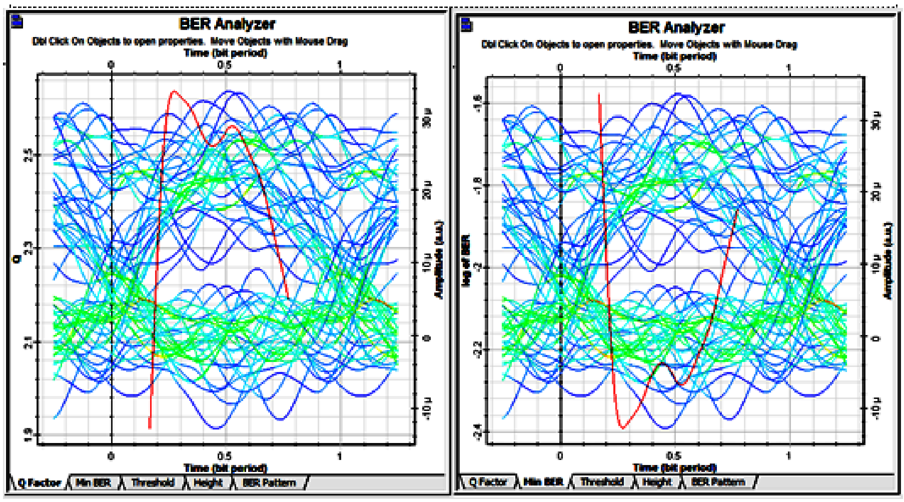

Figure 4.28: FP,Q-factor and BER(L=40Km,α=0.4dB/Km,P_in=0dBm)

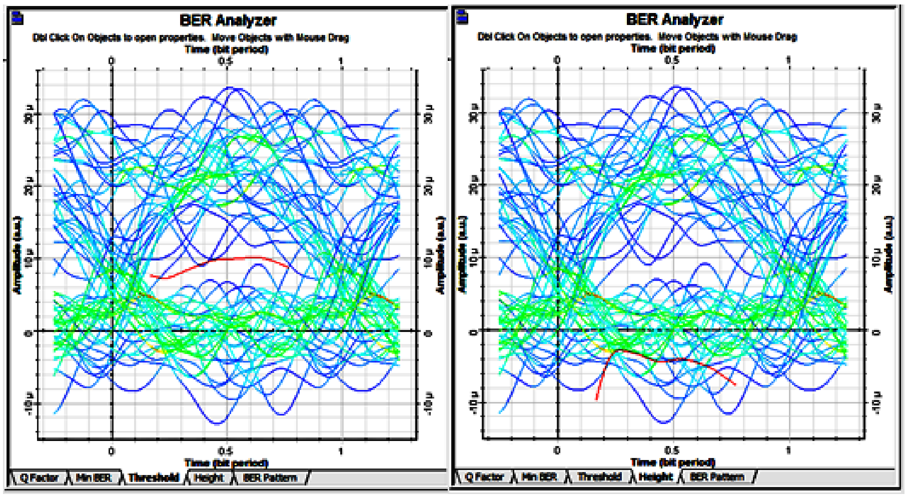

Figure 4.29: FP,Threshold and eye height(L=40Km,α=0.4dB/Km,P_in=0dBm)

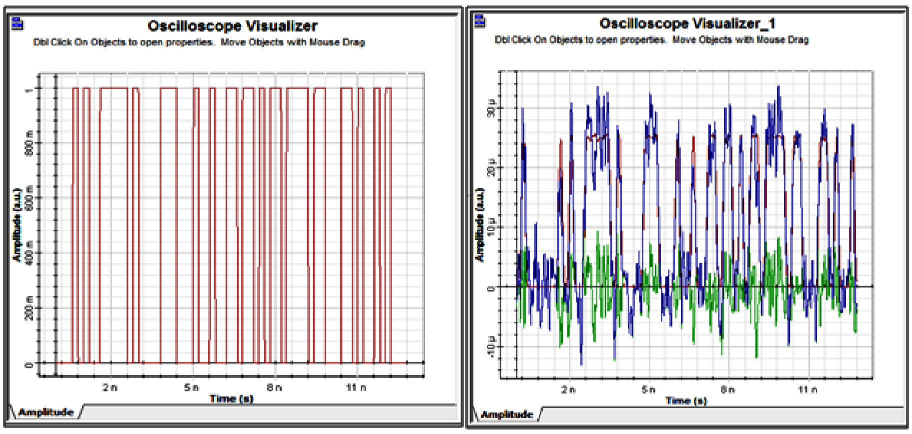

Figure 4.30: FP,Input and output signals(L=40Km,α=0.4dB/Km,P_in=0dBm)

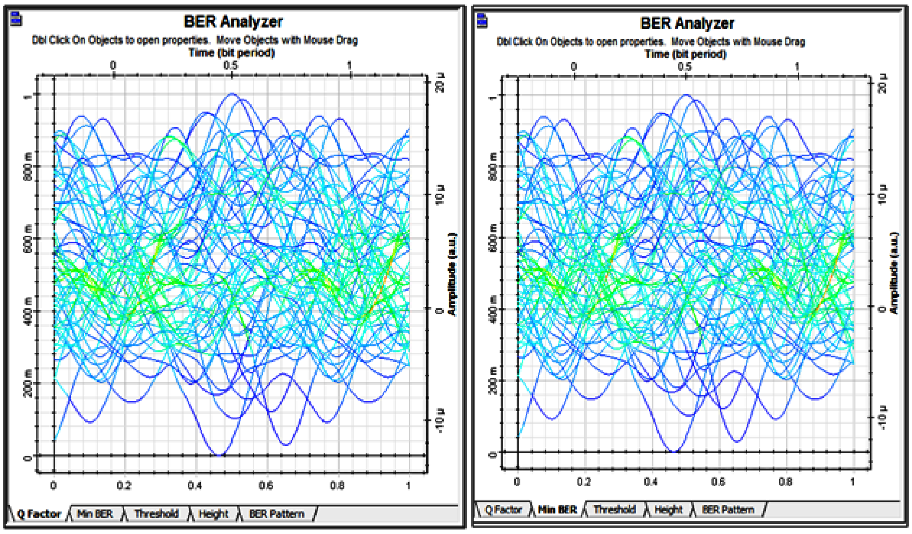

Figure 4.31: FP,Q-factor and BER(L=40Km,α=0.5dB/Km,P_in=0dBm)

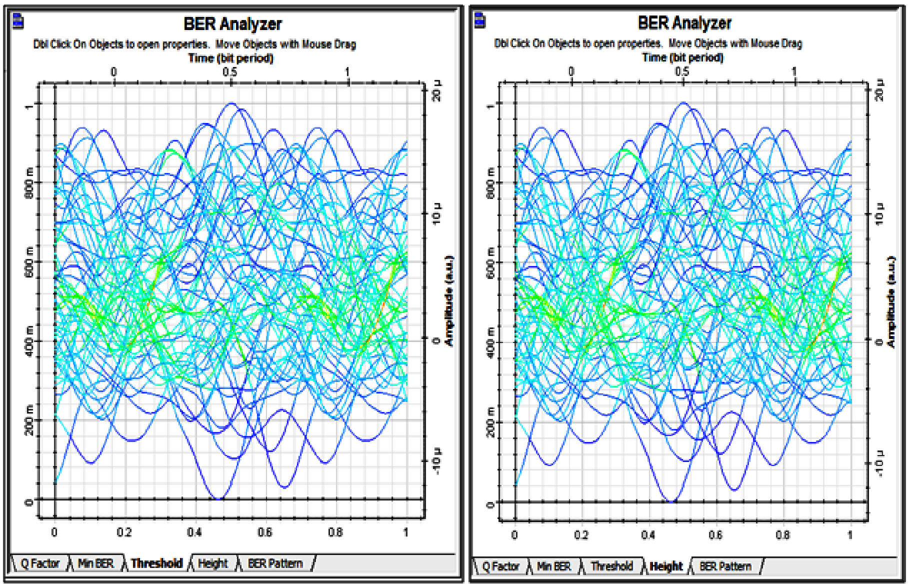

Figure 4.32: FP,Threshold and eye height(L=40Km,α=0.5dB/Km,P_in=0dBm)

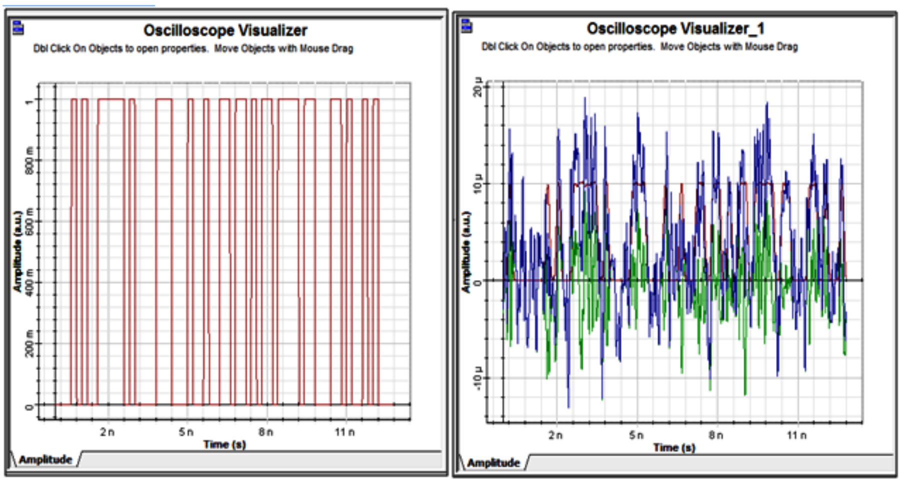

Figure 4.33: FP,Input and output signals(L=40Km,α=0.5dB/Km,P_in=0dBm)

4.2.1.3 Effect Of Input Power

In this case the following parameters are taken to see the effect of Input power.

- Attenuation coefficient: 0.3 dB/Km
- Fiber length: 40 Km

Figure 4.34, Figure 4.35, and Figure 4.36, show the system performance parameters when the Input power is equal to 0dBm. Next, the Input power is equal to 2dBm and the performance is shown in Figure 4.37, Figure 4.38, and Figure 4.39. Next, the Input power is equal to 5dBm and the performance is shown in Figure 4.40, Figure 4.41, and Figure 4.42. Next, the Input power is equal to 7dBm and the performance is shown in Figure 4.43, Figure 4.44, and Figure 4.45. Finally, the Input power is equal to 9dBm and the performance is shown in Figure 4.46, Figure 4.47, and Figure 4.48. The figures are presented in the next pages, which is shown that in the case of an input power 9 dBm (Highest Performance) a clearly output signal and open eye in the diagram also shown maximum Q-factor, Eye Height, Threshold and minimum BER. The performance gradually degraded until reach an input power 0 dBm (Lowest Performance), which is shown that a noisy output signal and closed eye in the diagram also shown minimum Q-factor, Eye Height, Threshold and maximum BER.

The following table, Tables 4.3 concluded the presents a summary of the results obtained from Figure 4.19 to Figure 4.33

Table 4.3: FP,Evaluation(L=40Km,α=0.3dB/Km,P_in=0 to 9dBm)

Input Power (dBm)	Max .Q-Factor	Min. BER	Eye Height	Threshold
0	5	6e-008	2.5e-005	2e-005
2	7	6e-013	5e-005	3e-005
5	10	2e-022	13e-005	4e-005
7	11	5e-029	21e-005	5e-005
9	12	7e-032	34e-005	6e-005

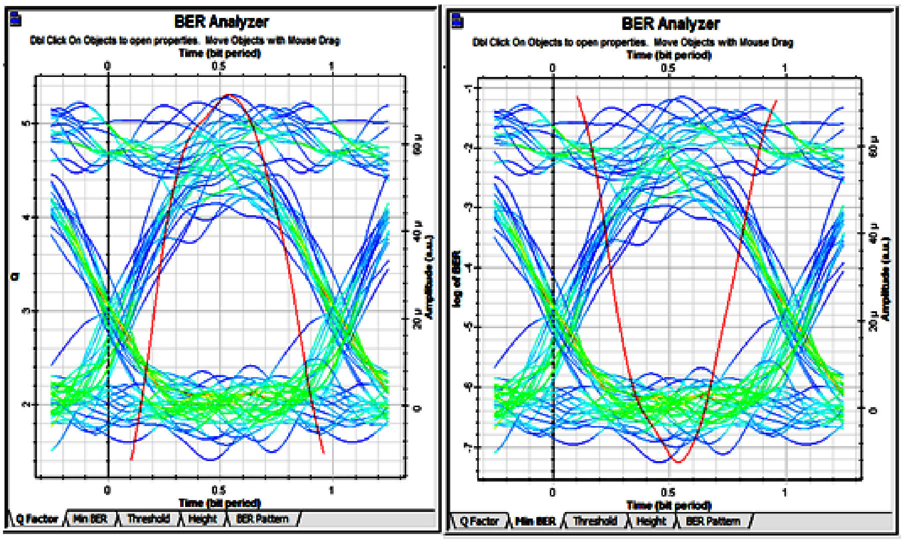

Figure 4.34: FP,Q-factor and BER(L=40Km,α=0.3dB/Km,P_in=0dBm)

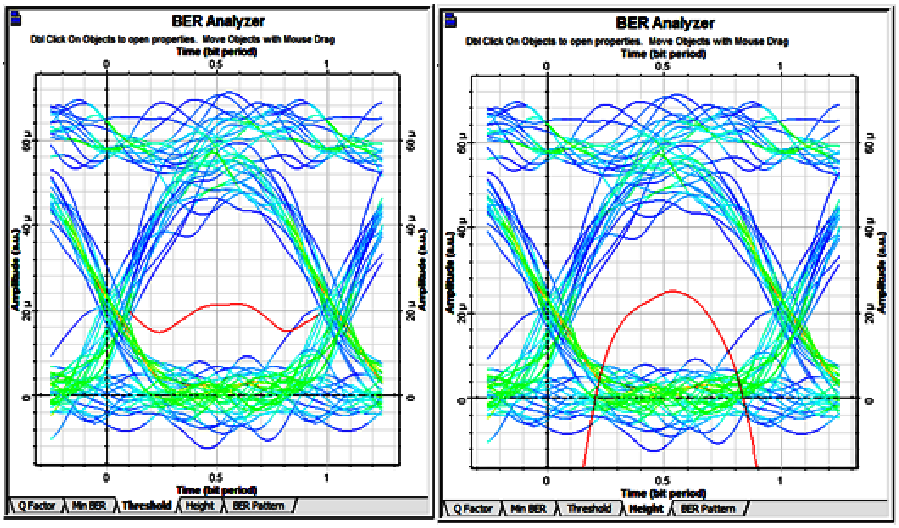

Figure 4.35: FP,Threshold and eye height(L=40Km,α=0.3dB/Km,P_in=0dBm)

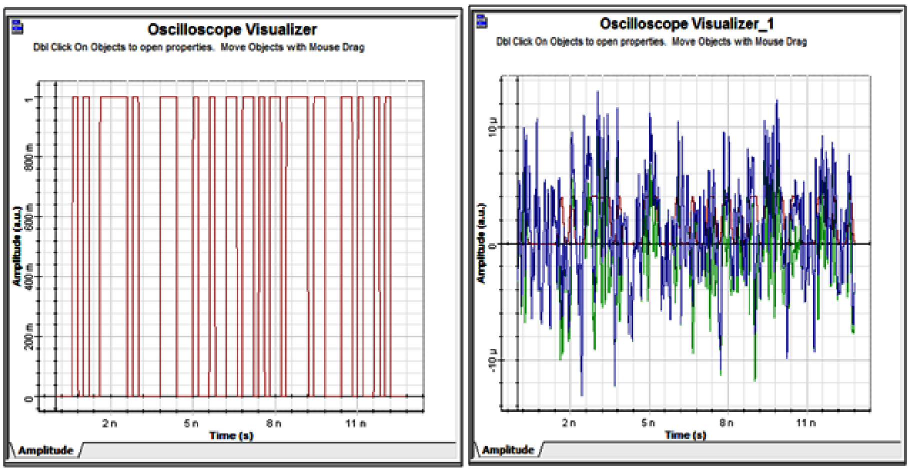

Figure 4.36: FP,Input and output signals(L=40Km,α=0.3dB/Km,P_in=0dBm)

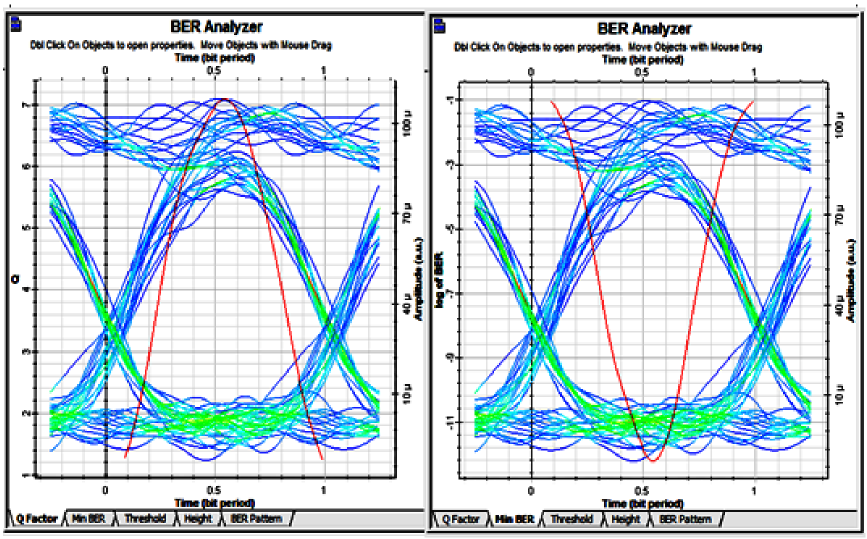

Figure 4.37: FP,Q-factor and BER(L=40Km,α=0.3dB/Km,P_in=2dBm)

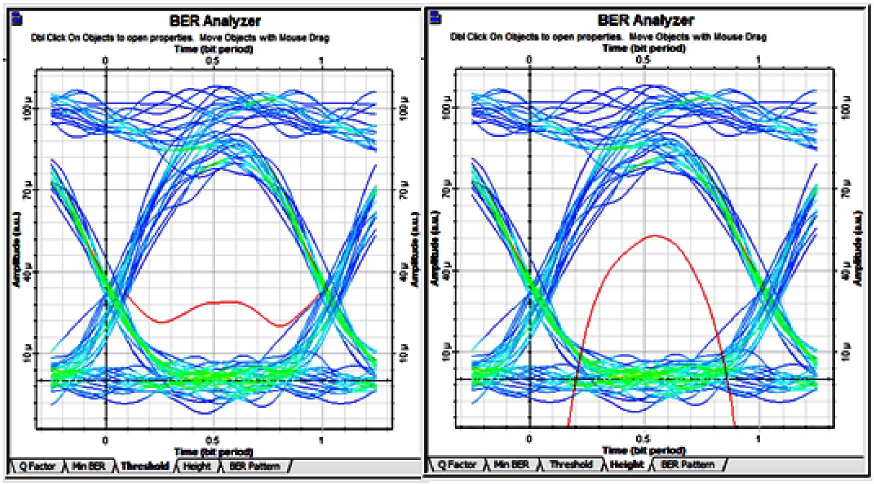

Figure 4.38: FP,Threshold and eye height(L=40Km,α=0.3dB/Km,P_in=2dBm)

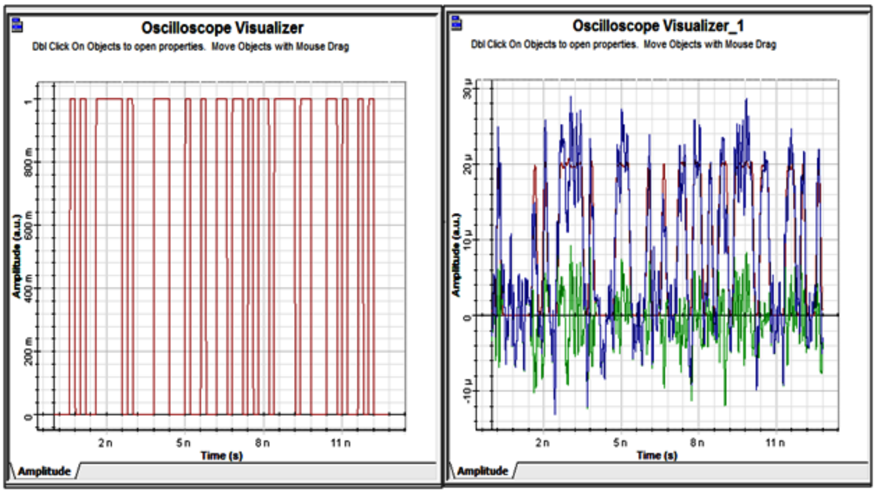

Figure 4.39: FP,Input and output signals(L=40Km,α=0.3dB/Km,P_in=2dBm)

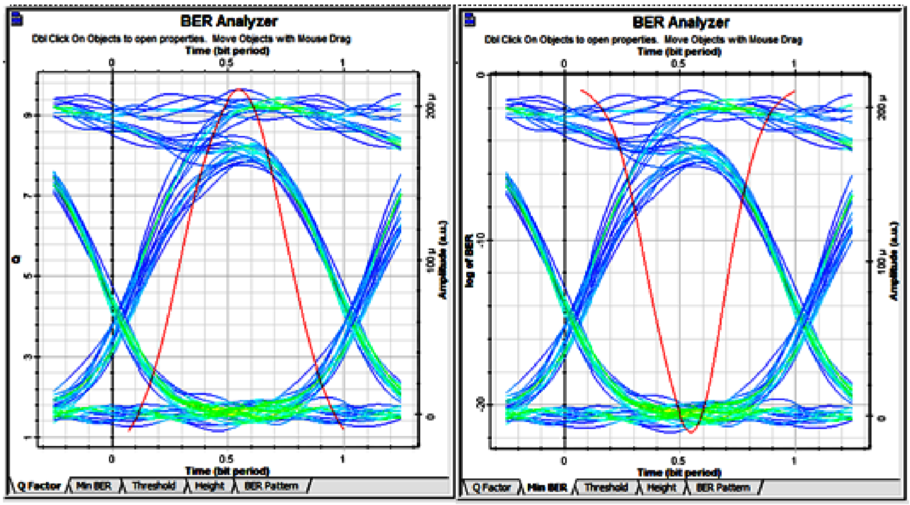

Figure 4.40: FP,Q-factor and BER(L=40Km,α=0.3dB/Km,P_in=5dBm)

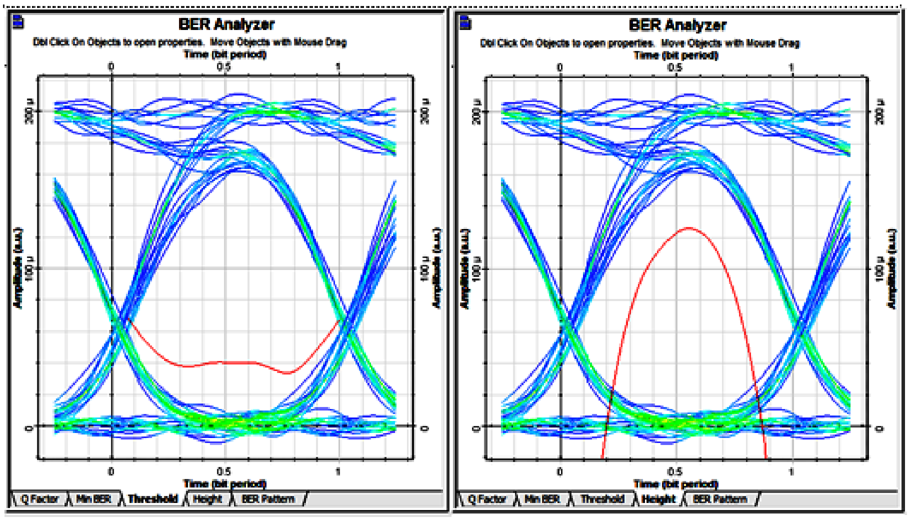

Figure 4.41: FP,Threshold and eye height(L=40Km,α=0.3dB/Km,P_in=5dBm)

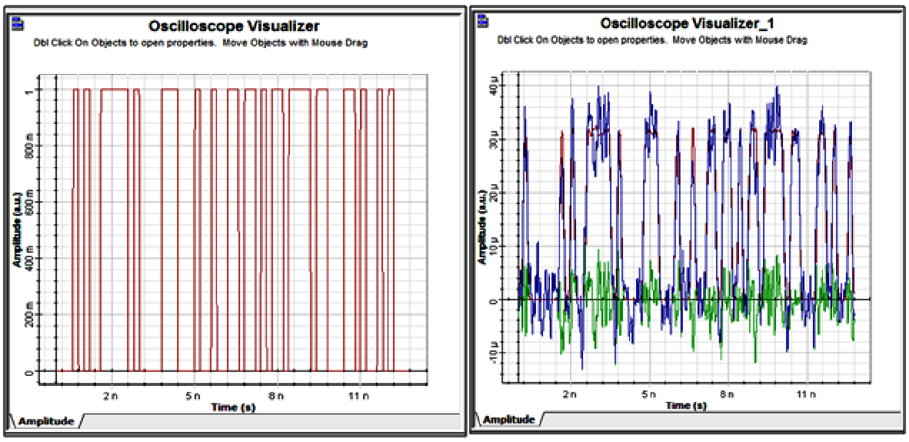

Figure 4.42: FP,Input and output signals(L=40Km,α=0.3dB/Km,P_in=5dBm)

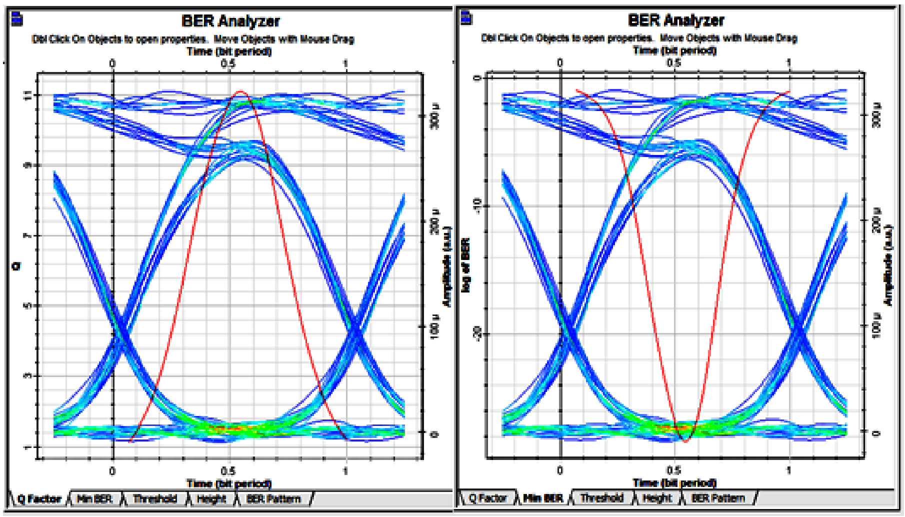

Figure 4.43: FP,Q-factor and BER(L=40Km,α=0.3dB/Km,P_in=7dBm)

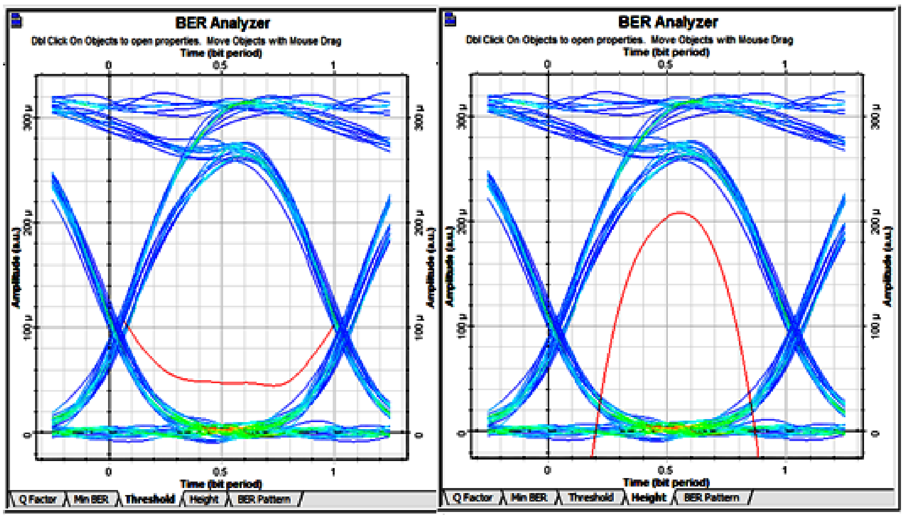

Figure 4.44: FP,Threshold and eye height(L=40Km,α=0.3dB/Km,P_in=7dBm)

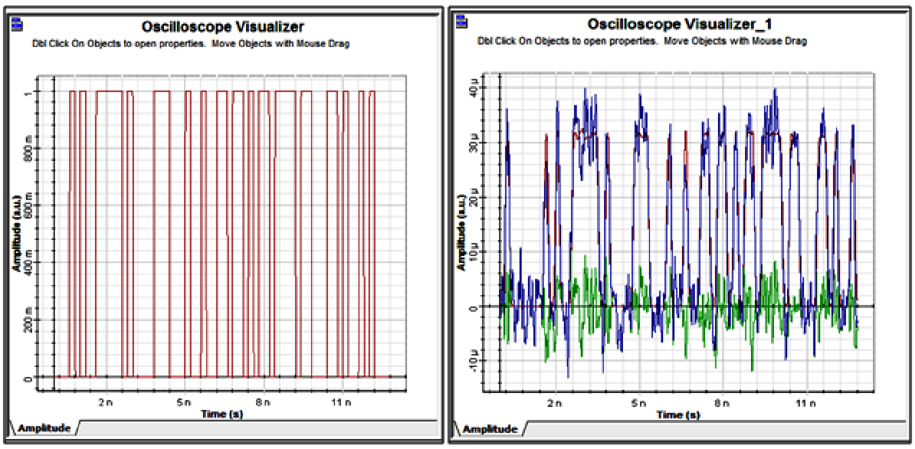

Figure 4.45: FP,Input and output signals(L=40Km,α=0.3dB/Km,P_in=7dBm)

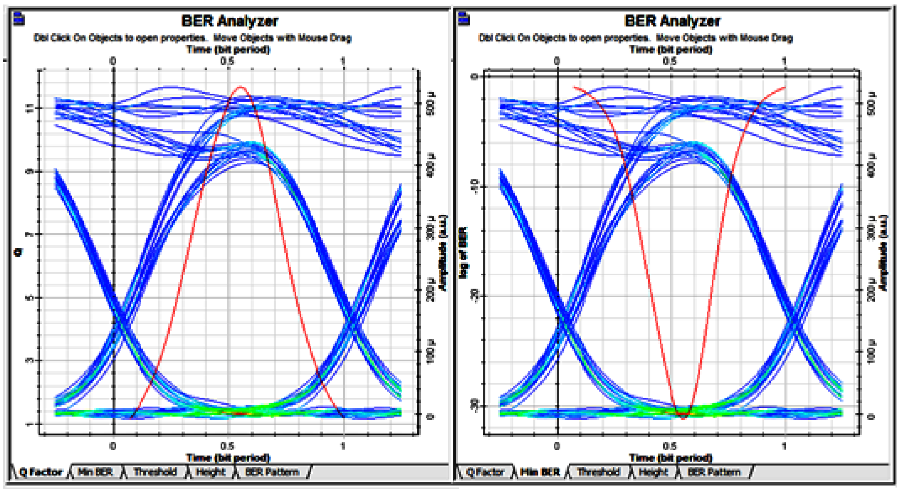

Figure 4.46: FP,Q-factor and BER(L=40Km,α=0.3dB/Km,P_in=9dBm)

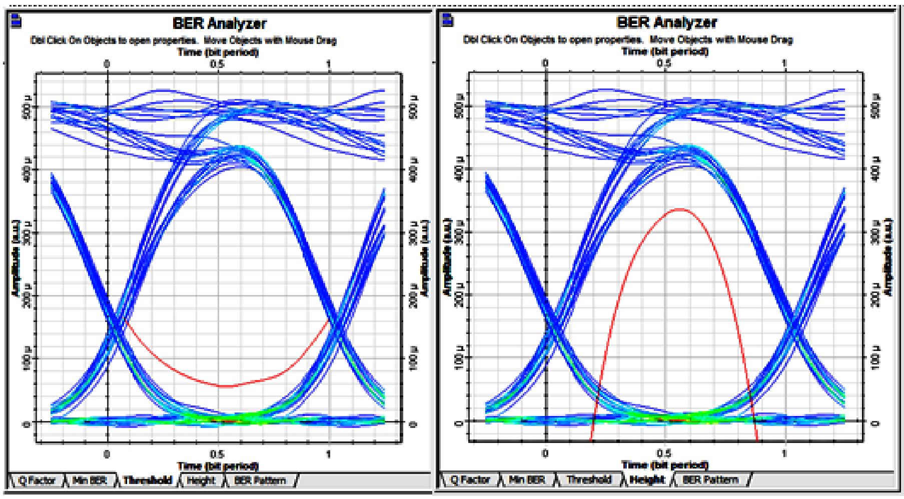

Figure 4.47: FP,Threshold and eye height(L=40Km,α=0.3dB/Km,P_in=9dBm)

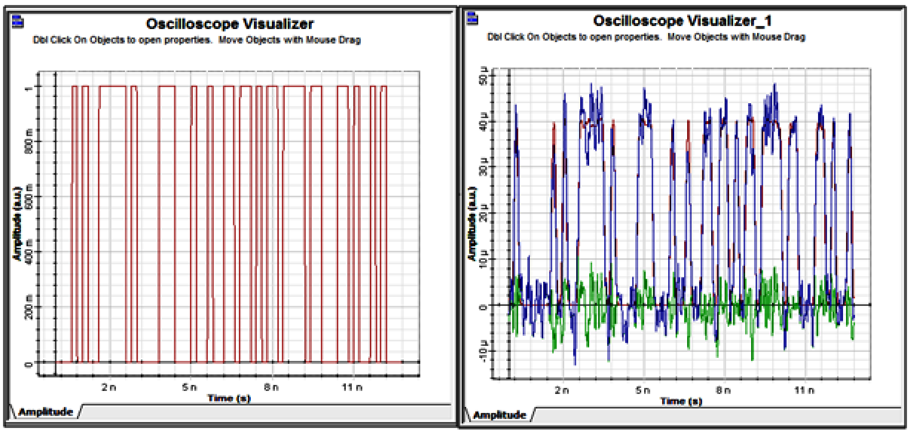

Figure 4.48: FP,Input and output signals(L=40Km,α=0.3dB/Km,P_in=9dBm)

4.2.2 Performance Analysis With a Mach-Zehnder Tunable Filter

The initial Mach-Zehnder optical filter properties as follow:

- Delay: 0 s
- Coupling coefficient: 0.5
- Additional loss: 0 dB

4.2.2.1 Effect Of Fiber Length

In this case the following parameters are taken to see the effect of fiber length.

- Input power: 0 dBm
- Attenuation coefficient: 0.1 dB/Km

Figure 4.50, Figure 4.51, and Figure 4.52, show the system performance parameters when the fiber length is equal to 40 Km. Next, the fiber length is equal to 80 Km. and the performance is shown in Figure 4.53, Figure 4.54, and Figure 4.55. Next, the fiber length is equal to 120 Km. and the performance is shown in Figure 4.56, Figure 4.57, and Figure 4.58. Next, the fiber length is equal to 160 Km. and the performance is shown in Figure 4.59, Figure 4.60, and Figure 4.61. Finally, the fiber length is equal to 200 Km. and the performance is shown in Figure 4.62, Figure 4.63, and Figure 4.64. The figures are presented in the next pages, which is shown that in the case of fiber length 40 Km (Highest Performance) a clearly output signal and open eye in the diagram also shown maximum Q-factor, Eye Height, Threshold and minimum BER. The performance gradually degraded until reach fiber length 200 Km (Lowest Performance), which is shown that a noisy output signal and closed eye in the diagram also shown minimum Q-factor, Eye Height, Threshold and maximum BER.

The following table, Tables 4.4 concluded the presents a summary of the results obtained from Figure 4.50 to Figure 4.56

Table 4.4: MZ,Evaluation(L=40 to 200Km,α=0.1dB/Km,P_in=0dBm)

Length (Km)	Max .Q-Factor	Min. BER	Eye Height	Threshold
40	39	0	4e-004	2e-004
80	19	1e-084	13e-005	7.3e-005
120	8	3e-014	4e-005	3e-005
160	3.3	5e-004	2e-006	1.2e-005
200	0	1	0	0

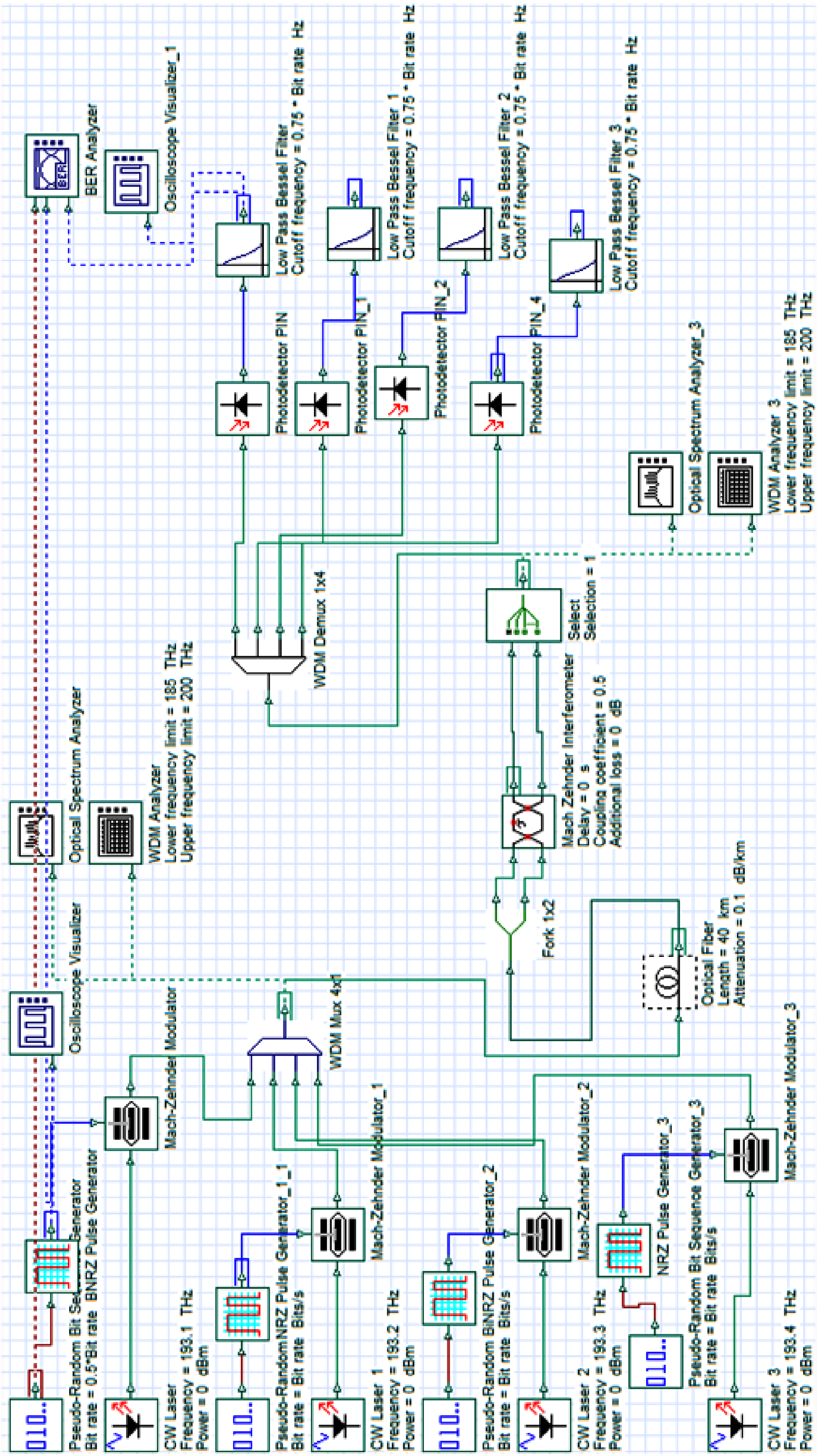

Figure 4.49: The system with MZ filter and Length=40Km

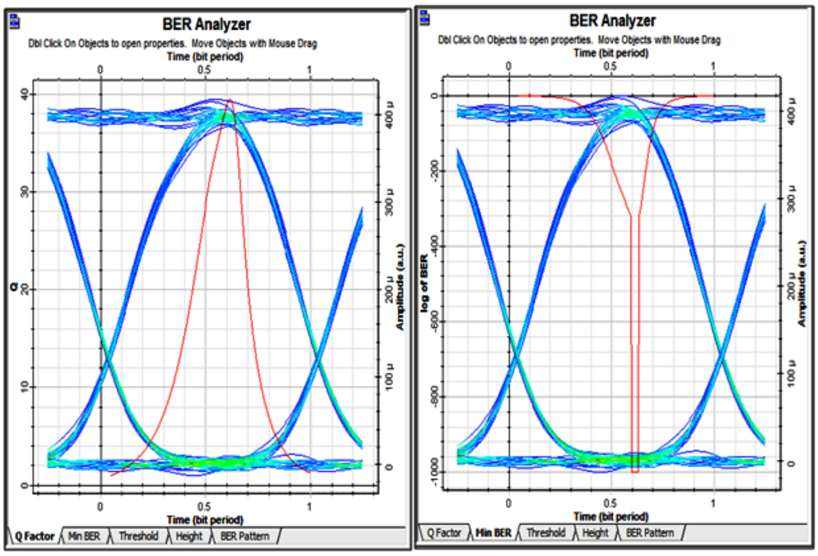

Figure 4.50: MZ,Q-factor and BER(L=40Km,α=0.1dB/Km,P_{in}=0dBm)

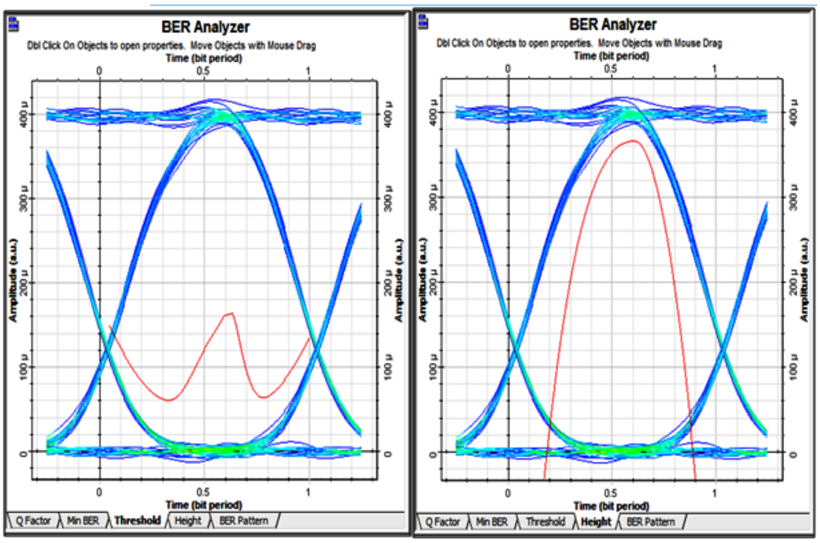

Figure 4.51: MZ, Threshold & eye height (L = 40Km, α = 0.1dB/Km, P_{in} = 0dBm)

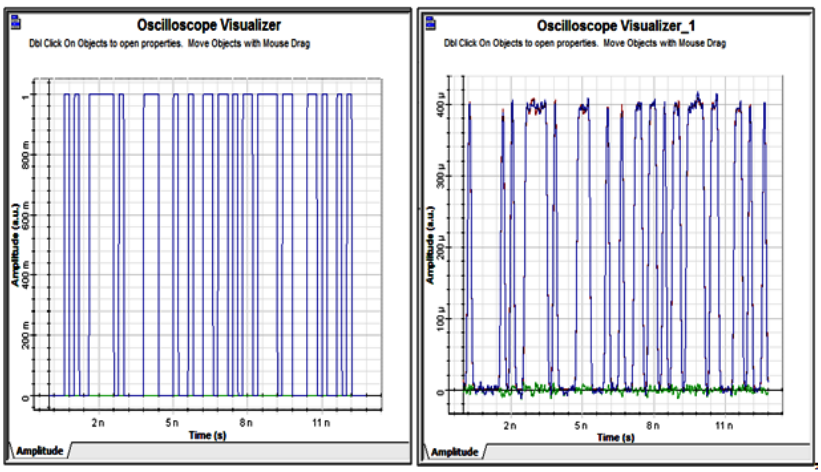

Figure 4.52: MZ, Input & output signals (L = 40Km,α = 0.1dB/Km, P_{in} = 0dBm)

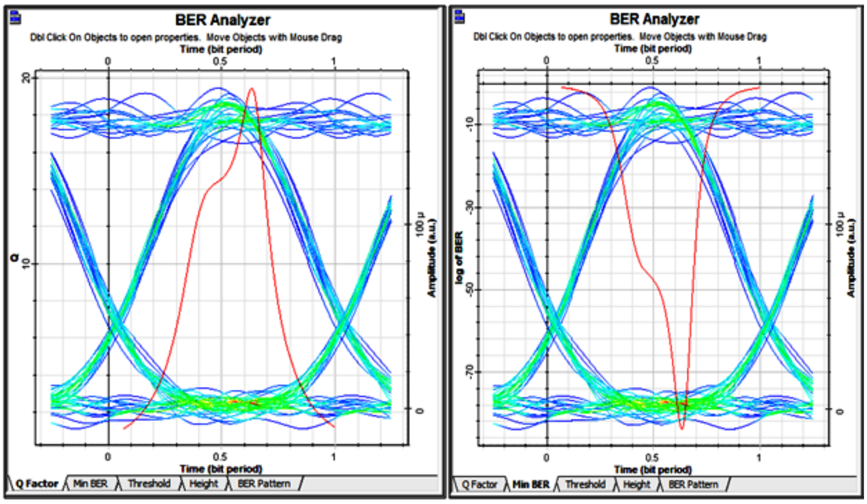

Figure 4.53: MZ,Q-factor and BER ($L = 80$Km, $\alpha = 0.1$dB/Km, $P_{in} = 0$dBm)

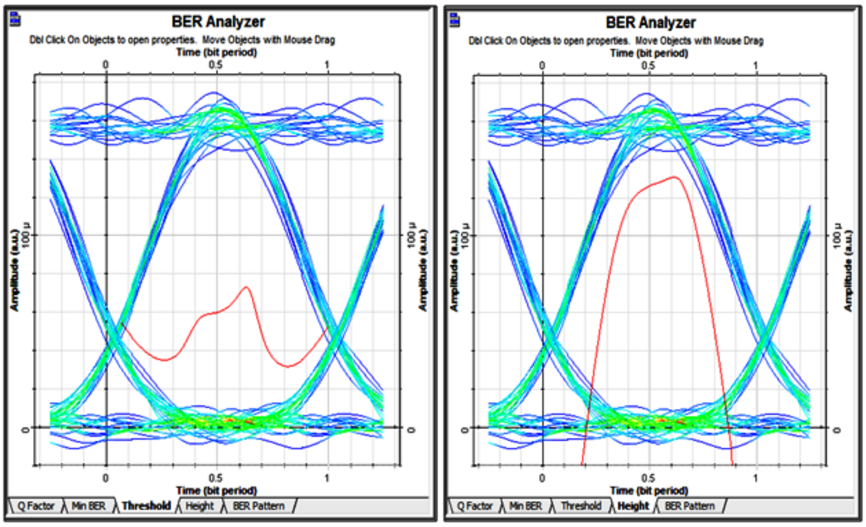

Figure 4.54: MZ,Threshold and eye height ($L = 80$Km, $\alpha = 0.1$dB/Km, $P_{in} = 0$dBm)

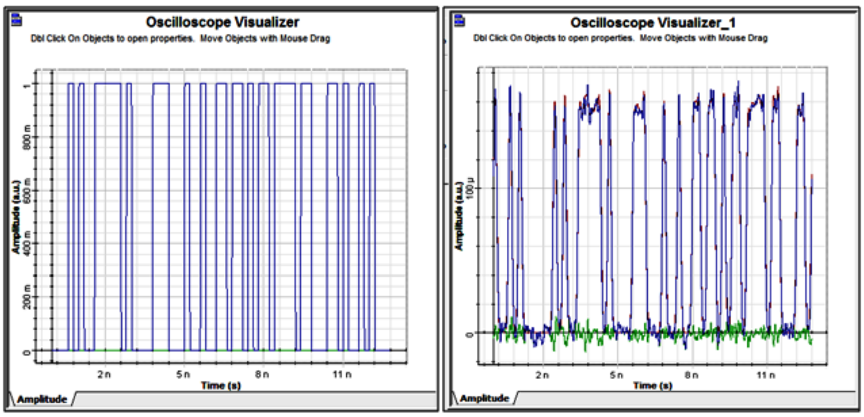

Figure 4.55: MZ,Input and output signals ($L = 80$Km,$\alpha = 0.1$dB/Km,$P_{in} = 0$dBm)

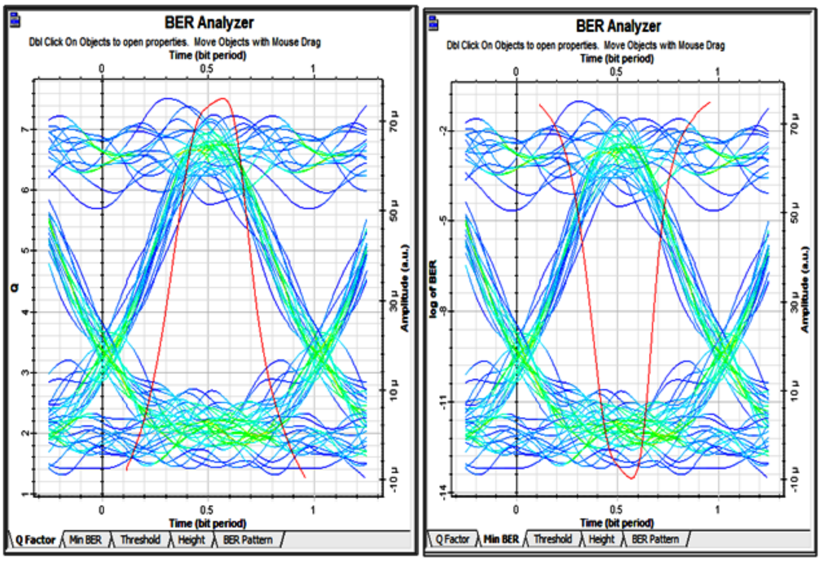

Figure 4.56: MZ,Q-factor and BER(L=120Km,α=0.1dB/Km,P_in=0dBm)

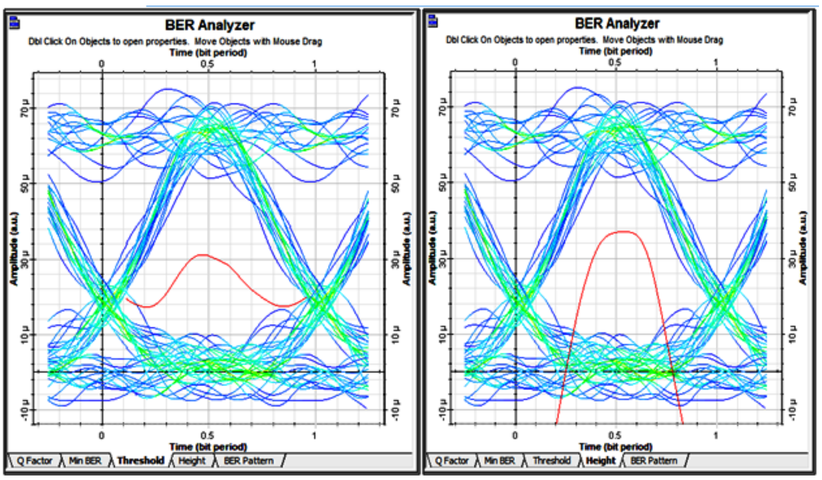

Figure 4.57: MZ,Threshold and eye height (L=120Km,α=0.1dB/Km,P_in=0dBm)

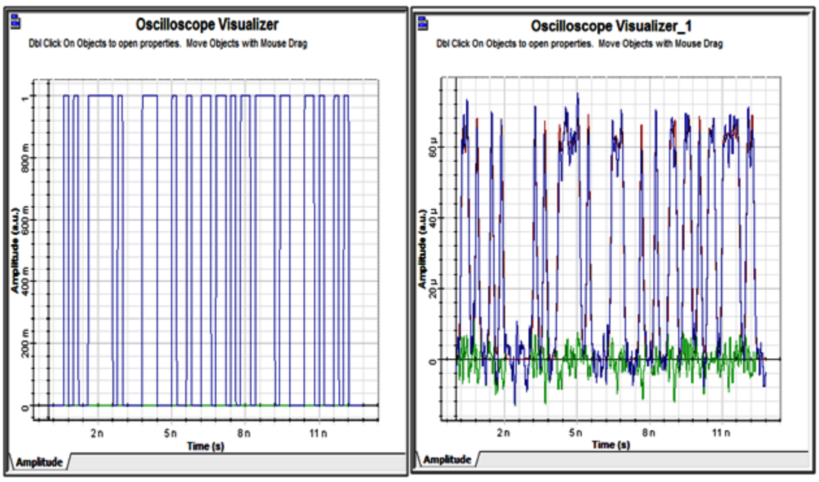

Figure 4.58: MZ,Input and output signals (L=120Km,α=0.1dB/Km,P_in=0dBm)

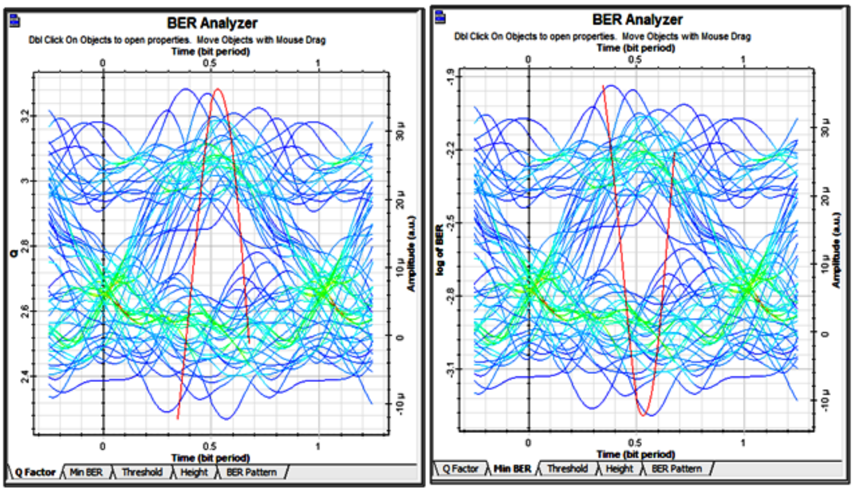

Figure 4.59: MZ,Q-factor and BER (L=160Km,α=0.1dB/Km,P_in=0dBm)

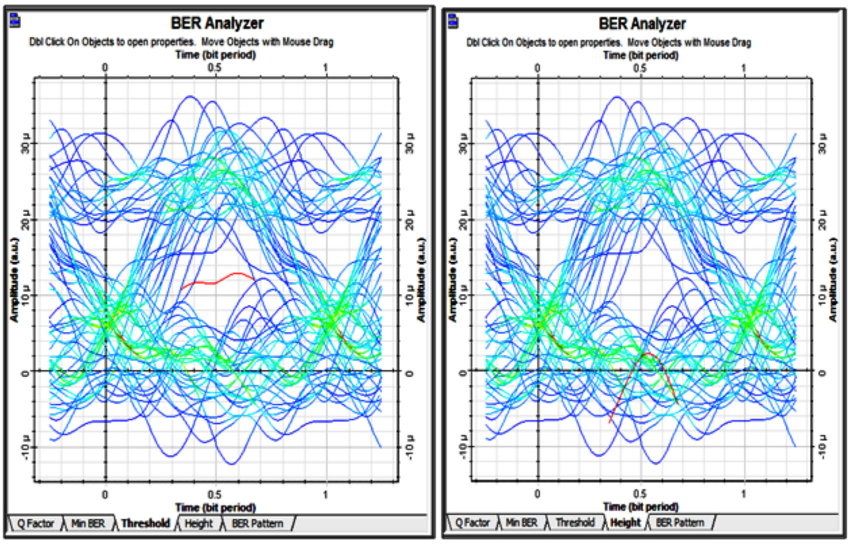

Figure 4.60: MZ,Threshold and eye height (L=160Km,α=0.1dB/Km,P_in=0dBm)

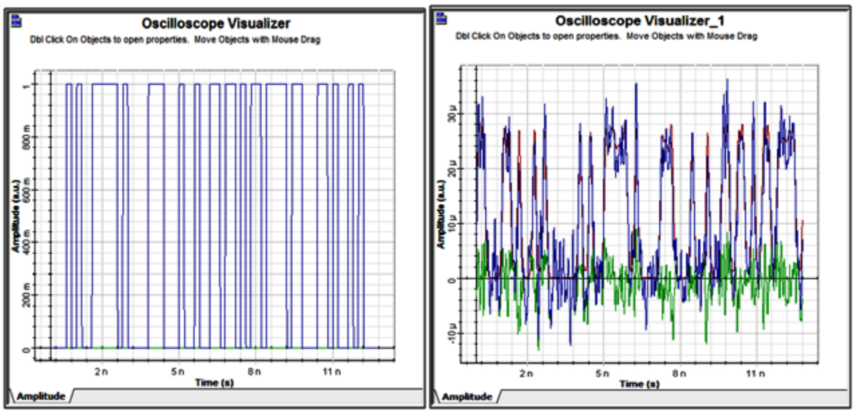

Figure 4.61: MZ,Input and output signals (L=160Km,α=0.1dB/Km,P_in=0dBm)

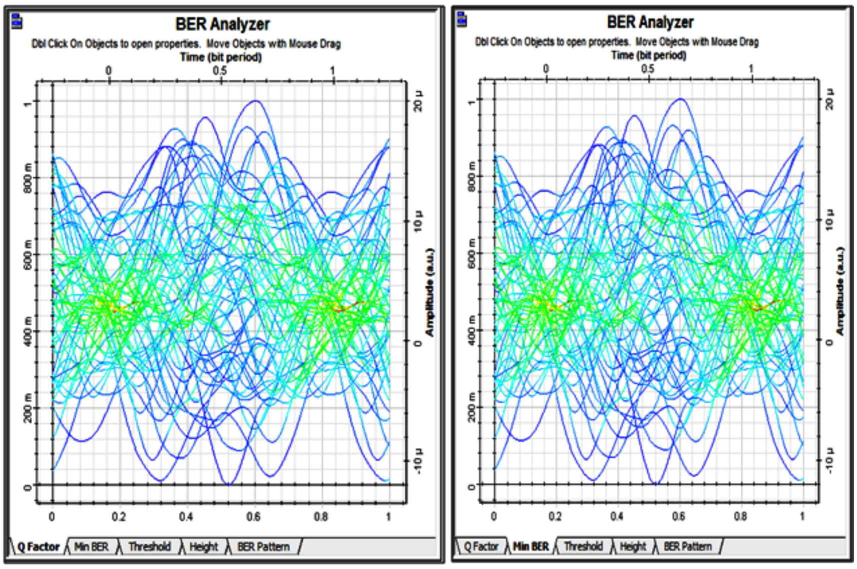

Figure 4.62: MZ,Q-factor and BER(L=200Km,α=0.1dB/Km,P_in=0dBm)

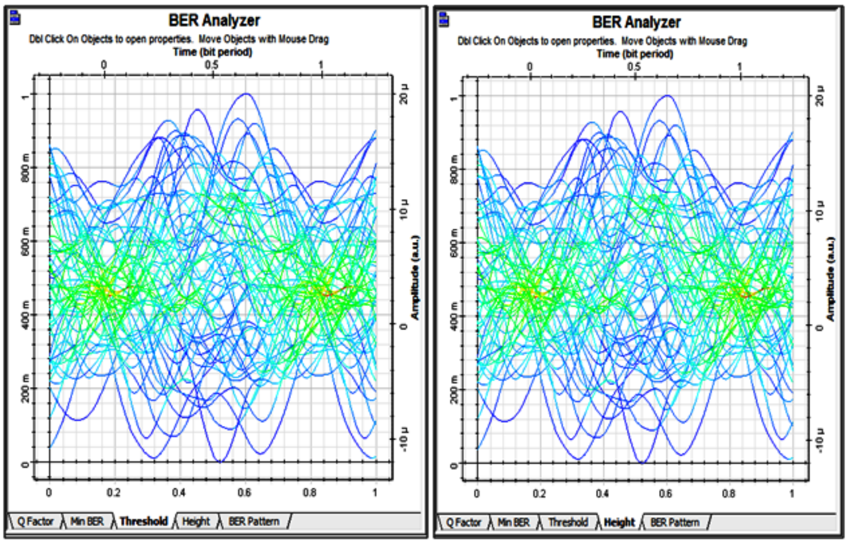

Figure 4.63: MZ,Threshold and eye height(L=200Km,α=0.1dB/Km,P_in=0dBm)

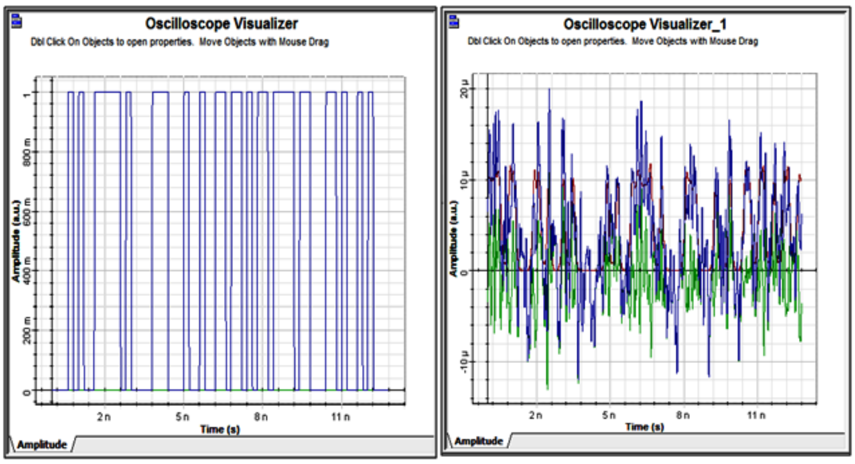

Figure 4.64: MZ,Input and output signals(L=200Km,α=0.1dB/Km,P_in=0dBm)

4.2.2.2 Effect of Attenuation Coefficient

In this case the following parameters are taken to see the effect of fiber attenuation coefficient.

- Input power: 0 dBm
- Fiber length: 40 Km

Figure 4.66, Figure 4.67, and Figure 4.68, show the system performance parameters when the fiber attenuation coefficient is equal to 0.1 dB/Km. Next, the attenuation is set to 0.2 dB/Km and the performance is shown in Figure 4.69, Figure 4.70, and Figure 4.71. Next, the attenuation is set to 0.3 dB/Km and the performance is shown in Figure 4.72, Figure 4.73, and Figure 4.74. Next, the attenuation is set to 0.4 dB/Km and the performance is shown in Figure 4.75, Figure 4.76, and Figure 4.77. Finally, the attenuation is set to 0.5 dB/Km and the performance is shown in Figure 4.78, Figure 4.79, and Figure 4.80. The figures are presented in the next pages, which is shown that in the case of an attenuation 0.1 dB/Km (Highest Performance) a clearly output signal and open eye in the diagram also shown maximum Q-factor, Eye Height, Threshold and minimum BER. The performance gradually degraded until reach an attenuation 0.5 dB/Km (Lowest Performance), which is shown that a noisy output signal and closed eye in the diagram also shown minimum Q-factor, Eye Height, Threshold and maximum BER.

The following table, Tables 4.5 concluded the presents a summary of the results obtained from Figure 4.66 to Figure 4.80

Table 4.5: MZ,Evaluation(L=40Km,α=0.1 to 0.5dB/Km,P_in=0dBm)

Attenuation (dB/Km)	Max .Q-Factor	Min. BER	Eye Height	Threshold
0.1	39	0	4e-004	2e-004
0.2	19	2e-080	13e-005	8e-005
0.3	8	2e-014	4e-005	3e-005
0.4	3.1	11e-004	6e-007	1.2e-005
0.5	0	1	0	0

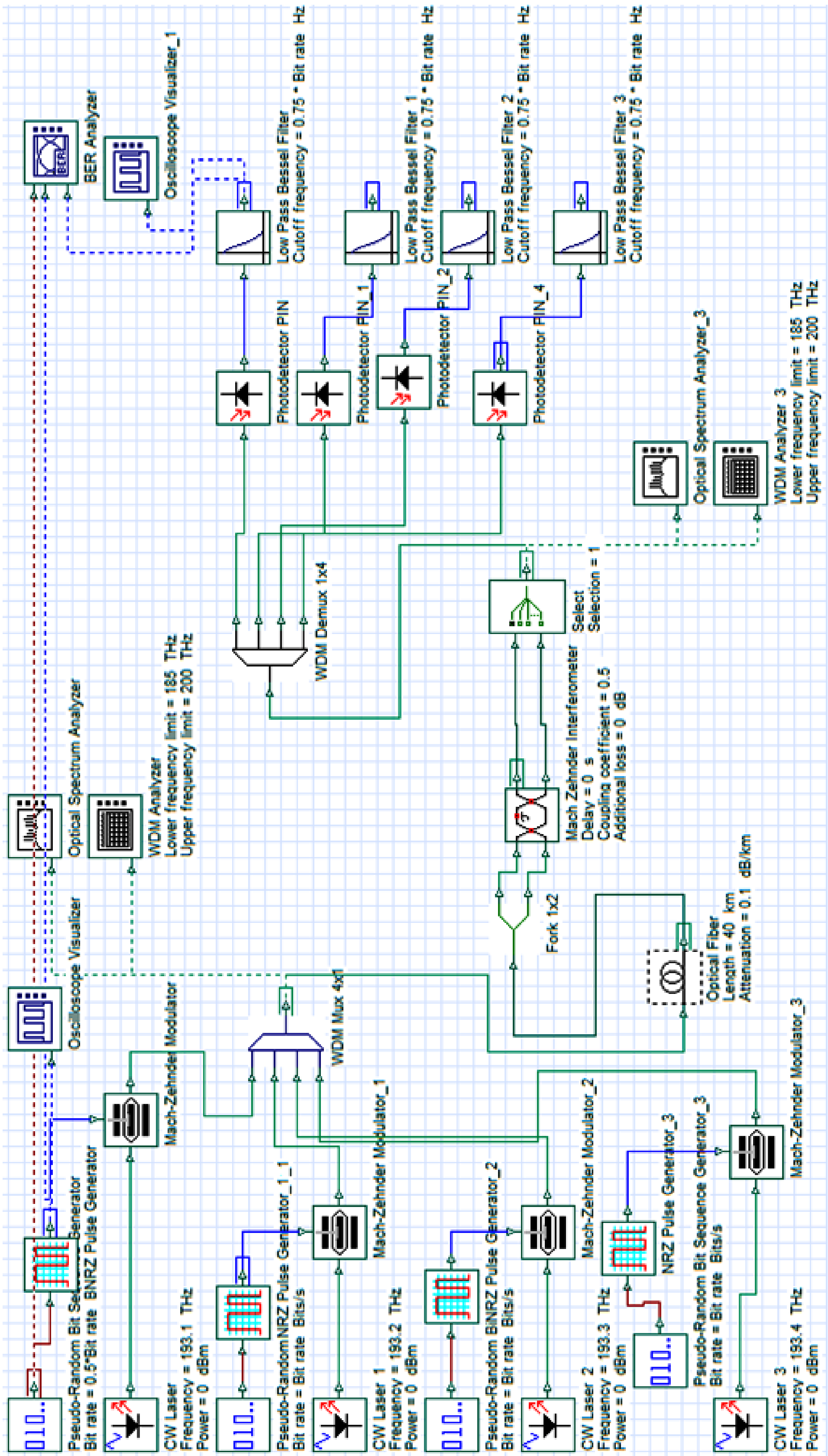

Figure 4.65: The system with MZ filter and Attenuation=0.1dB/Km

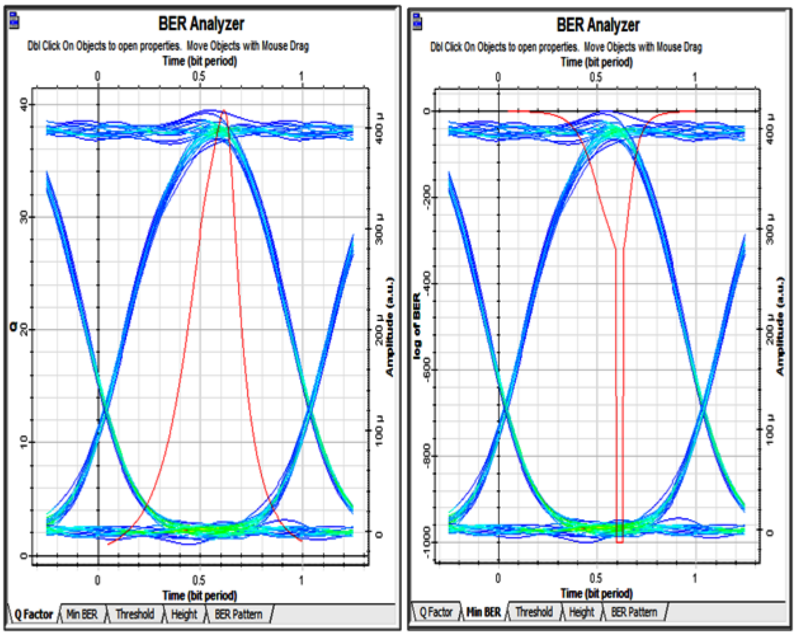

Figure 4.66: MZ,Q-factor and BER(L=40Km,α=0.1dB/Km,P_in=0dBm)

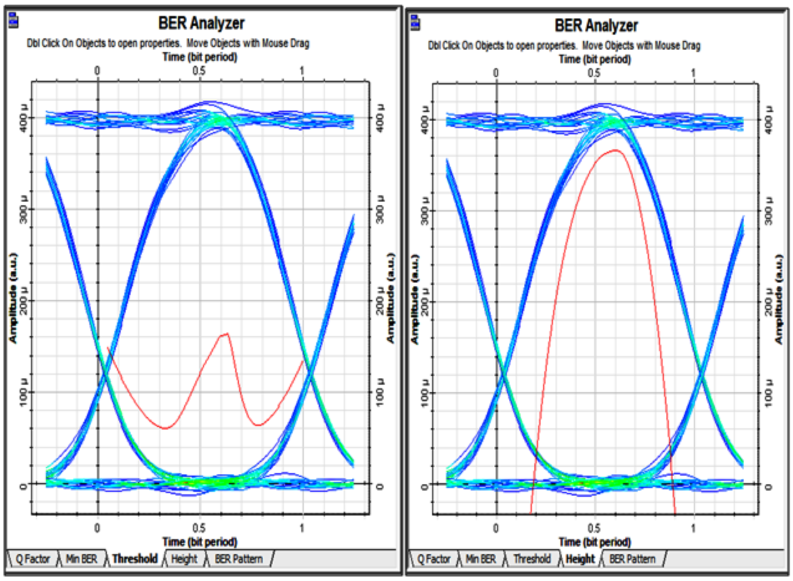

Figure 4.67: MZ,Threshold and eye height(L=40Km,α=0.1dB/Km,P_in=0dBm)

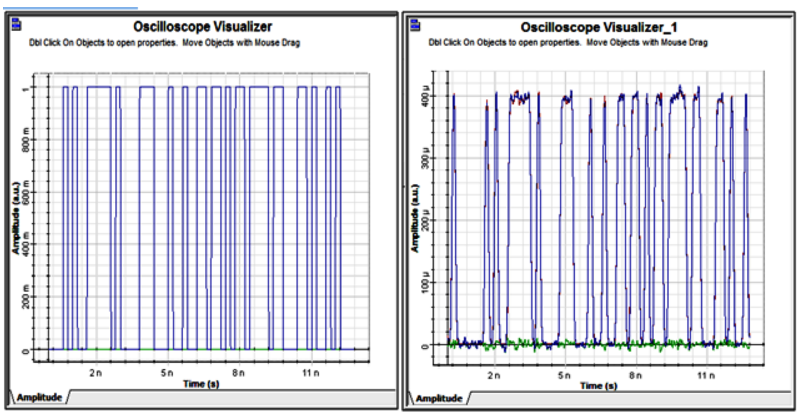

Figure 4.68: MZ,Input and output signals(L=40Km,α=0.1dB/Km,P_in=0dBm)

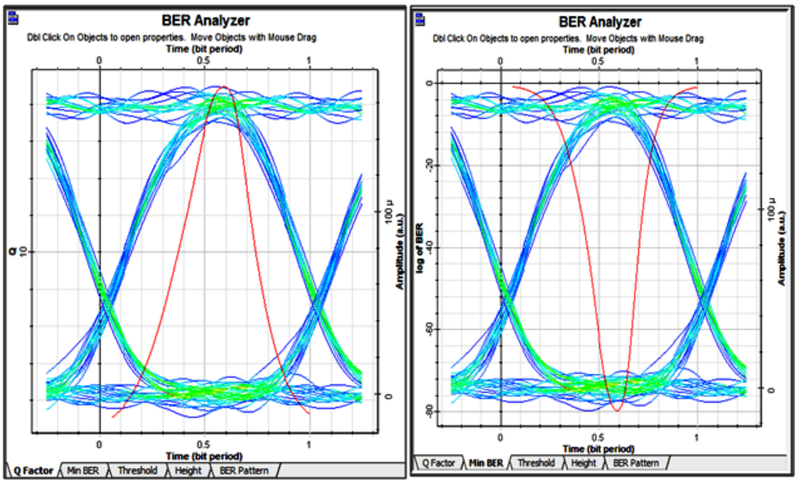

Figure 4.69: MZ,Q-factor and BER(L=40Km,α=0.2dB/Km,P_in=0dBm)

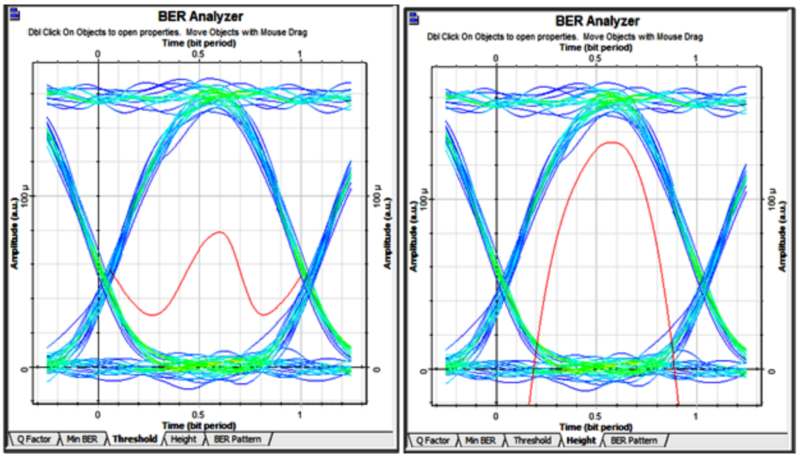

Figure 4.70: MZ,Threshold and eye height(L=40Km,α=0.2dB/Km,P_in=0dBm)

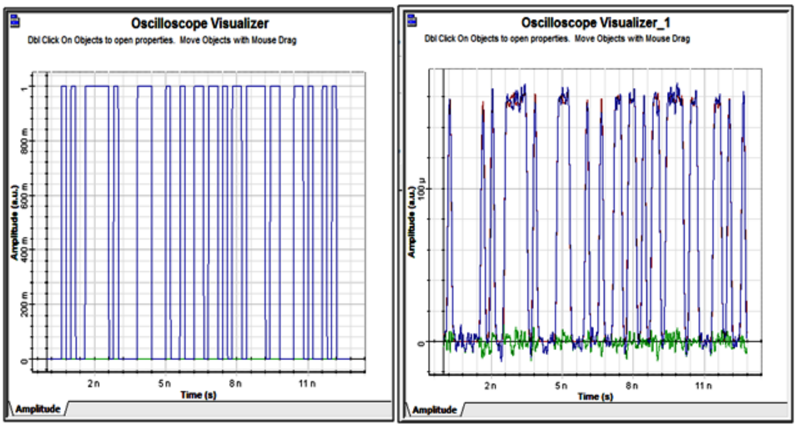

Figure 4.71: MZ,Input and output signals(L=40Km,α=0.2dB/Km,P_in=0dBm)

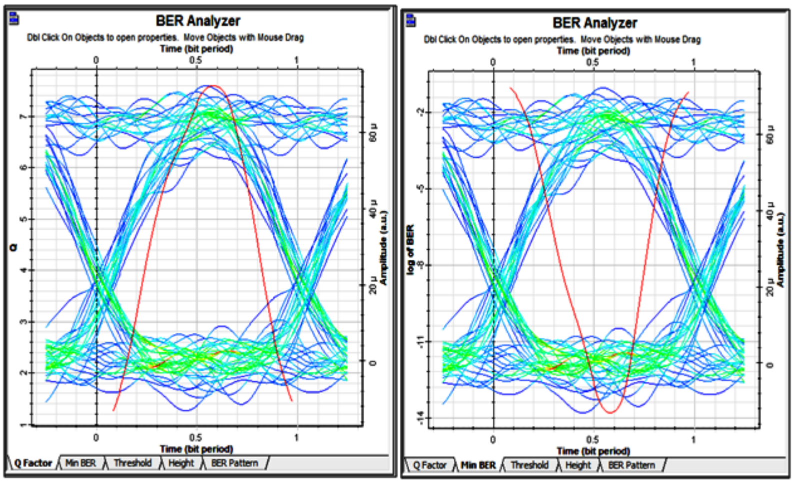

Figure 4.72: MZ,Q-factor and BER(L=40Km,α=0.3dB/Km,P_in=0dBm)

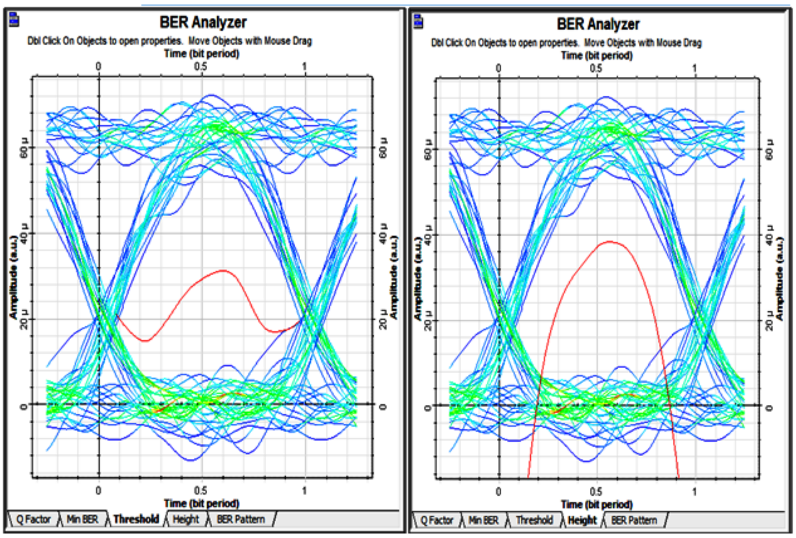

Figure 4.73: MZ,Threshold and eye height(L=40Km,α=0.3dB/Km,P_in=0dBm)

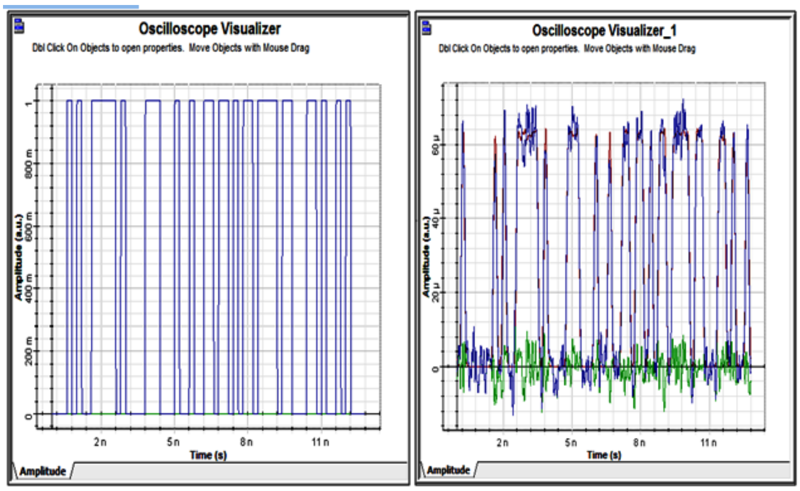

Figure 4.74: MZ,Input and output signals(L=40Km,α=0.3dB/Km,P_in=0dBm)

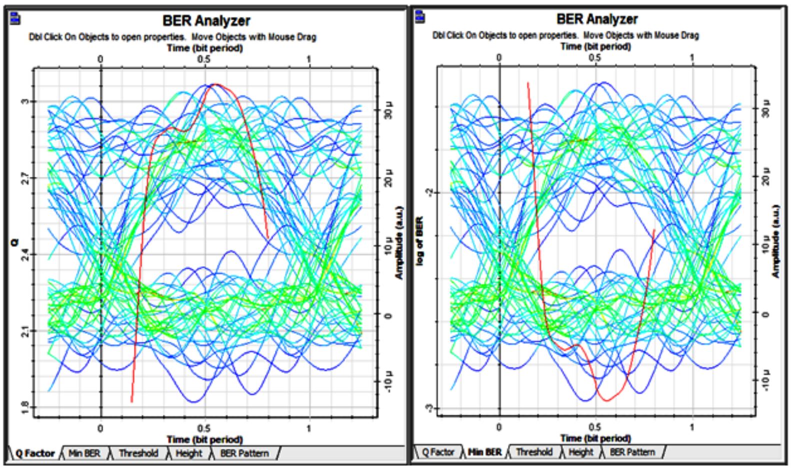

Figure 4.75: MZ,Q-factor and BER(L=40Km,α=0.4dB/Km,P_in=0dBm)

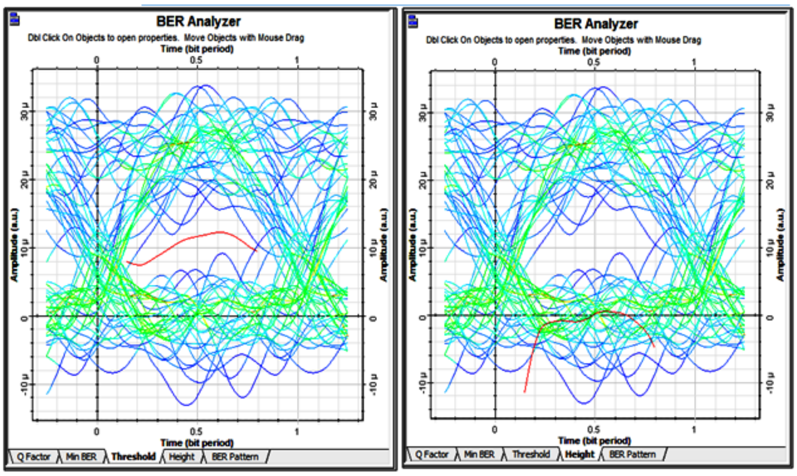

Figure 4.76: MZ,Threshold and eye height(L=40Km,α=0.4dB/Km,P_in=0dBm)

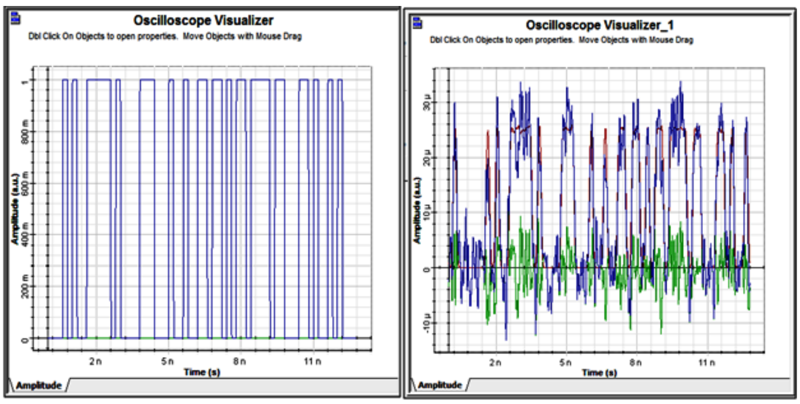

Figure 4.77: MZ,Input and output signals(L=40Km,α=0.4dB/Km,P_in=0dBm)

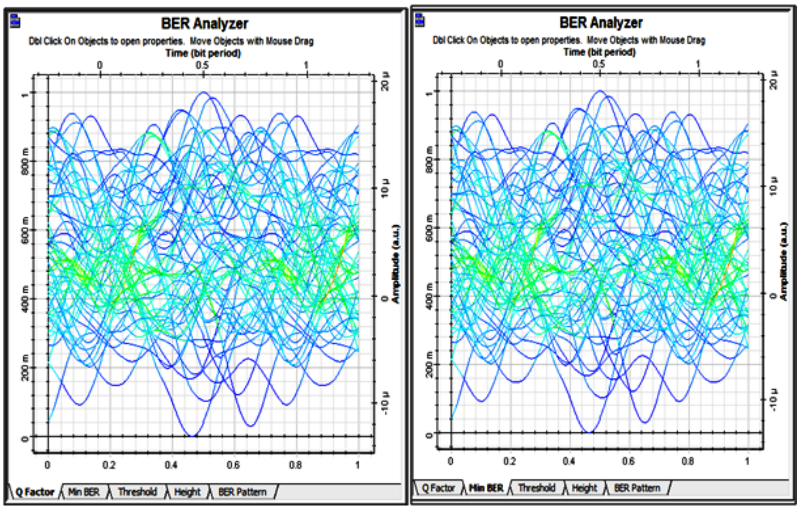

Figure 4.78: MZ,Q-factor and BER(L=40Km,α=0.5dB/Km,P_in=0dBm)

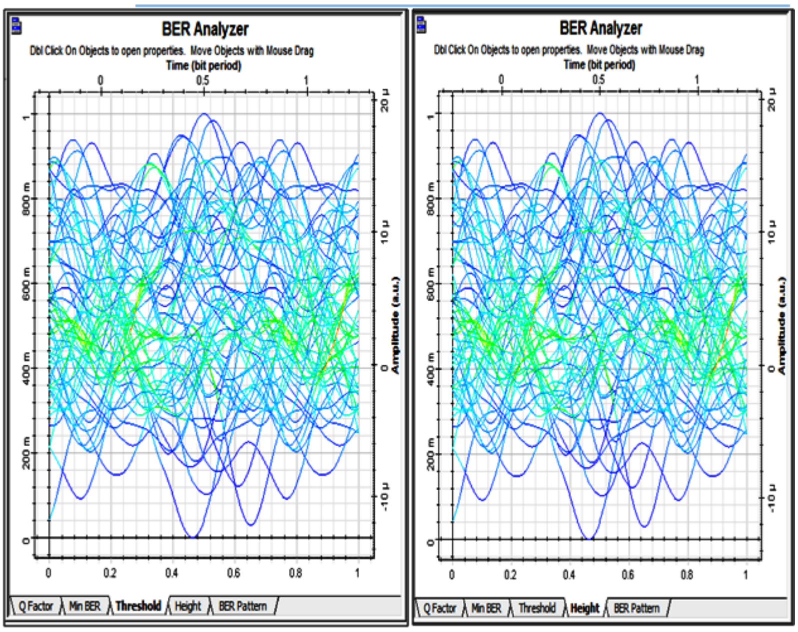

Figure 4.79: MZ,Threshold and eye height(L=40Km,α=0.5dB/Km,P_in=0dBm)

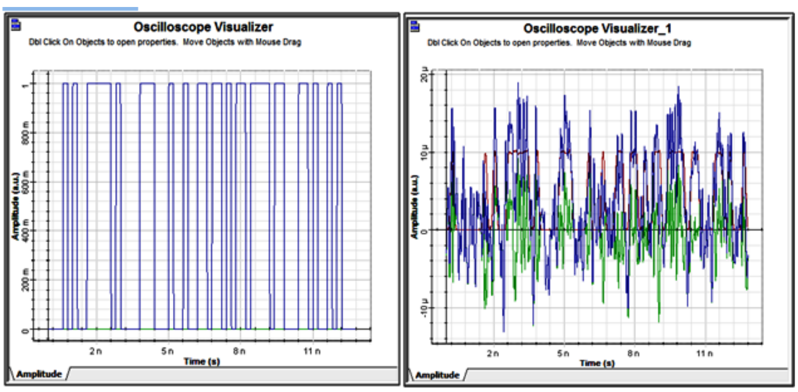

Figure 4.80: MZ,Input and output signals(L=40Km,α=0.5dB/Km,P_in=0dBm)

4.2.2.3 Effect Of Input Power

In this case the following parameters are taken to see the effect of Input power.

- Attenuation coefficient: 0.3 dB/Km
- Fiber length: 40 Km

Figure 4.82, Figure 4.83, and Figure 4.84, show the system performance parameters when the Input power is equal to 0dBm. Next, the Input power is equal to 2dBm and the performance is shown in Figure 4.85, Figure 4.86, and Figure 4.87. Next, the Input power is equal to 5dBm and the performance is shown in Figure 4.88, Figure 4.89, and Figure 4.90. Next, the Input power is equal to 7dBm and the performance is shown in Figure 4.91, Figure 4.92, and Figure 4.93. Finally, the Input power is equal to 9dBm and the performance is shown in Figure 4.94, Figure 4.95, and Figure 4.96. The figures are presented in the next pages, which is shown that in the case of an input power 9 dBm (Highest Performance) a clearly output signal and open eye in the diagram also shown maximum Q-factor, Eye Height, Threshold and minimum BER. The performance gradually degraded until reach an input power 0 dBm (Lowest Performance), which is shown that a noisy output signal and closed eye in the diagram also shown minimum Q-factor, Eye Height, Threshold and maximum BER.

The following table, Tables 4.6 concluded the presents a summary of the results obtained from Figure 4.82 to Figure 4.96

Table 4.6: MZ,Evaluation(L=40Km,α=0.3 dB/Km,$P_i n$=0 to 9dBm)

Input Power (dBm)	Max .Q-Factor	Min. BER	Eye Height	Threshold
0	8	2e-014	4e-005	3e-005
2	12	5e-035	8e-005	5e-005
5	22	2e-111	17e-005	9e-005
7	33	4e-241	29e-005	14e-005
9	36	2e-279	46e-005	15e-005

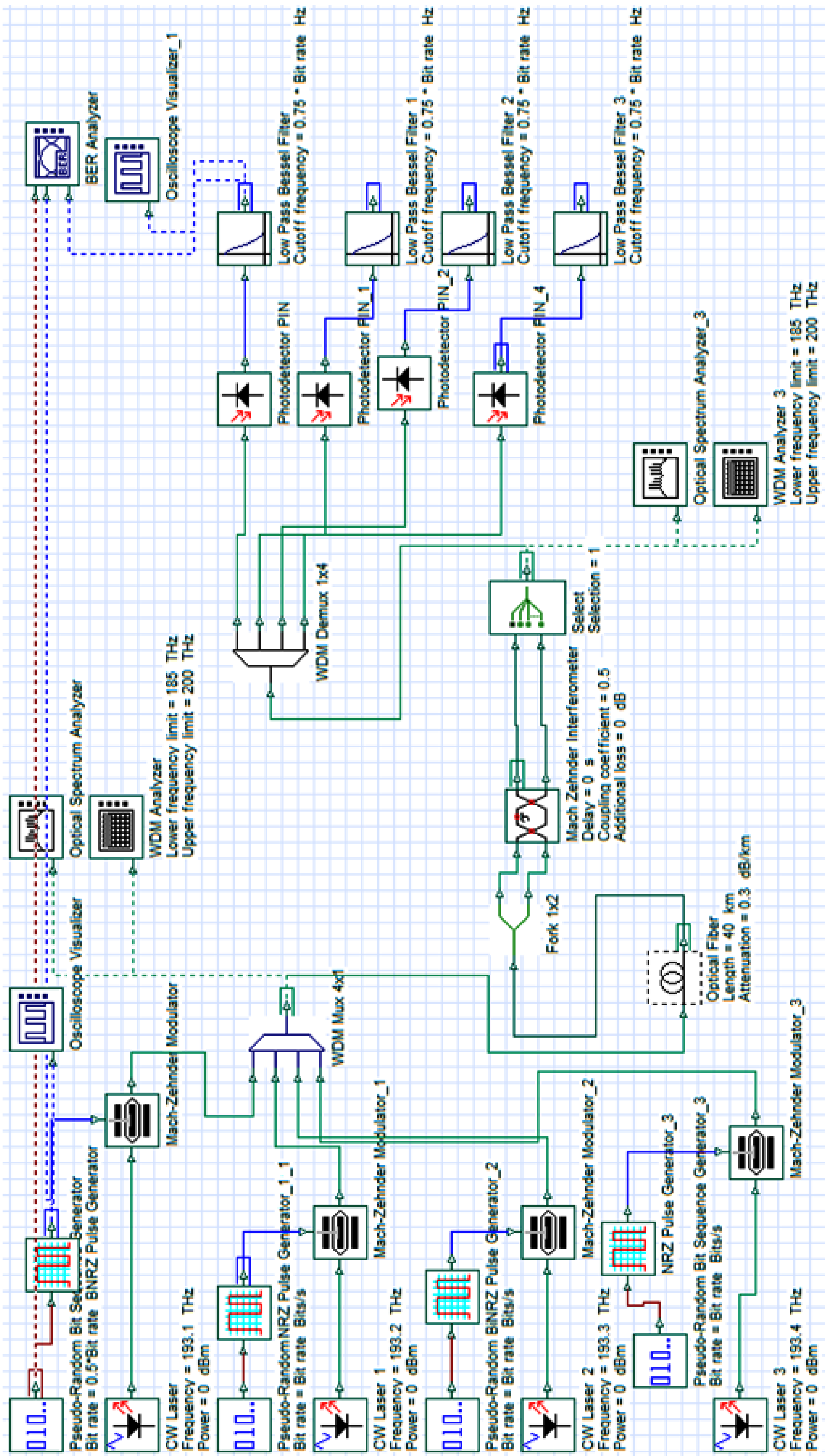

Figure 4.81: The system with MZ filter and Input Power=0dBm

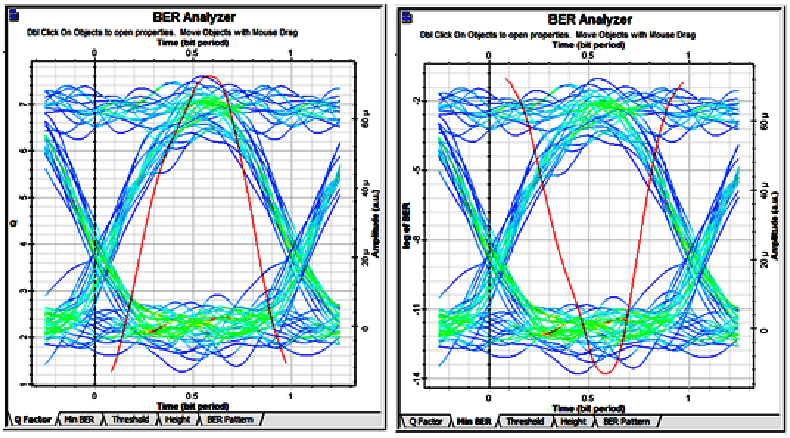

Figure 4.82: MZ,Q-factor and BER(L=40Km,α=0.3dB/Km,P_in=0dBm)

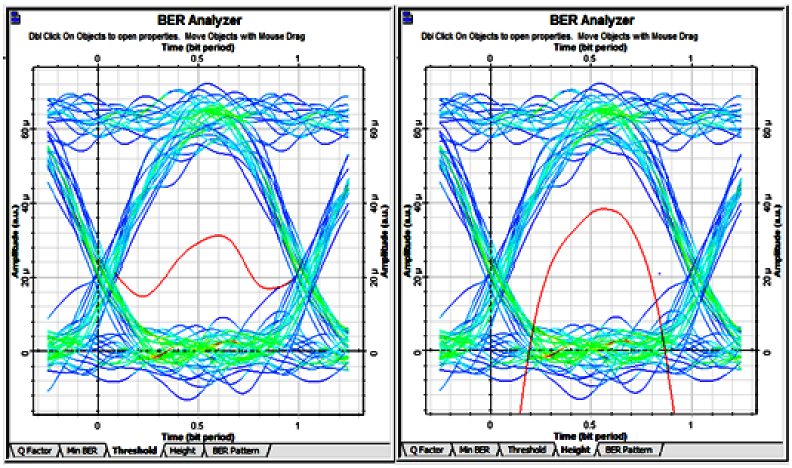

Figure 4.83: MZ,Threshold and eye height(L=40Km,α=0.3dB/Km,P_in=0dBm)

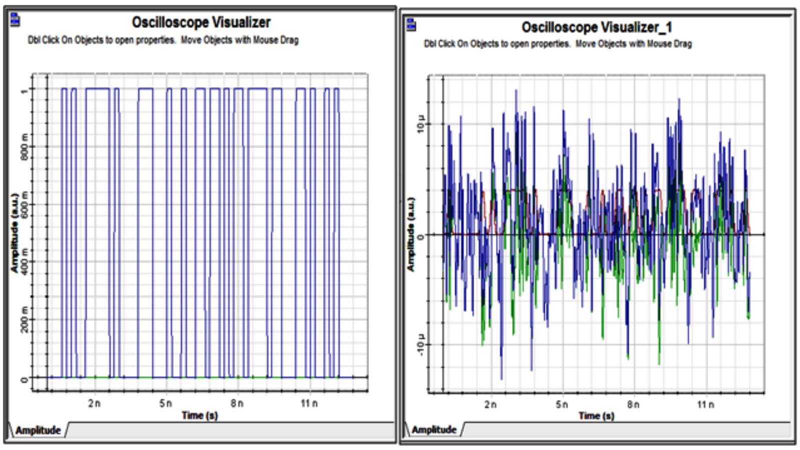

Figure 4.84: MZ,Input and output signals(L=40Km,α=0.3dB/Km,P_in=0dBm)

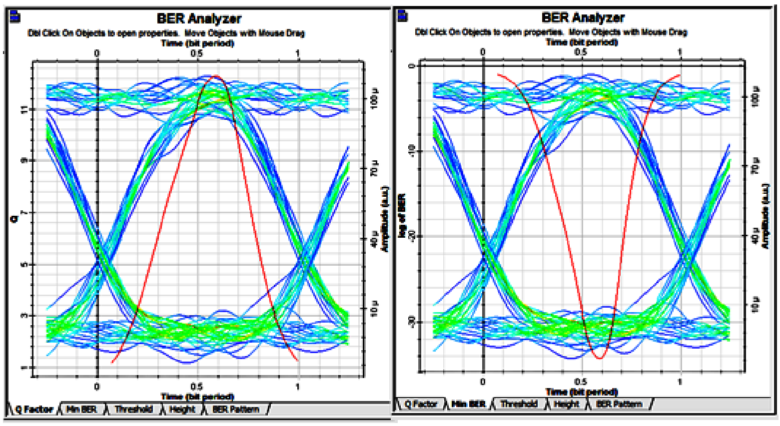

Figure 4.85: MZ,Q-factor and BER(L=40Km,α=0.3dB/Km,P_in=2dBm)

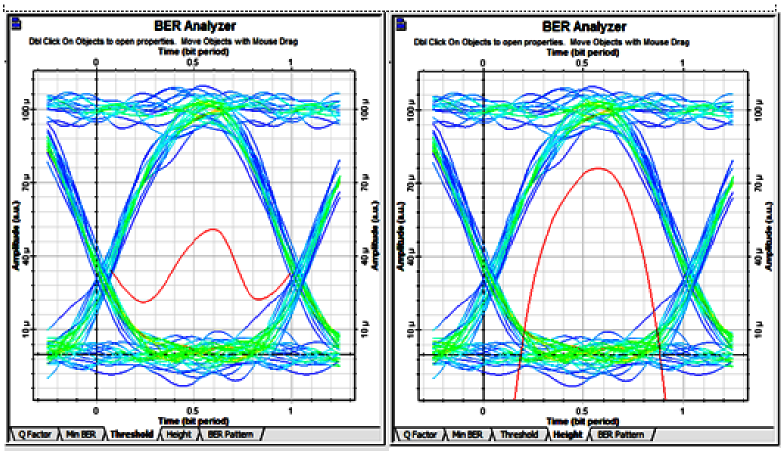

Figure 4.86: MZ,Threshold and eye height(L=40Km,α=0.3dB/Km,P_in=2dBm)

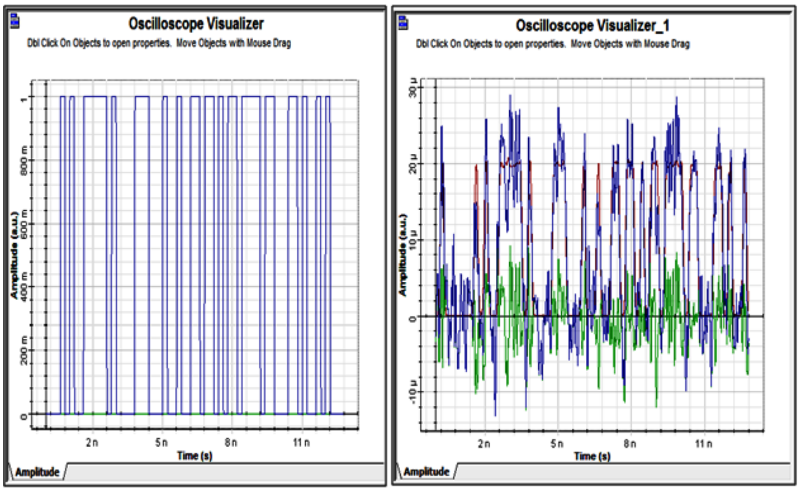

Figure 4.87: MZ,Input and output signals(L=40Km,α=0.3dB/Km,P_in=2dBm)

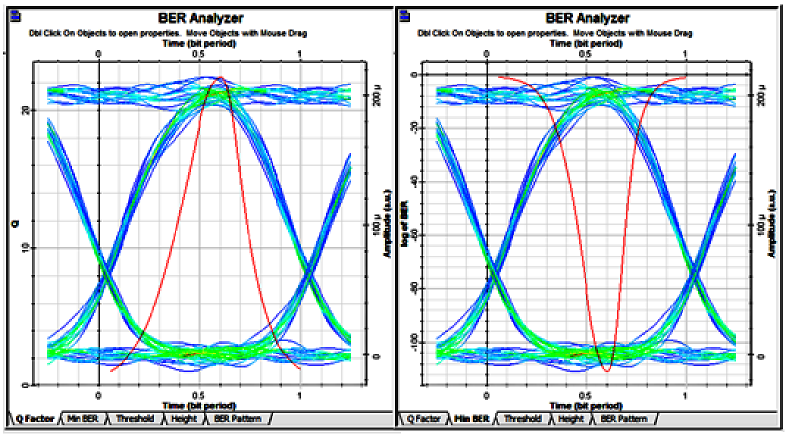

Figure 4.88: MZ,Q-factor and BER(L=40Km,α=0.3dB/Km,P_in=5dBm)

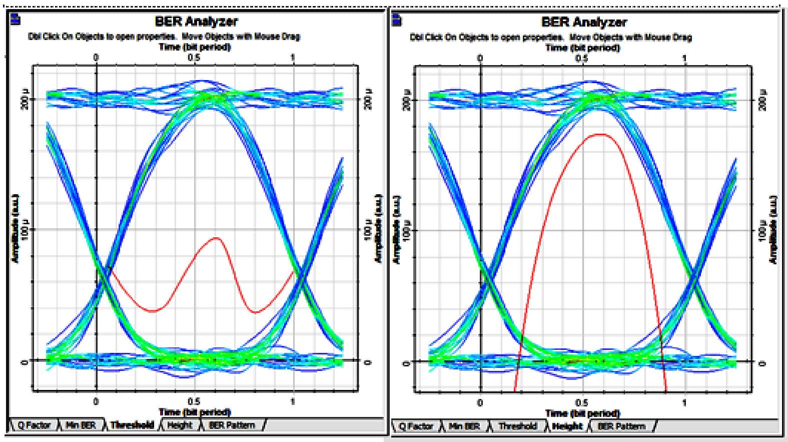

Figure 4.89: MZ,Threshold and eye height(L=40Km,α=0.3dB/Km,P_in=5dBm)

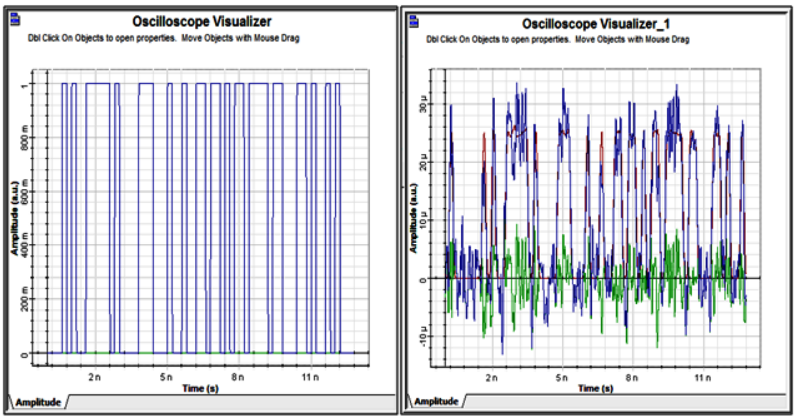

Figure 4.90: MZ,Input and output signals(L=40Km,α=0.3dB/Km,P_in=5dBm)

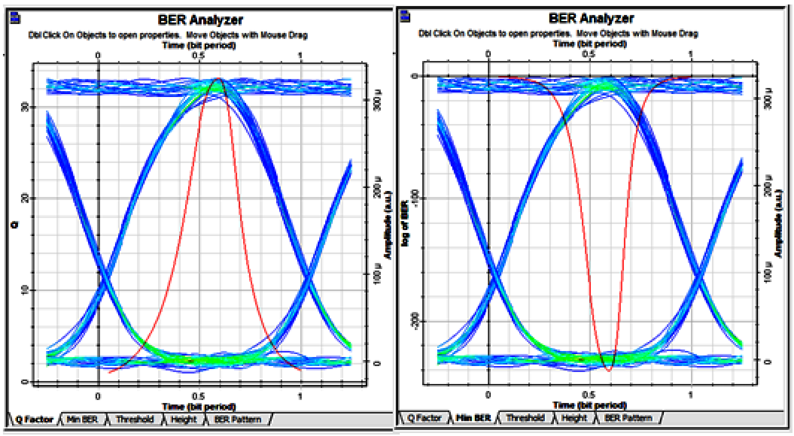

Figure 4.91: MZ,Q-factor and BER(L=40Km,α=0.3dB/Km,P_in=7dBm)

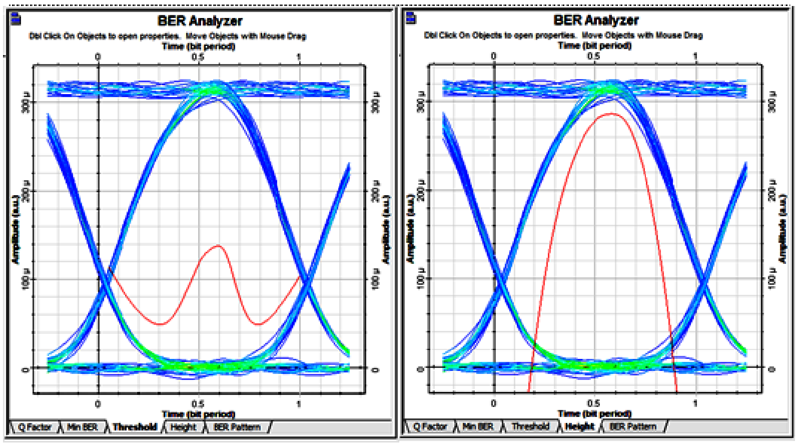

Figure 4.92: MZ,Threshold and eye height(L=40Km,α=0.3dB/Km,P_in=7dBm)

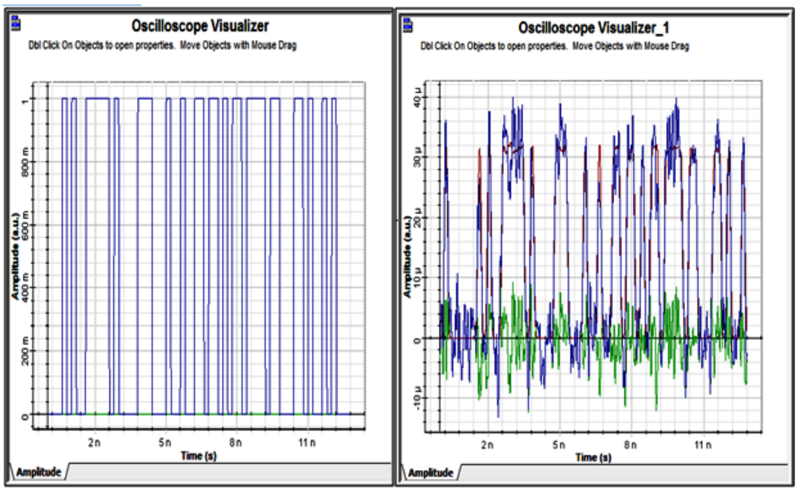

Figure 4.93: MZ,Input and output signals(L=40Km,α=0.3dB/Km,P_in=7dBm)

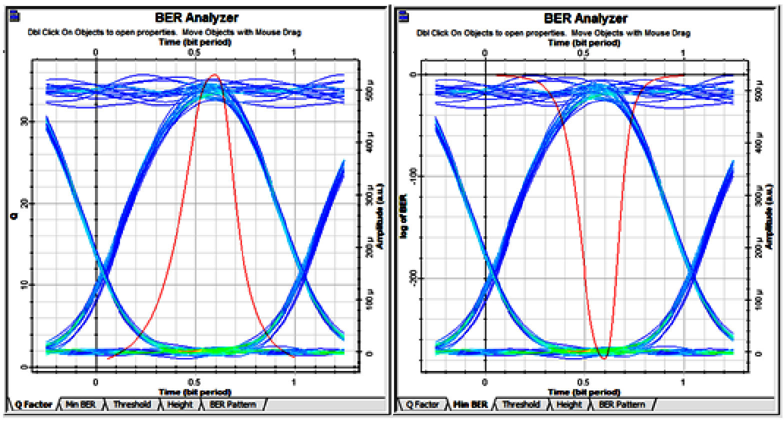

Figure 4.94: MZ,Q-factor and BER(L=40Km,α=0.3dB/Km,P_in=9dBm)

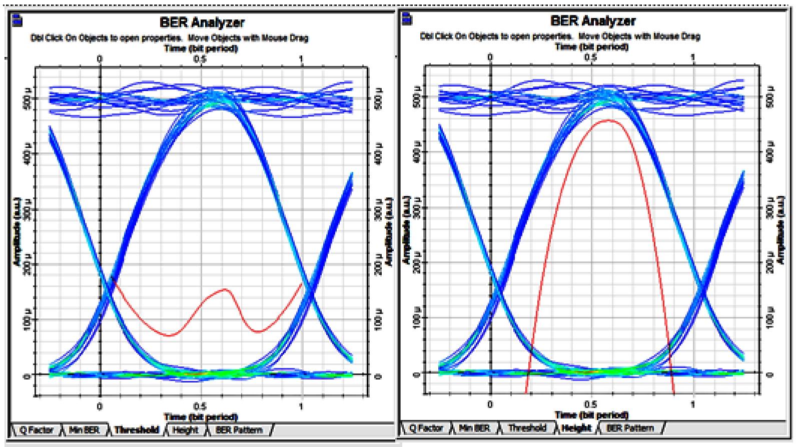

Figure 4.95: MZ,Threshold and eye height(L=40Km,α=0.3dB/Km,P_in=9dBm)

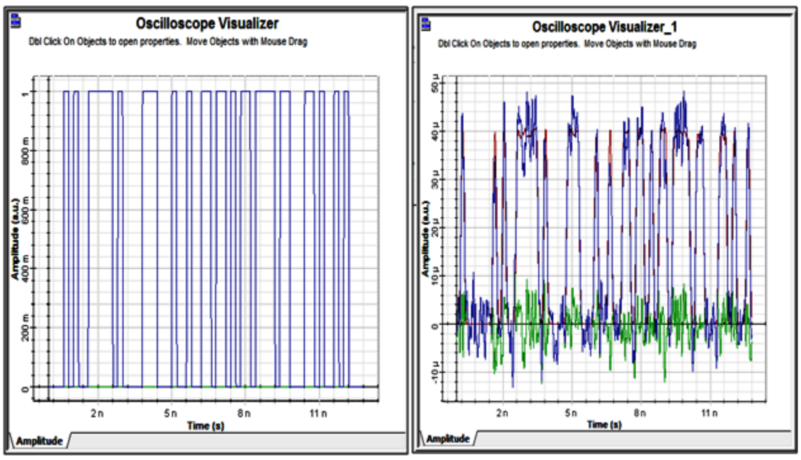

Figure 4.96: MZ,Input and output signals(L=40Km,α=0.3dB/Km,P_in=9dBm)

4.2.3 Performance Analysis With An Acousto-Optic Tunable Filter

4.2.3.1 Effect Of Fiber Length

In this case the following parameters are taken to see the effect of fiber length.

- Input power: 0 dBm
- Attenuation coefficient: 0.1 dB/Km

Figure 4.98, Figure 4.99, and Figure 4.100, show the system performance parameters when the fiber length is equal to 40 Km. Next, the fiber length is equal to 80 Km. and the performance is shown in Figure 4.101, Figure 4.102, and Figure 4.103. Next, the fiber length is equal to 120 Km. and the performance is shown in Figure 4.104, Figure 4.105, and Figure 4.106. Next, the fiber length is equal to 160 Km. and the performance is shown in Figure 4.107, Figure 4.108, and Figure 4.109. Finally, the fiber length is equal to 200 Km. and the performance is shown in Figure 4.110, Figure 4.111, and Figure 4.112. The figures are presented in the next pages, which is shown that in the case of fiber length 40 Km (Highest Performance) a clearly output signal and open eye in the diagram also shown maximum Q-factor, Eye Height, Threshold and minimum BER. The performance gradually degraded until reach fiber length 200 Km (Lowest Performance), which is shown that a noisy output signal and closed eye in the diagram also shown minimum Q-factor, Eye Height, Threshold and maximum BER.

The following table, Tables 4.7 concluded the presents a summary of the results obtained from Figure 4.98 to Figure 4.112

Table 4.7: AO,Evaluation(L=40 to 200Km,α=0.1dB/Km,P_in=0dBm)

Length (Km)	Max .Q-Factor	Min. BER	Eye Height	Threshold
40	9	3e-017	22e-005	5e-005
80	8	3e-015	8e-005	3.4e-005
120	5.2	1e-007	2e-005	2.2e-005
160	2.6	4e-003	-3e-006	9e-006
200	0	1	0	0

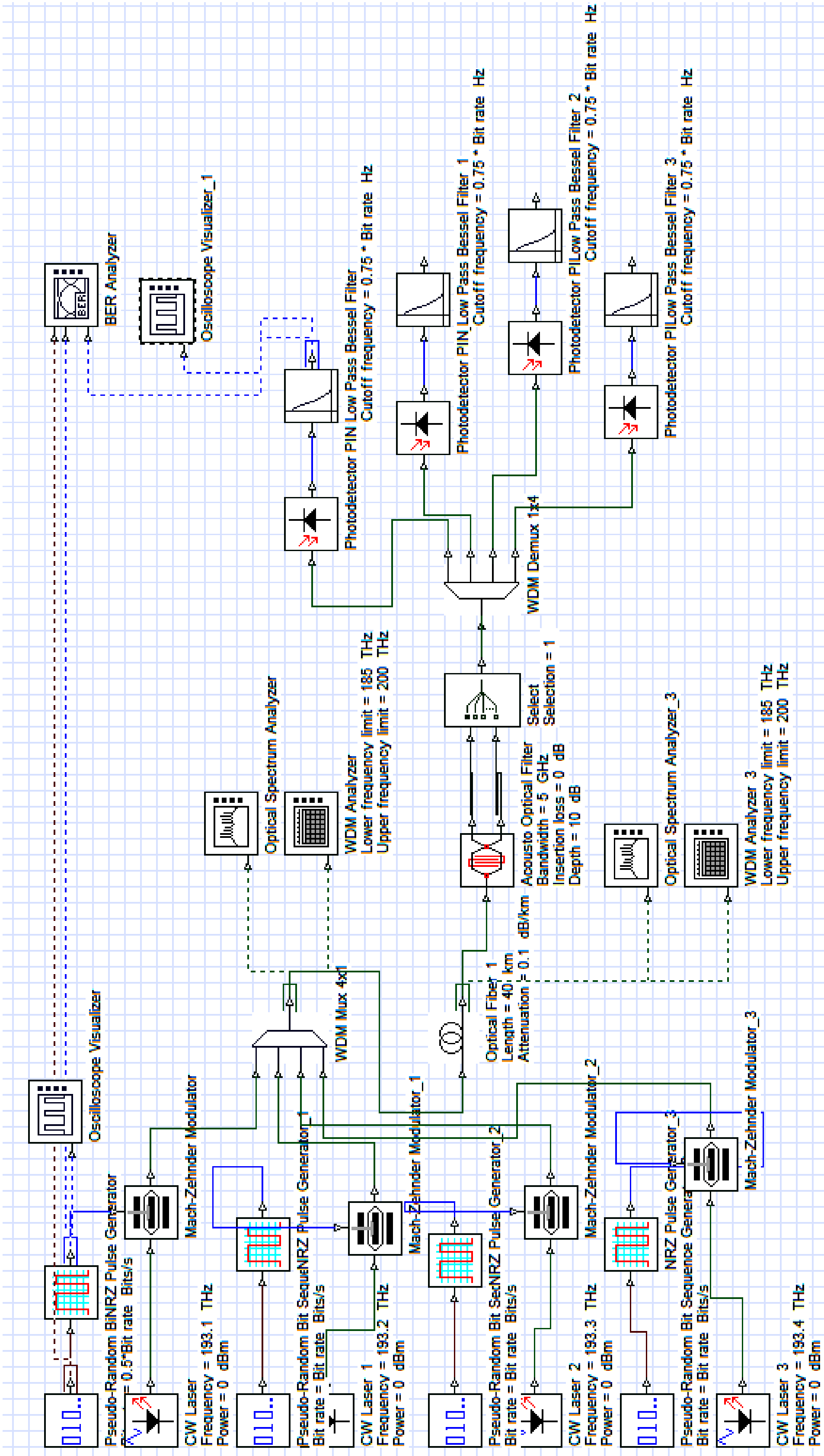

Figure 4.97: The system with AO filter and Length=40Km

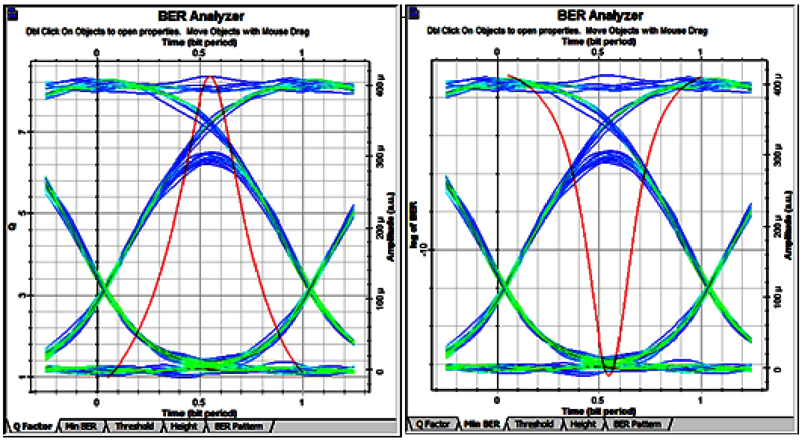

Figure 4.98: AO,Q-factor and BER(L=40Km,α=0.1dB/Km,P_in=0dBm)

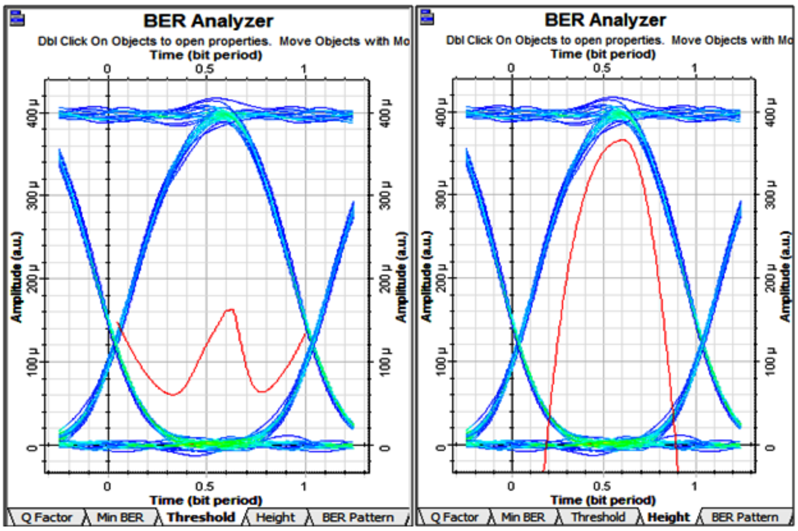

Figure 4.99: AO,Threshold and eye height(L=40Km,α=0.1dB/Km,P_in=0dBm)

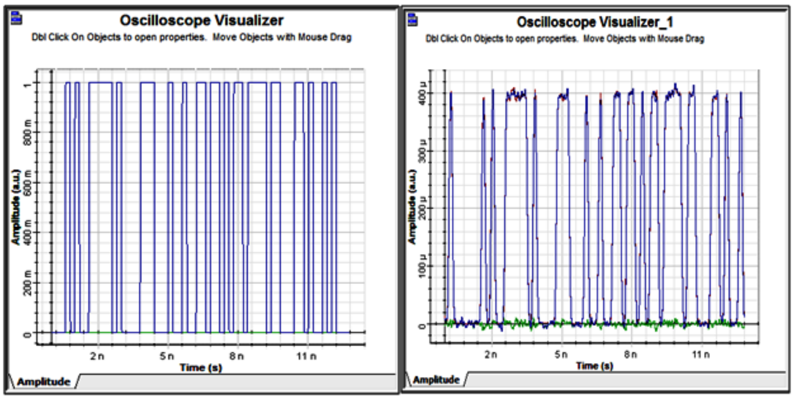

Figure 4.100: AO,Input and output signals(L=40Km,α=0.1dB/Km,P_in=0dBm)

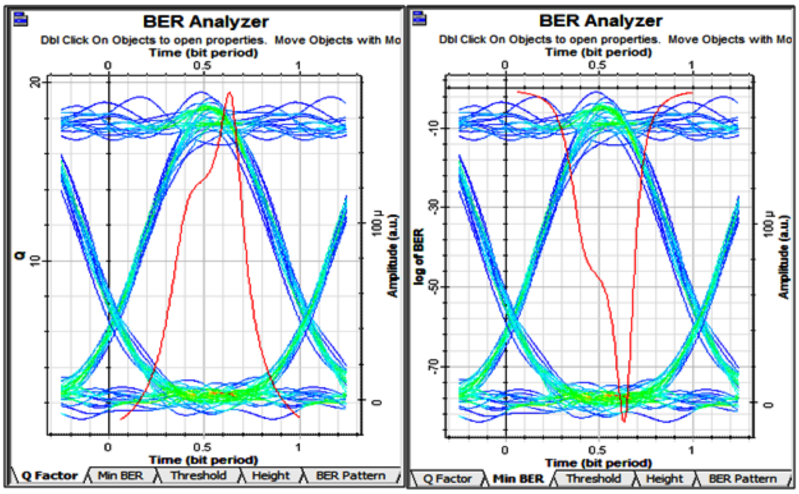

Figure 4.101: AO,Q factor and BER(L=80Km,α=0.1dB/Km,P_in=0dBm)

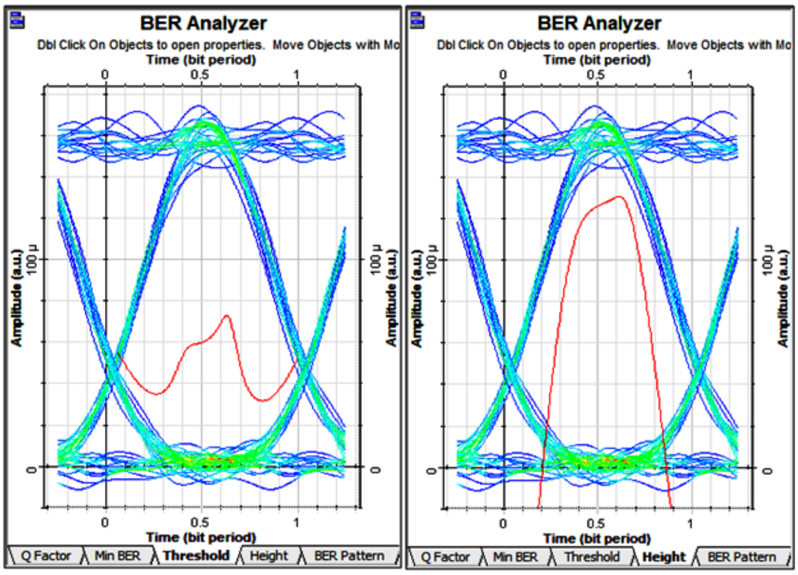

Figure 4.102: AO,Threshold and eye height(L=80Km,α=0.1dB/Km,P_in=0dBm)

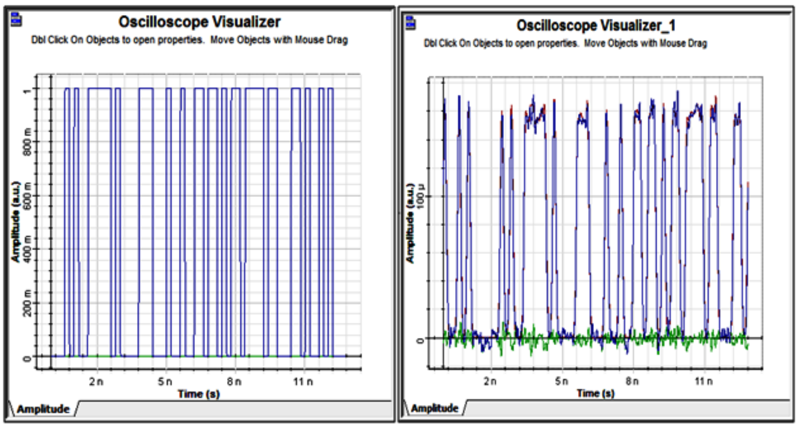

Figure 4.103: AO,Input and output signals(L=80Km,α=0.1dB/Km,P_in=0dBm)

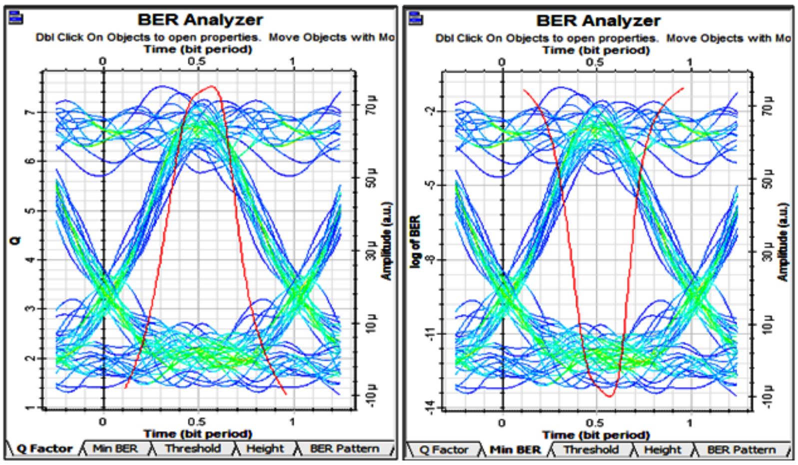

Figure 4.104: AO,Q-factor and BER(L=120Km,α=0.1dB/Km,P_in=0dBm)

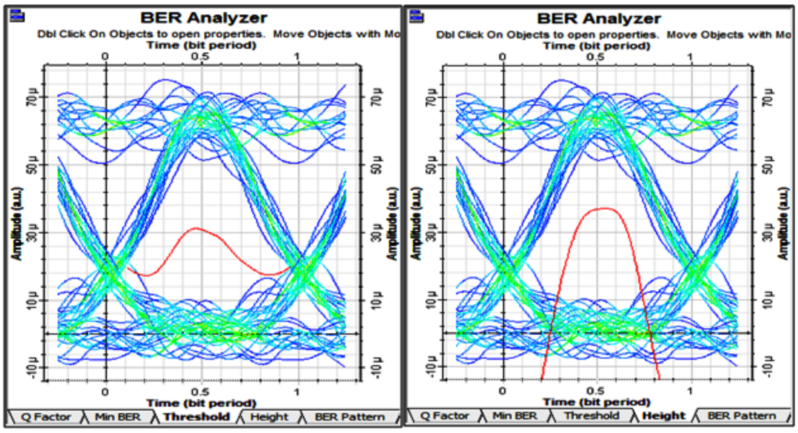

Figure 4.105: AO,Threshold and eye height(L=120Km,α=0.1dB/Km,P_in=0dBm)

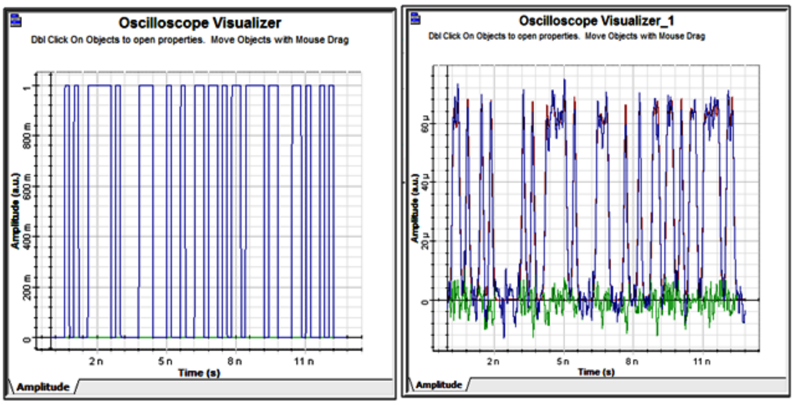

Figure 4.106: AO,Input and output signals(L=120Km,α=0.1dB/Km,P_in=0dBm)

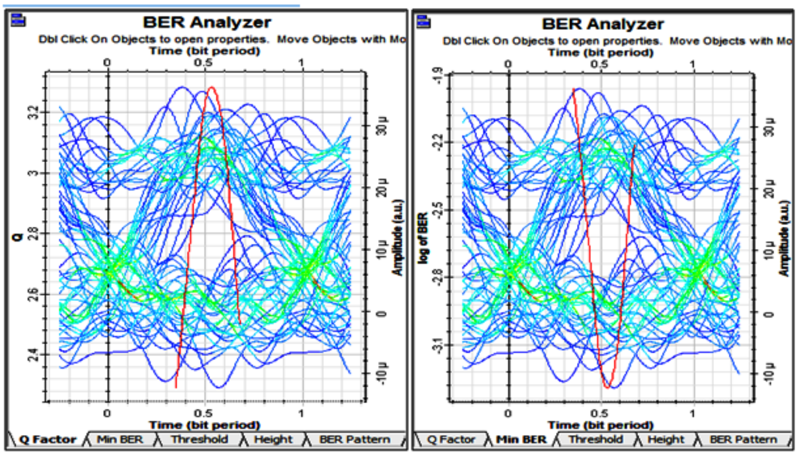

Figure 4.107: AO,Q-factor and BER(L=160Km,α=0.1dB/Km,P_in=0dBm)

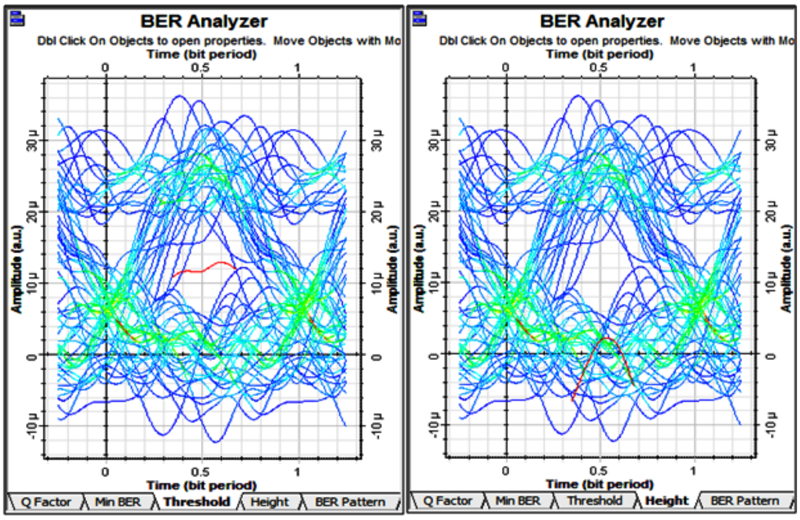

Figure 4.108: AO,Threshold and eye height(L=160Km,α=0.1dB/Km,P_in=0dBm)

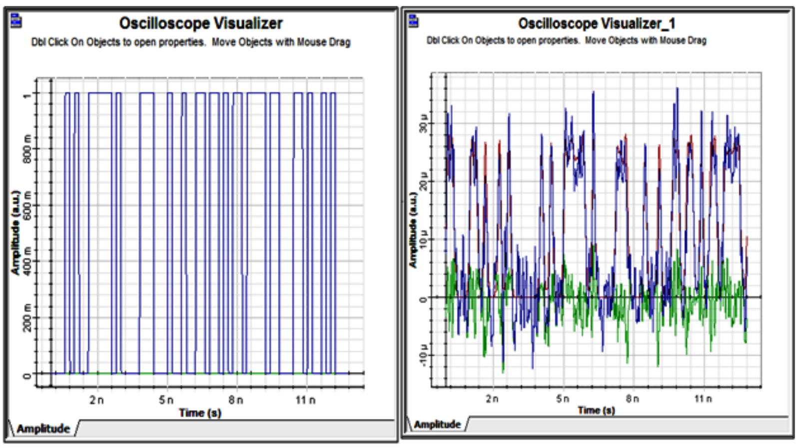

Figure 4.109: AO,Input and output signals(L=160Km,α=0.1dB/Km,P_in=0dBm)

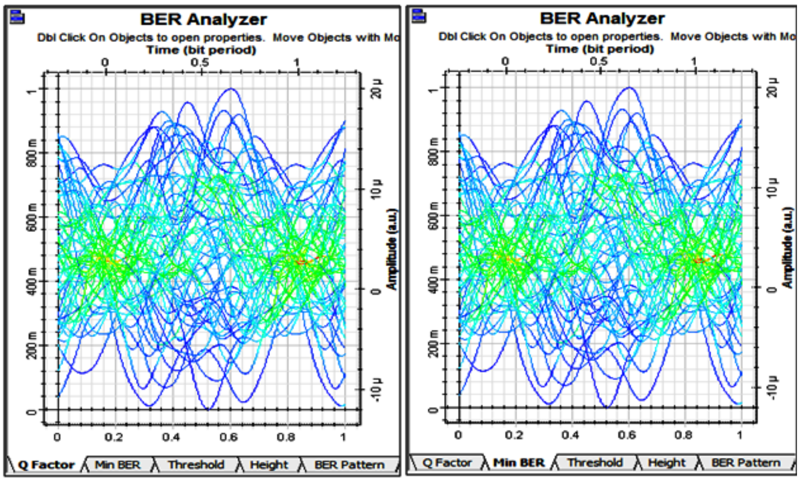

Figure 4.110: AO,Q-factor and BER(L=200Km,α=0.1dB/Km,P_in=0dBm)

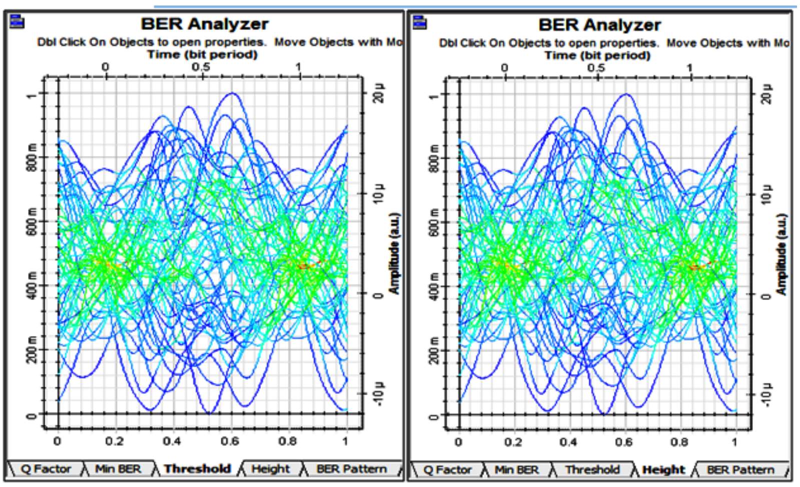

Figure 4.111: AO,Threshold and eye height(L=200Km,α=0.1dB/Km,P_in=0dBm)

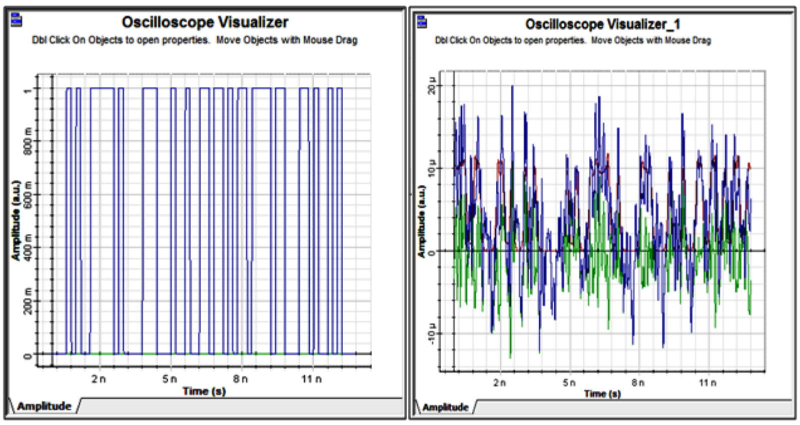

Figure 4.112: AO,Input and output signals(L=200Km,α=0.1dB/Km,P_in=0dBm)

4.2.3.2 Effect Of Attenuation Coefficient

In this case the following parameters are taken to see the effect of fiber attenuation coefficient.

- Input power: 0 dBm
- Fiber length: 40 Km

Figure 4.113, Figure 4.114, and Figure 4.115, show the system performance parameters when the fiber attenuation coefficient is equal to 0.1 dB/Km. Next, the attenuation is set to 0.2 dB/Km and the performance is shown in Figure 4.116, Figure 4.117, and Figure 4.118. Next, the attenuation is set to 0.3 dB/Km and the performance is shown in Figure 4.119, Figure 4.120, and Figure 4.121. Next, the attenuation is set to 0.4 dB/Km and the performance is shown in Figure 4.122, Figure 4.123, and Figure 4.124. Finally, the attenuation is set to 0.5 dB/Km and the performance is shown in Figure 4.125, Figure 4.126, and Figure 4.134. The figures are presented in the next pages, which is shown that in the case of an attenuation 0.1 dB/Km (Highest Performance) a clearly output signal and open eye in the diagram also shown maximum Q-factor, Eye Height, Threshold and minimum BER. The performance gradually degraded until reach an attenuation 0.5 dB/Km (Lowest Performance), which is shown that a noisy output signal and closed eye in the diagram also shown minimum Q-factor, Eye Height, Threshold and maximum BER.

The following table, Tables 4.8 concluded the presents a summary of the results obtained from Figure 4.113 to Figure 4.134

Table 4.8: AO,Evaluation(L=40Km,α=0.1 to 0.5dB/Km,P_in=0dBm)

Attenuation (dB/Km)	Max .Q-Factor	Min. BER	Eye Height	Threshold
0.1	9	3e-017	22e-005	5e-005
0.2	7	2e-012	8e-005	3e-005
0.3	4	3e-006	1e-005	1e-005
0.4	2	107e-004	-7e-006	9e-006
0.5	0	1	0	0

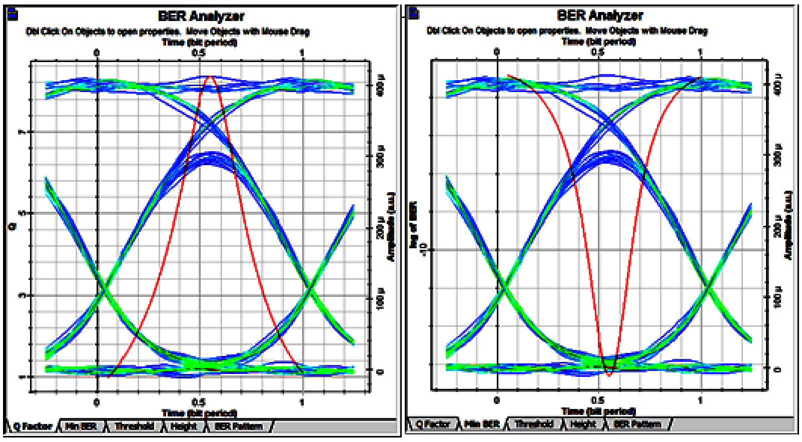

Figure 4.113: AO,Q-factor and BER(L=40Km,α=0.1dB/Km,P_in=0dBm)

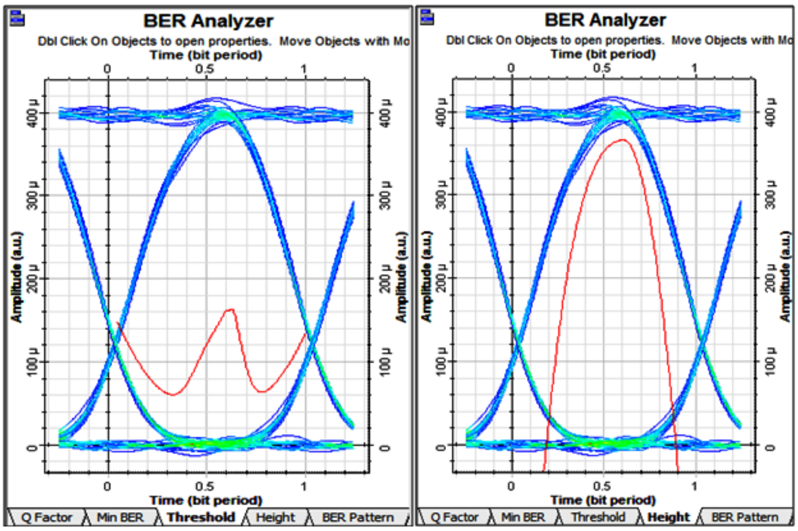

Figure 4.114: AO,Threshold and eye height(L=40Km,α=0.1dB/Km,P_in=0dBm)

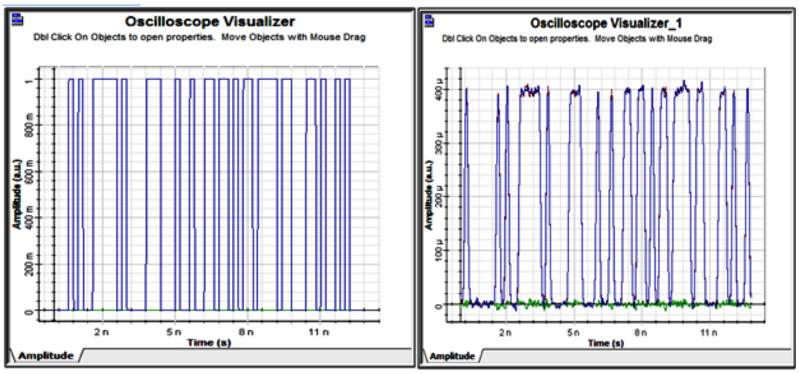

Figure 4.115: AO,Input and output signals(L=40Km,α=0.1dB/Km,P_in=0dBm)

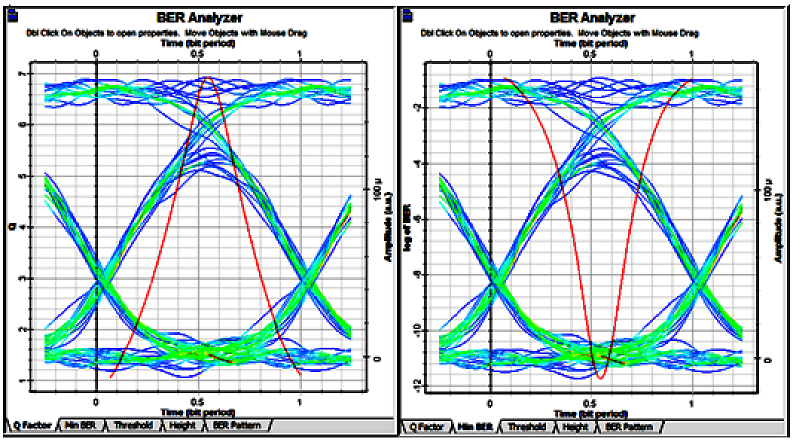

Figure 4.116: AO,Q-factor and BER(L=40Km,α=0.2dB/Km,P_in=0dBm)

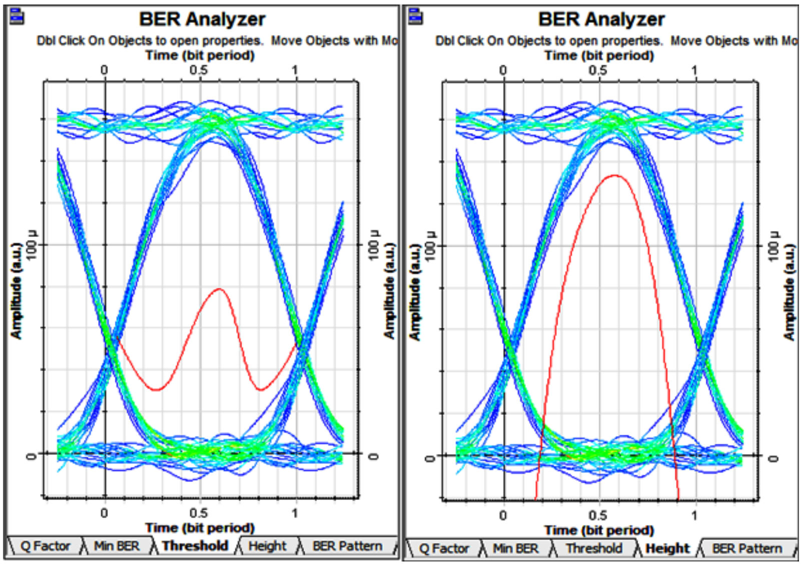

Figure 4.117: AO,Threshold and eye height(L=40Km,α=0.2dB/Km,P_in=0dBm)

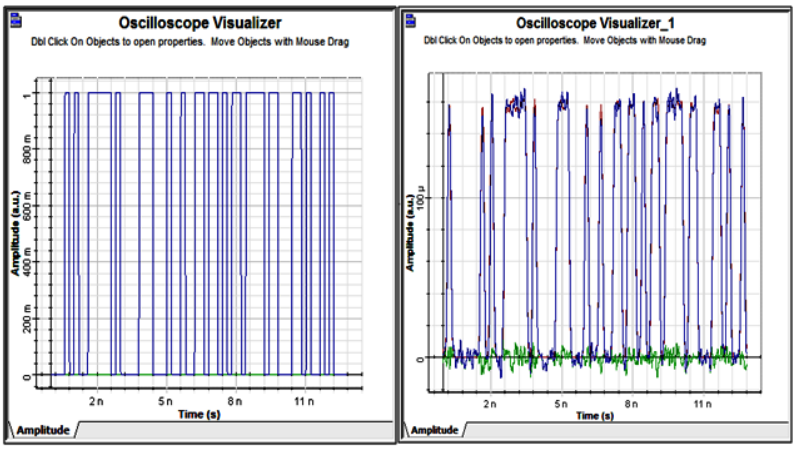

Figure 4.118: AO,Input and output signals(L=40Km,α=0.2dB/Km,P_in=0dBm)

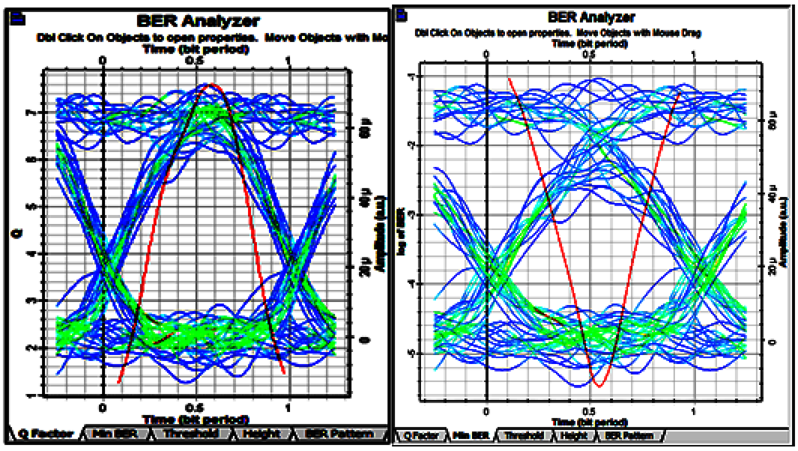

Figure 4.119: AO,Q-factor and BER(L=40Km,α=0.3dB/Km,P_in=0dBm)

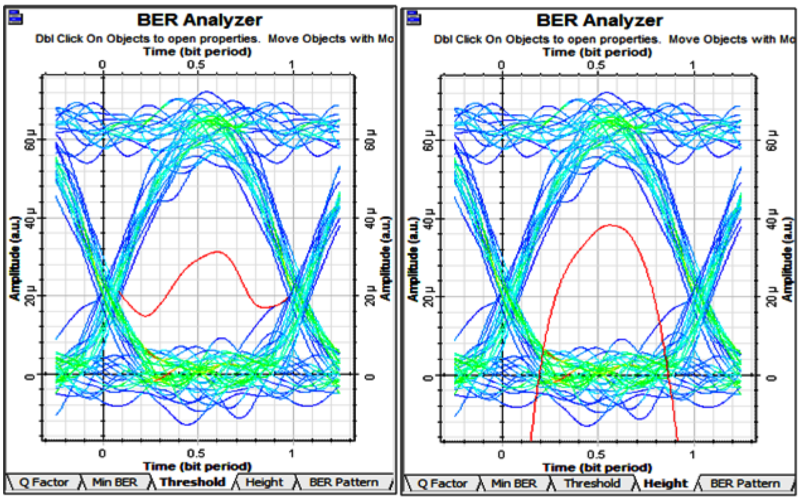

Figure 4.120: AO,Threshold and eye height(L=40Km,α=0.3dB/Km,P_in=0dBm)

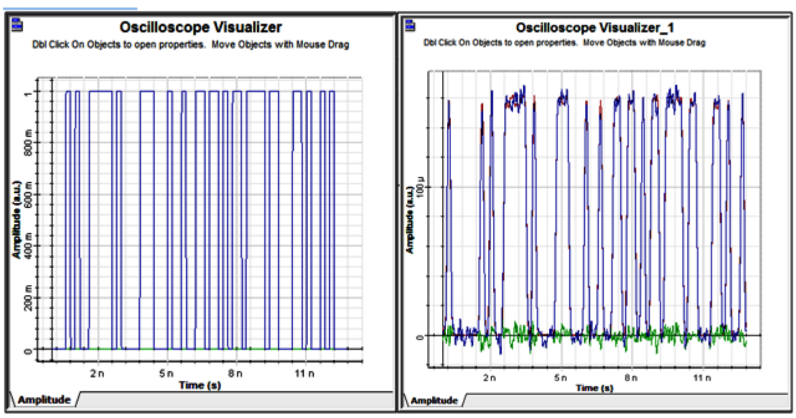

Figure 4.121: AO,Input and output signals(L=40Km,α=0.3dB/Km,P_in=0dBm)

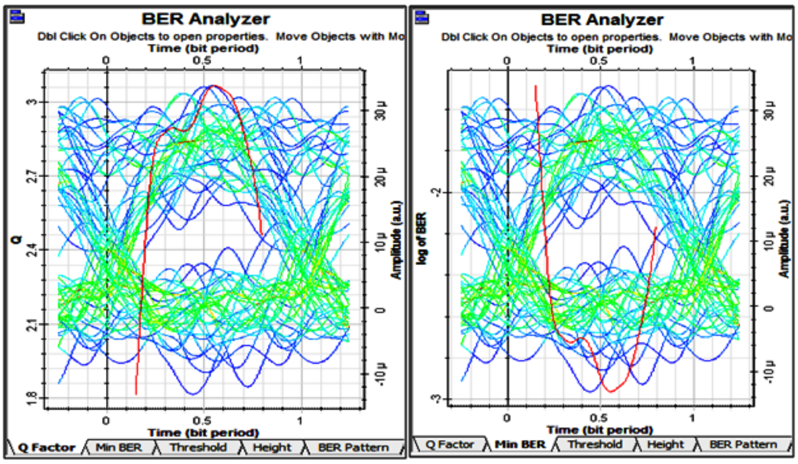

Figure 4.122: AO,Q-factor and BER(L=40Km,α=0.4dB/Km,P_in=0dBm)

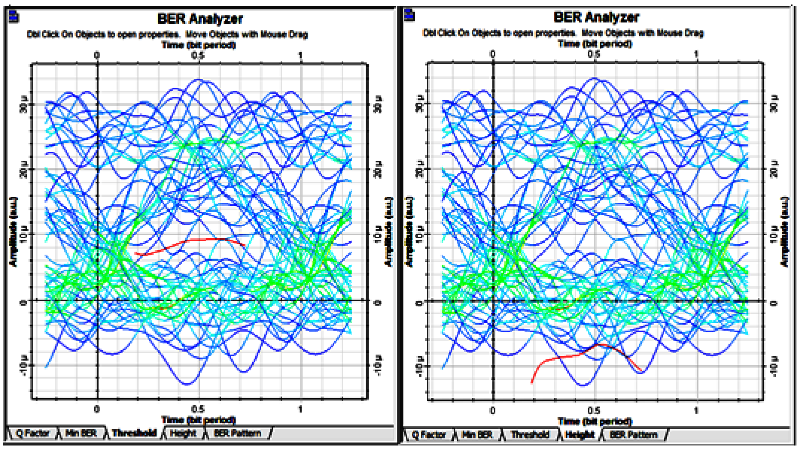

Figure 4.123: AO,Threshold and eye height(L=40Km,α=0.4dB/Km,P_in=0dBm)

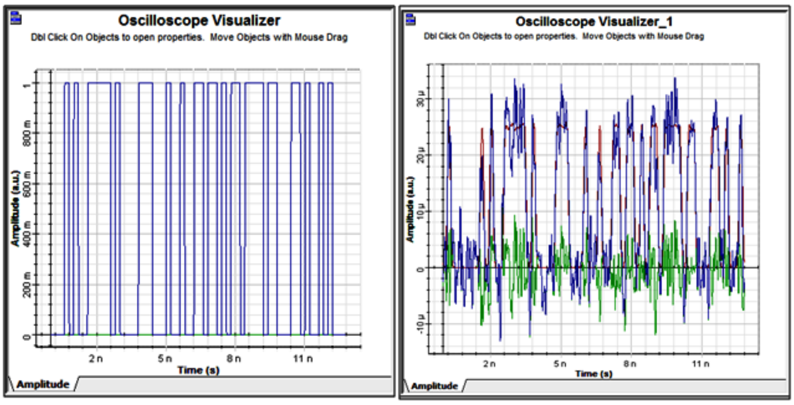

Figure 4.124: AO,Input and output signals(L=40Km,α=0.4dB/Km,P_in=0dBm)

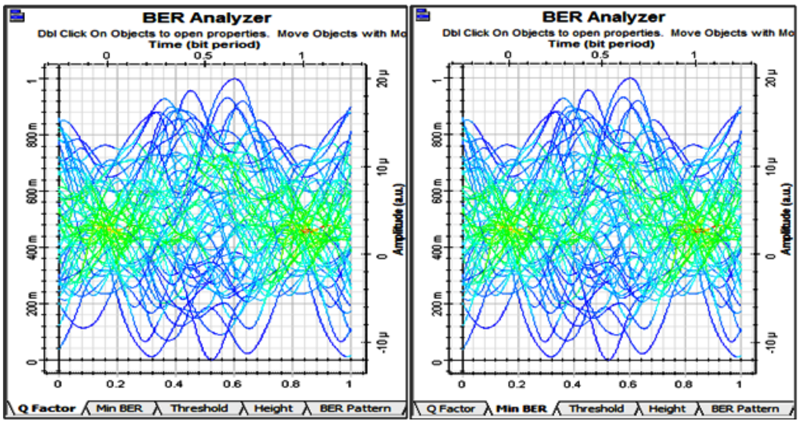

Figure 4.125: AO,Q-factor and BER(L=40Km,α=0.5dB/Km,P_in=0dBm)

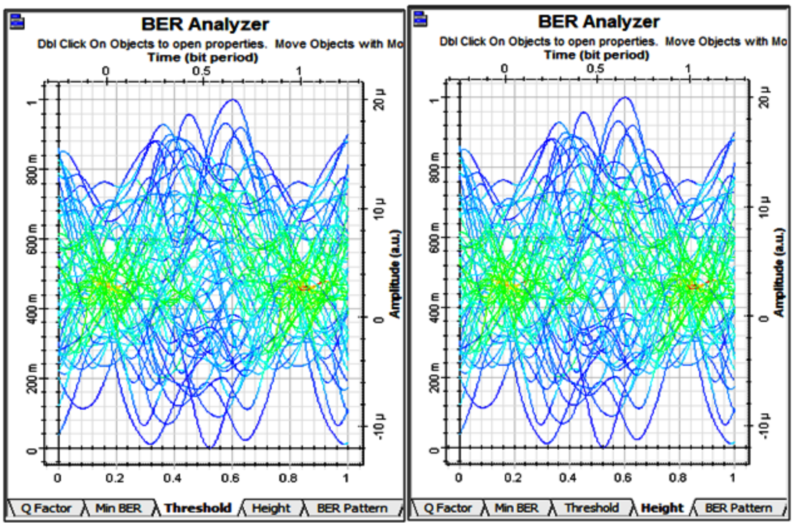

Figure 4.126: AO,Threshold and eye height(L=40Km,α=0.5dB/Km,P_in=0dBm)

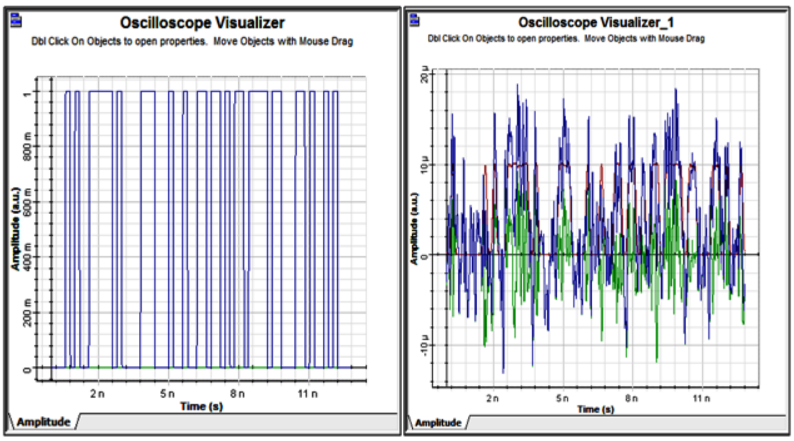

Figure 4.127: AO,Input and output signals(L=40Km,α=0.5dB/Km,P_in=0dBm)

4.2.3.3 Effect Of Input Power

In this case the following parameters are taken to see the effect of Input power.

- Attenuation coefficient: 0.3 dB/Km
- Fiber length: 40 Km

Figure 4.128, Figure 4.129, and Figure 4.130, show the system performance parameters when the Input power is equal to 0dBm. Next, the Input power is equal to 2dBm and the performance is shown in Figure 4.131, Figure 4.132, and Figure 4.133. Next, the Input power is equal to 5dBm and the performance is shown in Figure 4.134, Figure 4.135, and Figure 4.136. Next, the Input power is equal to 7dBm and the performance is shown in Figure 4.137, Figure 4.138, and Figure 4.139. Finally, the Input power is equal to 9dBm and the performance is shown in Figure 4.140, Figure 4.141, and Figure 4.142. The figures are presented in the next pages, which is shown that in the case of an input power 9 dBm (Highest Performance) a clearly output signal and open eye in the diagram also shown maximum Q-factor, Eye Height, Threshold and minimum BER. The performance gradually degraded until reach an input power 0dBm (Lowest Performance), which is shown that a noisy output signal and closed eye in the diagram also shown minimum Q-factor, Eye Height, Threshold and maximum BER.

The following table, Tables 4.9 concluded the presents a summary of the results obtained from Figure 4.128 to Figure 4.142

Table 4.9: AO,Evaluation(L=40Km,α=0.3 dB/Km,P_in=0 to 9dBm

Input Power (dBm)	Max .Q-Factor	Min. BER	Eye Height	Threshold
0	4	3e-006	1.7e-005	1.8e-005
2	6	4e-009	4e-005	2.5e-005
5	7	5e-014	10e-005	3.6e-005
7	8	7e-017	17e-005	4.5e-005
9	8.5	1e-017	27e-005	6e-005

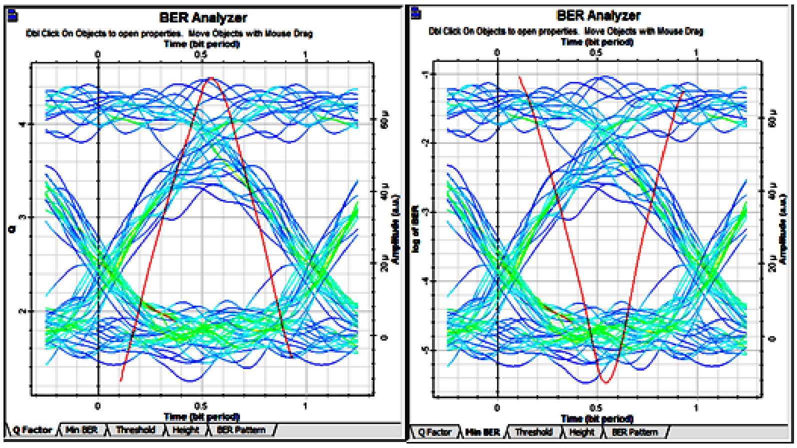

Figure 4.128: AO,Q-factor and BER(L=40Km,α=0.3dB/Km,P_in=0dBm)

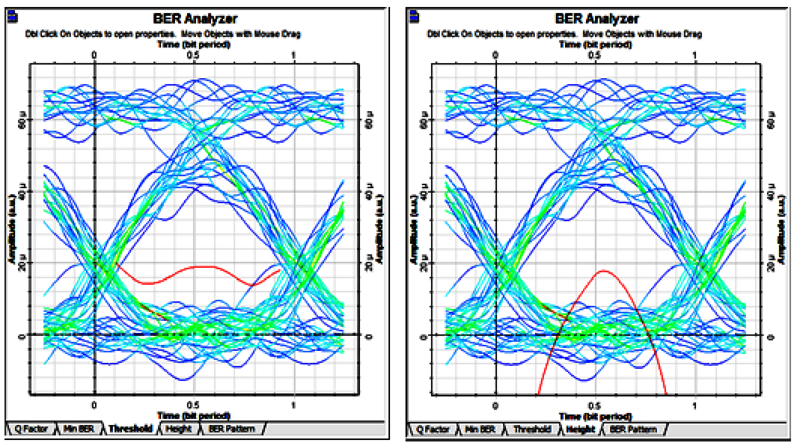

Figure 4.129: AO,Threshold and eye height(L=40Km,α=0.3dB/Km,P_in=0dBm)

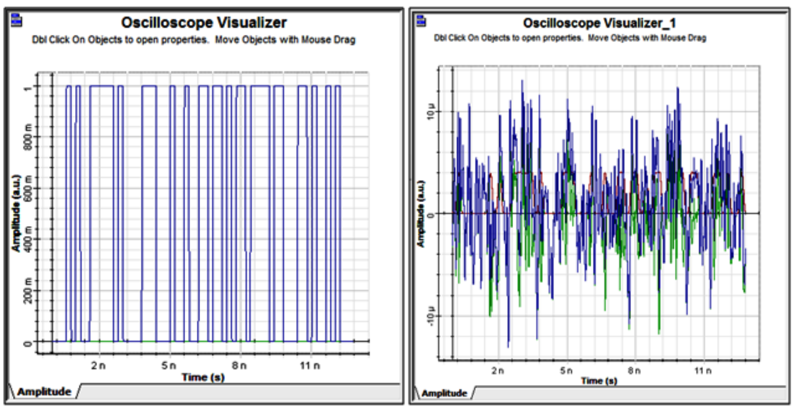

Figure 4.130: AO,Input and output signals(L=40Km,α=0.3dB/Km,P_in=0dBm)

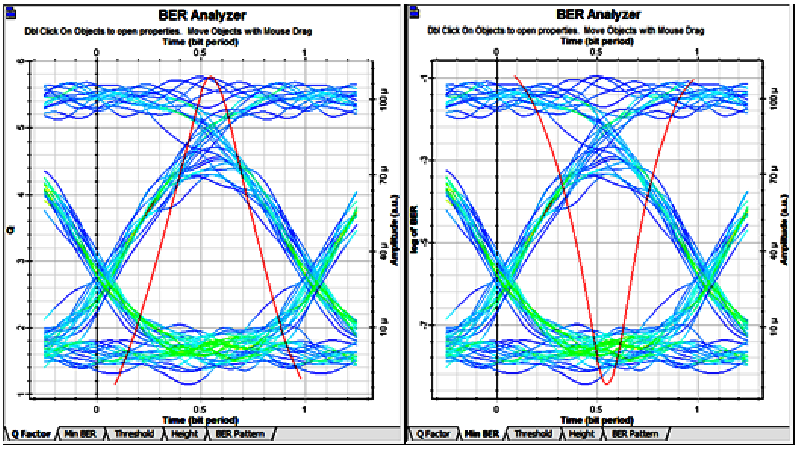

Figure 4.131: AO,Q-factor and BER(L=40Km,α=0.3dB/Km,P_in=2dBm)

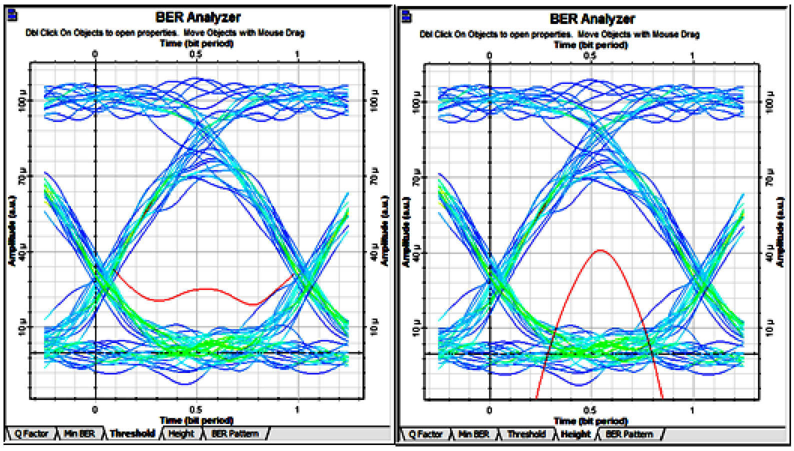

Figure 4.132: AO,Threshold and eye height(L=40Km,α=0.3dB/Km,P_in=2dBm)

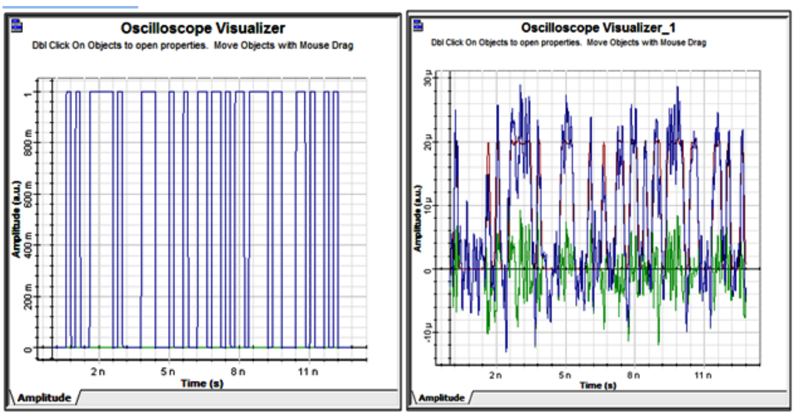

Figure 4.133: AO,Input and output signals(L=40Km,α=0.3dB/Km,P_in=2dBm)

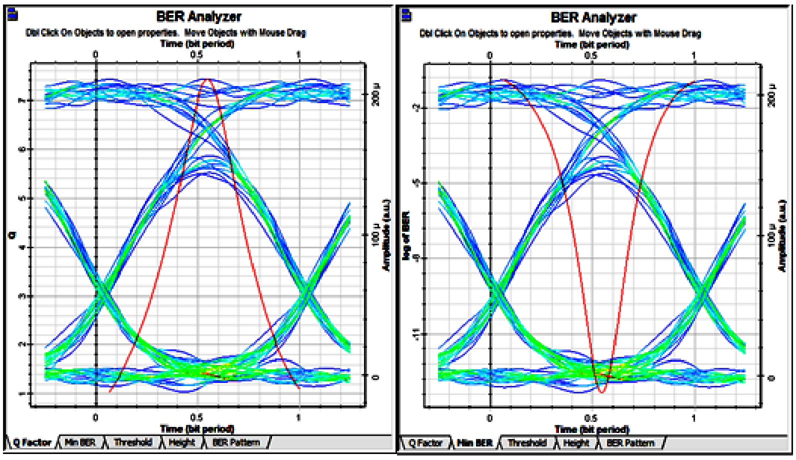

Figure 4.134: AO,Q-factor and BER(L=40Km,α=0.3dB/Km,P_in=5dBm)

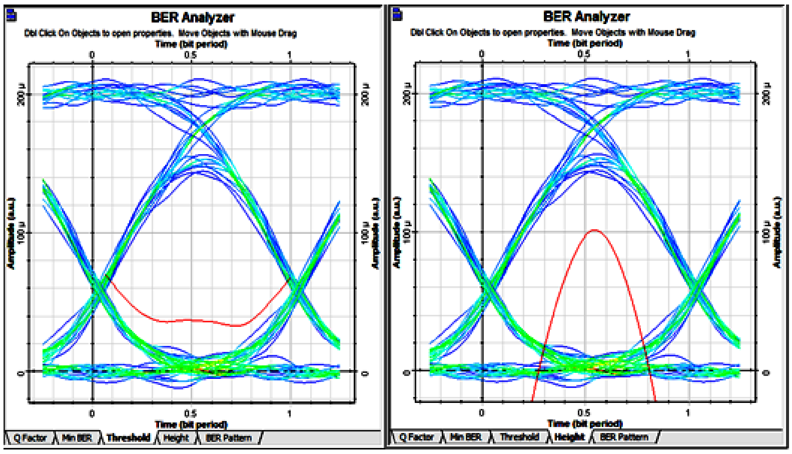

Figure 4.135: AO,Threshold and eye height(L=40Km,α=0.3dB/Km,P_in=5dBm)

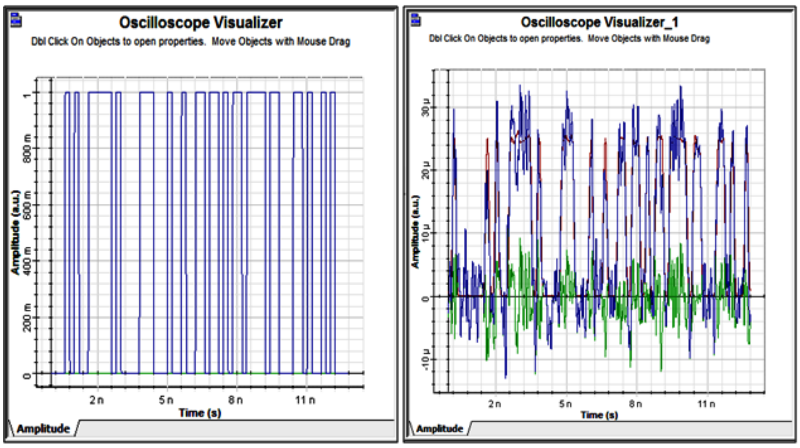

Figure 4.136: AO,Input and output signals(L=40Km,α=0.3dB/Km,P_in=5dBm)

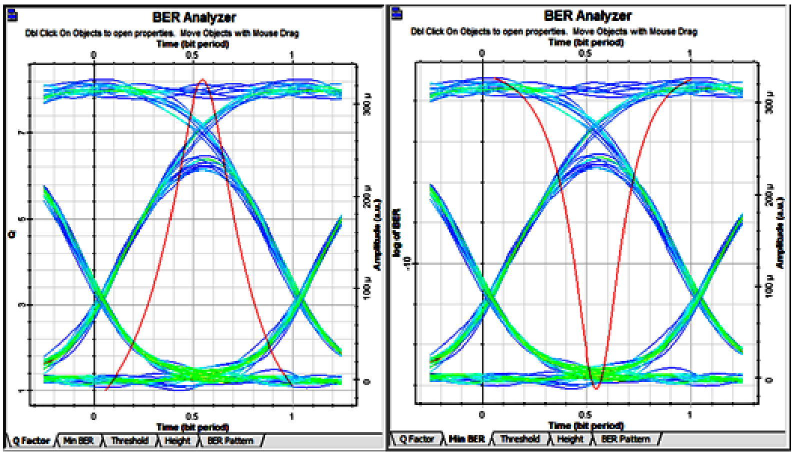

Figure 4.137: AO,Q-factor and BER(L=40Km,α=0.3dB/Km,P_in=7dBm)

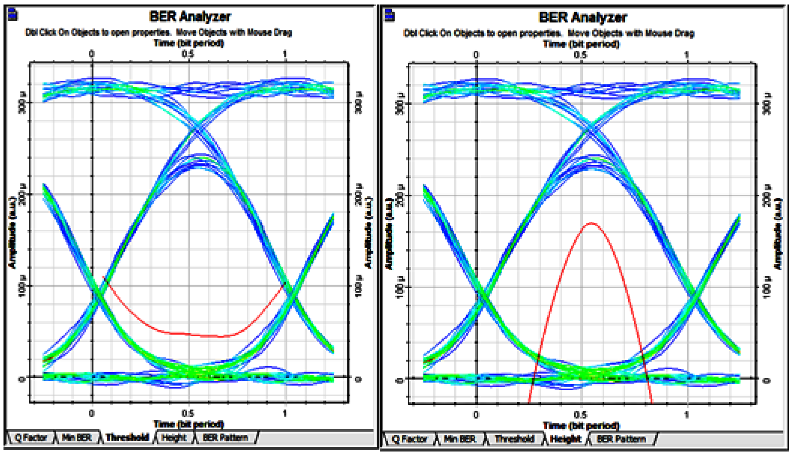

Figure 4.138: AO,Threshold and eye height(L=40Km,α=0.3dB/Km,P_in=7dBm)

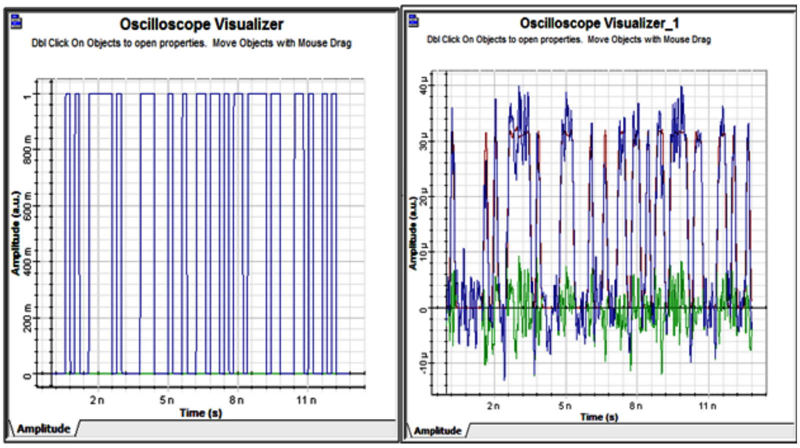

Figure 4.139: AO,Input and output signals(L=40Km,α=0.3dB/Km,P_in=7dBm)

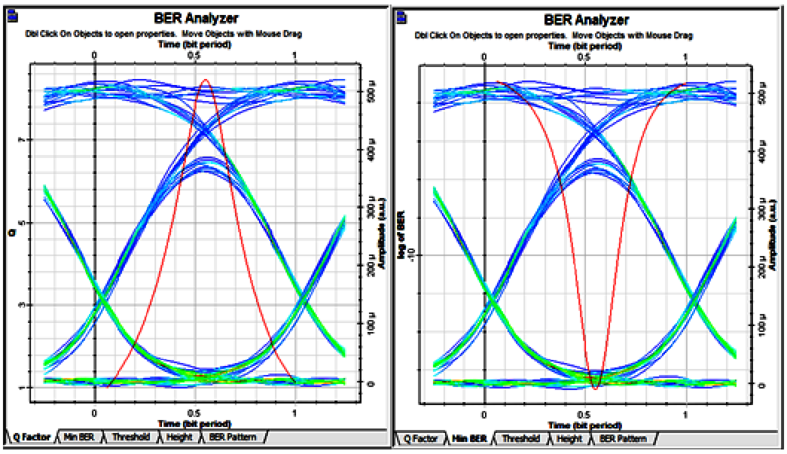

Figure 4.140: AO,Q-factor and BER(L=40Km,α=0.3dB/Km,P_in=9dBm)

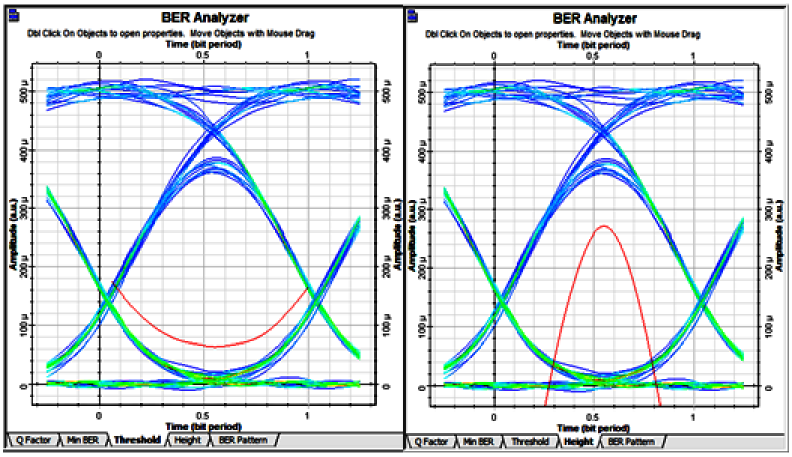

Figure 4.141: AO,Threshold and eye height(L=40Km,α=0.3dB/Km,P_in=9dBm)

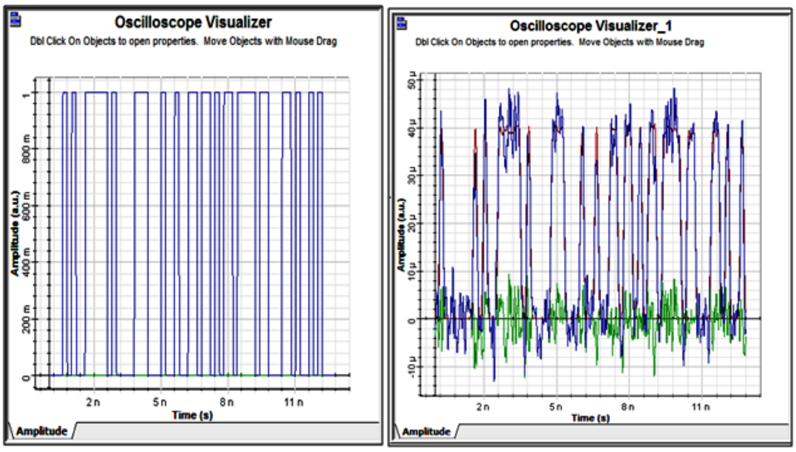

Figure 4.142: AO,Input and output signals(L=40Km,α=0.3dB/Km,P_in=9dBm)

4.2.4 Comparison Of Performance Evaluation Of Filtering For WDM Based Optical Fiber Networks

The tables presented in the following subsections presents a conclusion of the previous experimental observation. The results are summarized for various cases of the fiber length (see section 4.2.4.1), different values of attenuation (see section 4.2.4.2) and the impact of input power (see section 4.2.4.3).

4.2.4.1 Different Fiber Length

The parameters used to test the cases of different fiber lengths are listed as follows.

- Fiber Length = 40,80,120,160 and 200 Km
- Fiber Attenuation = 0.1 dB/Km
- Input Power = 0 dBm

Table 4.10 and Figure 4.143 summarizes the results maximum Q-factor given for different fiber lengths. Table 4.11 and Figure 4.144 summarizes the results minimum BER given for different fiber lengths. Table 4.12 and Figure 4.145 lists the results for maximum eye-height, and finally, Table 4.13 and Figure 4.146 lists the results for maximum threshold, which is shown that when a fiber length changed from 40 to 200 Km the Q-factor, Eye Height and Threshold when: (1)MZ filter used will be maximum, (2)FP used will be moderate and (3)AO used will be minimum. Also shown that the BER when: (1)MZ filter used will be minimum, (2)FP used will be moderate and (3)AO used will be maximum.

Table 4.10: Max .Q-Factor (MZ, FP, AO) with different fiber length

Length (Km)	MZ Filter	FP Filter	AO Filter
40	39	12	9
80	19	11	8
120	8	6.7	5.2
160	3.3	2.9	2.6
200	0	0	0

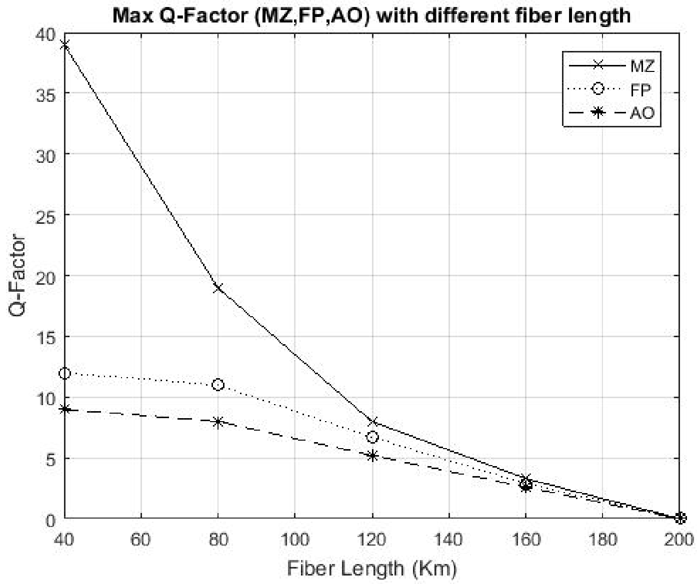

Figure 4.143: Max .Q-Factor (MZ, FP, AO) with different fiber length

Table 4.11: Min. BER (MZ, FP, AO) with different fiber length

Length (Km)	MZ Filter	FP Filter	AO Filter
40	0	9e-032	3e-017
80	1e-084	5e-030	3e-015
120	3e-014	9e-012	1e-007
160	5e-004	2e-003	4e-003
200	1	1	1

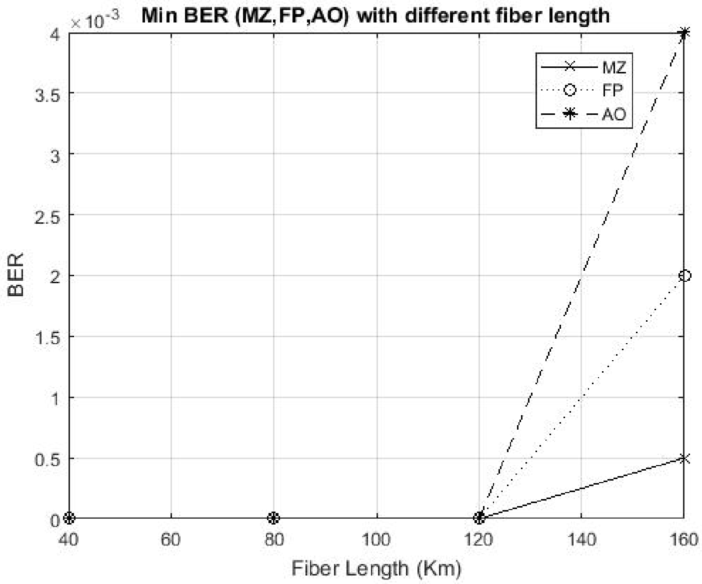

Figure 4.144: Min. BER (MZ, FP, AO) with different fiber length

Table 4.12: Max .Eye Height (MZ, FP, AO) with different fiber length

Length (Km)	MZ Filter	FP Filter	AO Filter
40	4e-004	3e-004	22e-005
80	13e-005	10e-005	8e-005
120	4e-005	3e-005	2e-005
160	2e-006	-6e-007	-3e-006
200	0	0	0

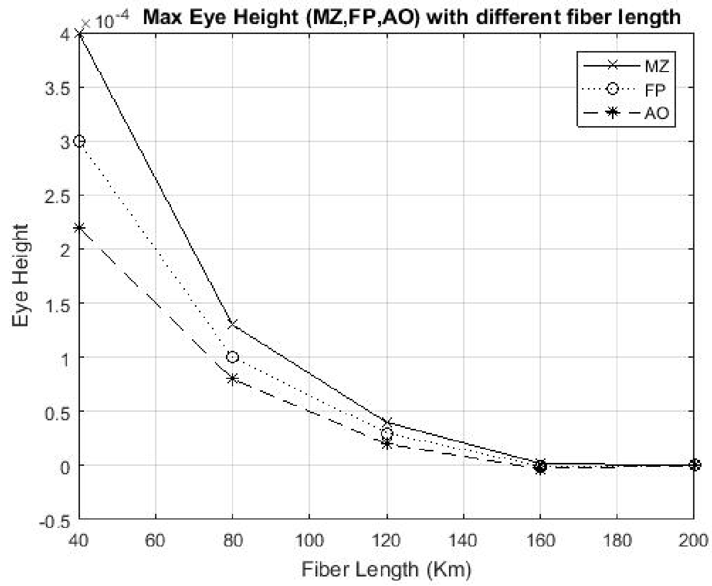

Figure 4.145: Max .Eye Height (MZ, FP, AO) with different fiber length

Table 4.13: Max. Threshold (MZ, FP, AO) with different fiber length

Length (Km)	MZ Filter	FP Filter	AO Filter
40	2e-004	5e-005	5e-005
80	7.3e-005	5e-005	3.4e-005
120	3e-005	2.9e-005	2.2e-005
160	1.2e-005	1e-005	9e-006
200	0	0	0

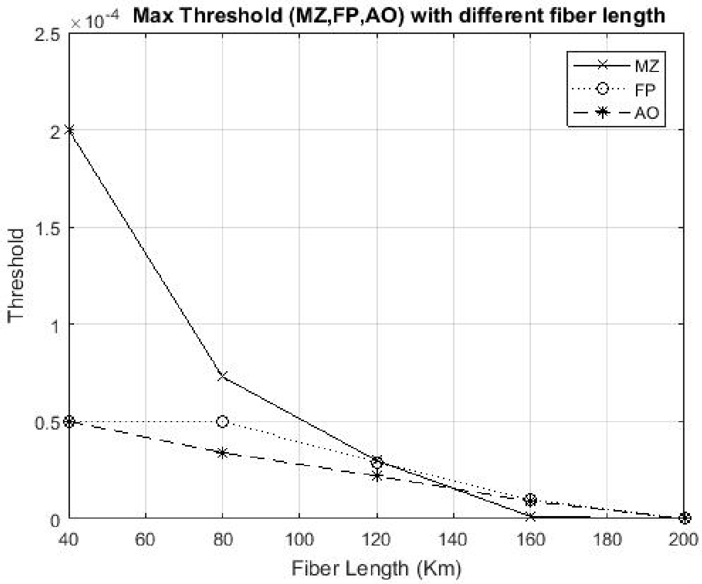

Figure 4.146: Max. Threshold (MZ, FP, AO) with different fiber length

According to all above results when a fiber length is changed, the Mach-Zehnder Filter gives best results than others filters. Also Fabry–Perot Filter gives better results than Acousto-Optic Filter in terms of Q-factor, BER, Eye height and Threshold.

4.2.4.2 Different Fiber Attenuation

The parameters used to test the cases of fiber attenuation are listed as follows.

- Fiber Length = 40 Km
- Fiber Attenuation = 0.1,0.2,0.3,0.4,0.5 dB/Km
- Input Power = 0 dBm

Table 4.14 and Figure 4.147 summarizes the results the maximum Q-factor given for different cases of fiber attenuation. Table 4.15 and Figure 4.148 summarizes the results the minimum BER given for different cases of fiber attenuation. Table 4.16 and Figure 4.149 lists the results for the maximum eye-height, and finally, Table 4.17 and Figure 4.150 lists the results for maximum threshold, which is shown that when a fiber attenuation changed from 0.1 to 0.5 dB/Km the Q-factor, Eye Height and Threshold when: (1)MZ filter used will be maximum, (2)FP used will be moderate and (3)AO used will be minimum. Also shown that the BER when: (1)MZ filter used will be minimum, (2)FP used will be moderate and (3)AO used will be maximum.

Table 4.14: Max .Q-Factor (MZ, FP, AO) with different fiber attenuation

Fiber Attenuation (dB/Km)	MZ Filter	FP Filter	AO Filter
0.1	39	12	9
0.2	19	9	7
0.3	8	5	4
0.4	3.1	2.6	2
0.5	0	0	0

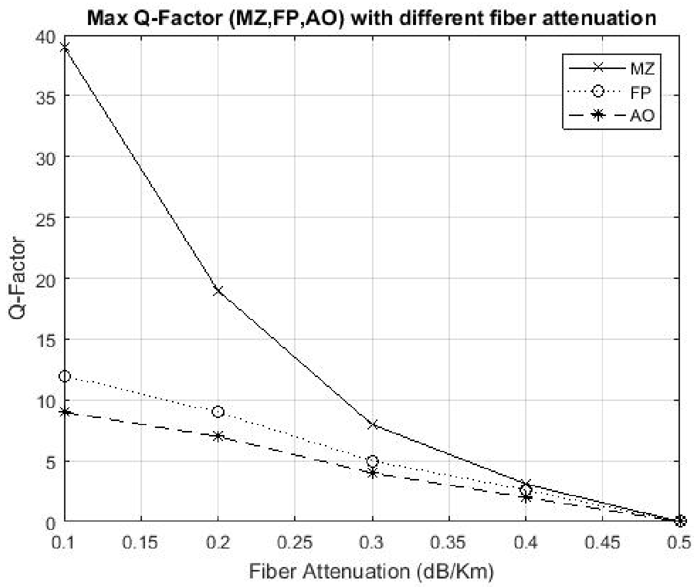

Figure 4.147: Max .Q-Factor (MZ, FP, AO) with different fiber attenuation

Table 4.15: Min. BER (MZ, FP, and AO) with different fiber attenuation

Fiber Attenuation (dB/Km)	MZ Filter	FP Filter	AO Filter
0.1	0	9e-032	3e-017
0.2	2e-080	2e-019	2e-012
0.3	2e-014	6e-008	3e-006
0.4	11e-004	41e-004	107e-004
0.5	1	1	1

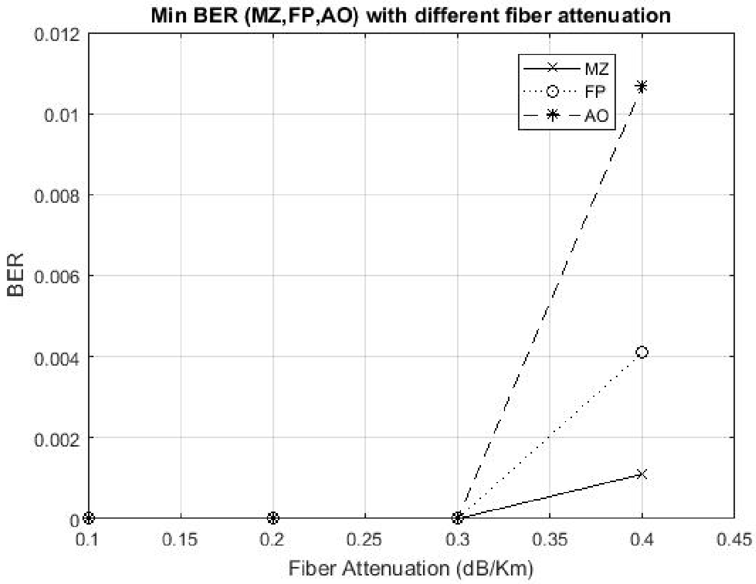

Figure 4.148: Min. BER (MZ, FP, and AO) with different fiber attenuation

Table 4.16: Max .Eye Height (MZ, FP, AO) with different fiber attenuation

Fiber Attenuation (dB/Km)	MZ Filter	FP Filter	AO Filter
0.1	4e-004	3e-004	22e-005
0.2	13e-005	9.6e-005	8e-005
0.3	4e-005	2.5e-005	1e-005
0.4	6e-007	-3e-006	-7e-006
0.5	0	0	0

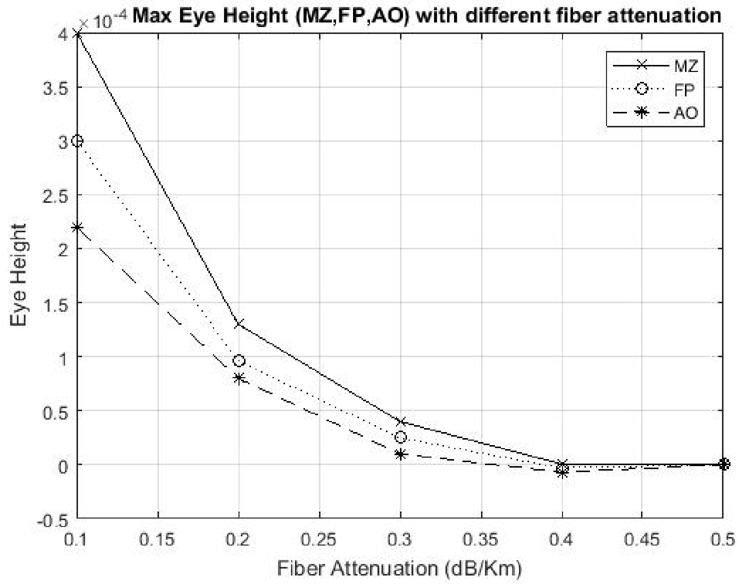

Figure 4.149: Max .Eye Height (MZ, FP, AO) with different fiber attenuation

Table 4.17: Max. Threshold (MZ, FP, AO) with different fiber attenuation

Fiber Attenuation (dB/Km)	MZ Filter	FP Filter	AO Filter
0.1	2e-004	5e-005	5e-005
0.2	8e-005	4e-005	3e-005
0.3	3e-005	2e-005	1e-005
0.4	1.2e-005	8e-006	9e-006
0.5	0	0	0

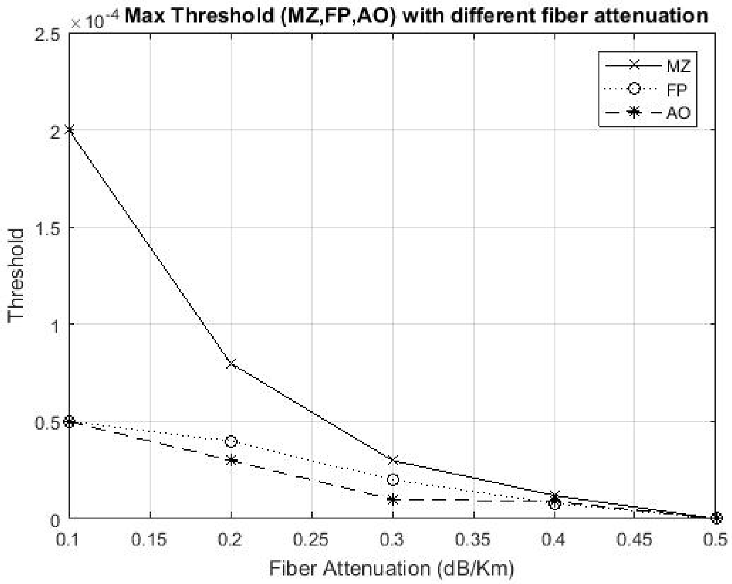

Figure 4.150: Max. Threshold (MZ, FP, AO) with different fiber attenuation

According to all above results when attenuation coefficient of a fiber is changed, Mach-Zehnder Filters gives best results than Fabry–Perot and Acousto-Optic Filters in terms of Q-factor, BER, Eye height and Threshold.

4.2.4.3 Different Input Power

The parameters used to test the cases of input power are listed as follows.

- Fiber Length = 40 Km
- Fiber Attenuation = 0.3 dB/Km
- Input Power = 0,2,5,7 and 9 dBm

Table 4.18 and Figure 4.151 summarizes the results the maximum Q-factor given for different cases of input power. Table 4.19 and Figure 4.152 summarizes the results minimum BER given for different cases of input power. Table 4.20 and Figure 4.153 lists the results for maximum eye-height, and finally, Table 4.21 and Figure 4.154 lists the results for maximum threshold, which is shown that when a fiber input power changed from 0 to 9 dBm the Q-factor, Eye Height and Threshold when: (1)MZ filter used will be maximum, (2)FP used will be moderate and (3)AO used will be minimum. Also shown that the BER when: (1)MZ filter used will be minimum, (2)FP used will be moderate and (3)AO used will be maximum.

Table 4.18: Max .Q-Factor (MZ, FP, AO) with different Input Power

Input Power (dBm)	MZ Filter	FP Filter	AO Filter
0	8	5	4
2	12	7	6
5	22	10	7
7	33	11	8
9	36	12	8.5

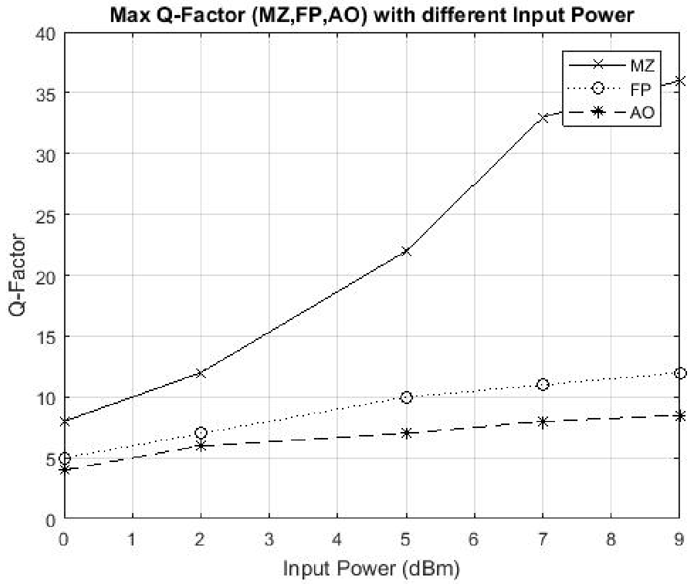

Figure 4.151: Max .Q-Factor (MZ, FP, AO) with different Input Power

Table 4.19: Min. BER (MZ, FP, and AO) with different Input Power

Input Power (dBm)	MZ Filter	FP Filter	AO Filter
0	2e-014	6e-008	3e-006
2	5e-035	6e-013	4e-009
5	2e-111	2e-022	5e-014
7	4e-241	5e-029	7e-017
9	2e-279	7e-032	1e-017

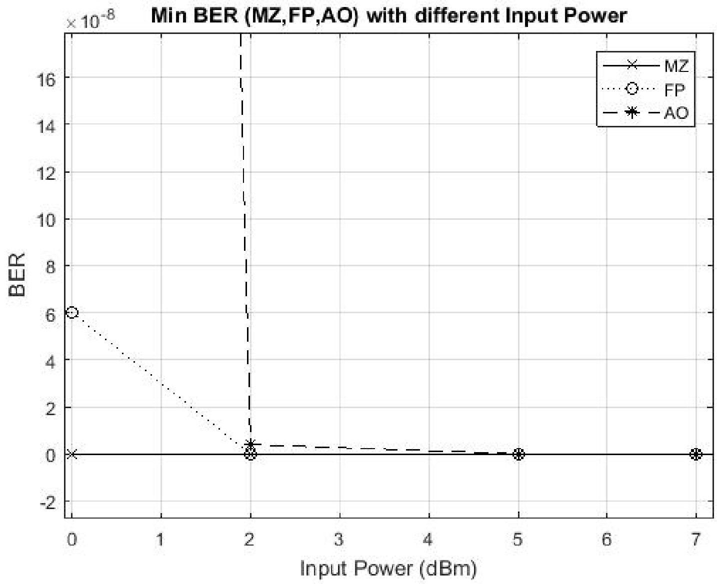

Figure 4.152: Min. BER (MZ, FP, and AO) with different Input Power

Table 4.20: Max .Eye Height (MZ, FP, AO) with different Input Power

Input Power (dBm)	MZ Filter	FP Filter	AO Filter
0	4e-005	2.5e-005	1.7e-005
2	8e-005	5e-005	4e-005
5	17e-005	13e-005	10e-005
7	29e-005	21e-005	17e-005
9	46e-005	34e-005	27e-005

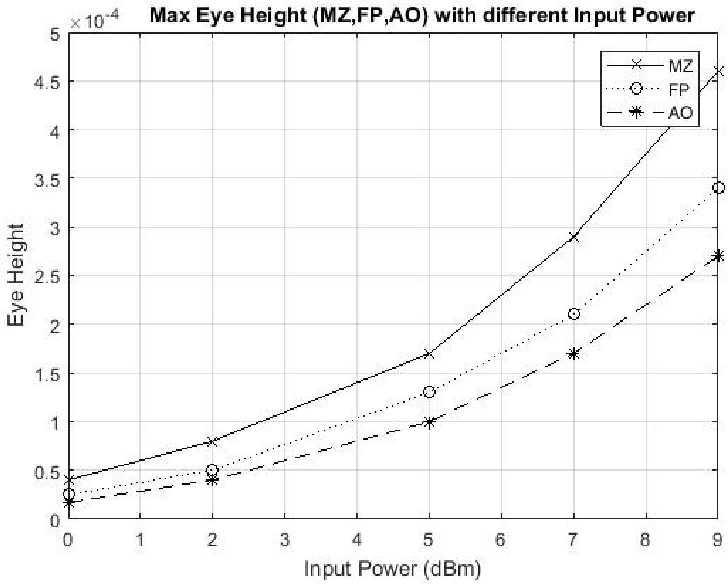

Figure 4.153: Max .Eye Height (MZ, FP, AO) with different Input Power

Table 4.21: Max. Threshold (MZ, FP, AO) with different Input Power

Input Power (dBm)	MZ Filter	FP Filter	AO Filter
0	3e-005	2e-005	1.8e-005
2	5e-005	3e-005	2.5e-005
5	9e-005	4e-005	3.6e-005
7	14e-005	5e-005	4.5e-005
9	15e-005	6e-005	6e-005

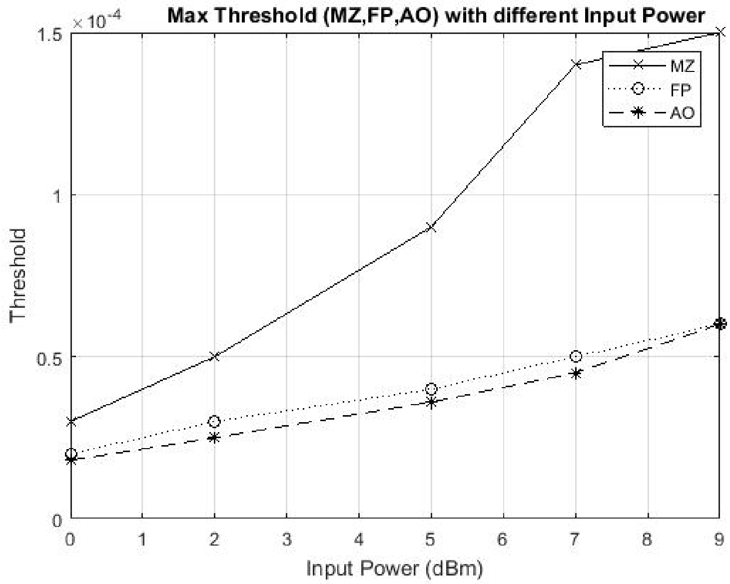

Figure 4.154: Max. Threshold (MZ, FP, AO) with different Input Power

According to all above results when an input power to the fiber is changed, also, Mach-Zehnder Filter gives best results than Fabry–Perot and Acousto-Optic Filters in terms of Q-factor, BER, Eye height and Threshold.

4.3 The pass band characteristics of tunable optical filters

Figure 4.155, Figure 4.156, and Figure 4.157, show the pass band characteristics of Fabry–Perot, Mach-Zehnder and Acousto-Optic Filters respectively.

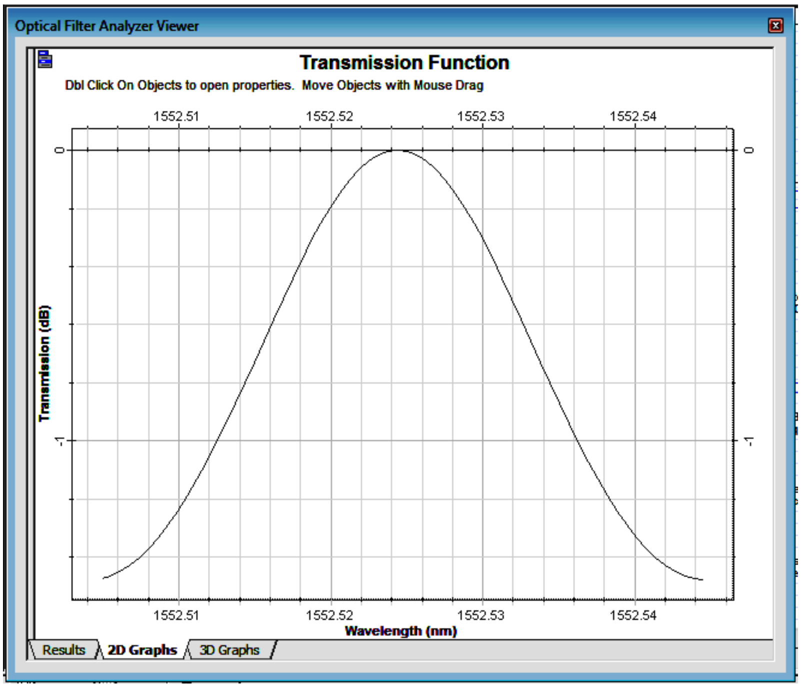

Figure 4.155: The pass band of FP filter

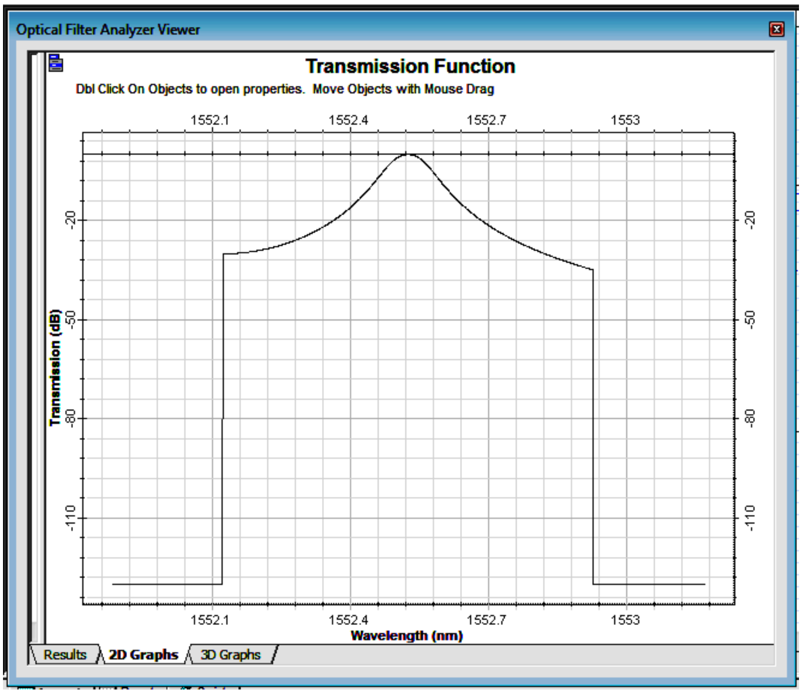

Figure 4.156: The pass band of MZ filter

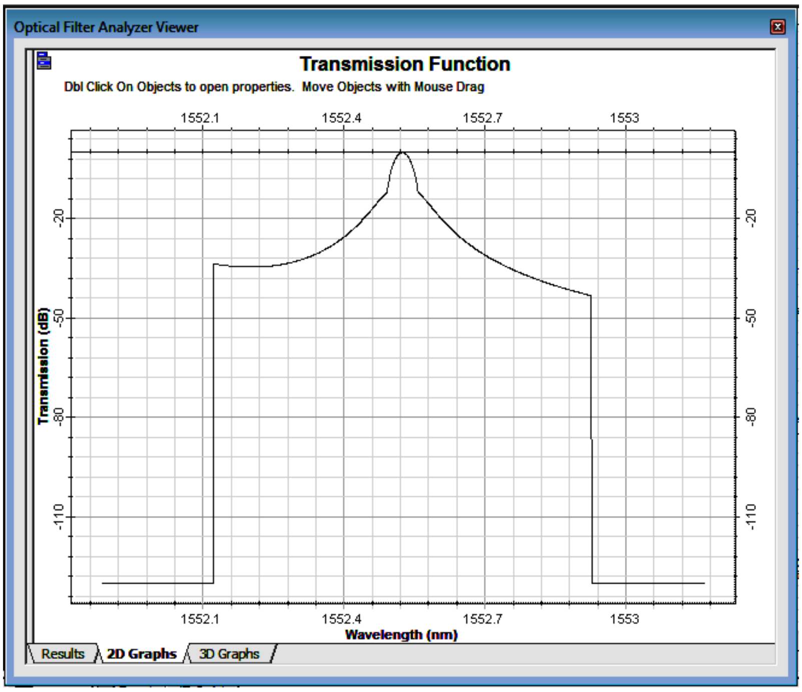

Figure 4.157: The pass band of AO filter

Chapter Five
Conclusions and Recommendations

5.1 Conclusions

This thesis concentrates on the different tunable filtering types for WDM based optical fiber networks, which is an important optical component in multi-channel systems. We analyzed the effects of fiber length, fiber attenuation coefficient and an input power from the laser source to the optical fiber on the performance of tunable optical filters in terms of Q-factor, BER, Eye-height and Threshold and we achieved a good results when we use both optical filters Fabry–Perot and Mach-Zehnder than Acousto-Optic Filter.
In chapter'2 we introduced the literature Reviewer on the different tunable optical filters types. The following two aspects are presented in this literature Reviewer: 1) the basic principle of tunable filters is introduced and classified into three Fabry–Perot (FP), Mach-Zehnder (MZ) and Acousto-Optic (AO) tunable filter. In FP, an interferometer can be electronically controlled its length by using a piezoelectric transducer, also the air gap can be used between two optical fibers to get a high-reflectivity mirrors. In MZ, an interferometer can be made by using two a 3-dB couplers for splitting and interfering process. In AO, a grating dynamically formed by use acoustic waves and it has tuning range wider as possible to match an applications in optical FDM. 2) Reviewed an improvements in a mathematical model of FP interferometer in s-domain and improve a novel absolute strain measurement system by using the same interferometer with high properties. Also there are an improvements in a MZ interferometer (MZI) by using Athermal, flat-topped, compact low-loss thermo-optic single (MZIs) and two cascaded MZIs with high performance transmission. Also there are an improvements in AO filter to operate in 2-4 m region by using carefully optimized resonant designs.
In chapter'3 we concentrated the analyze system model of this thesis and we have considered the system design of filtering for Wavelength Division Multiplexing (WDM) based optical fiber networks, then we discussed the effect

of limiting factors (fiber length, attenuation coefficient and input power) in terms of quality (Q) factor, bit-error rate (BER), eye height and threshold when we use a Fabry–Perot, Mach-Zehnder and Acousto-Optic tunable filters. In chapter'4 we discussed the performance analysis of filtering for WDM based optical fiber networks was evaluated by OptiSystem simulation. We discussed the result of performance analysis for WDM based optical fiber networks in different filtering types and limiting factors then compared with each other and we observe that when a fiber length, attenuation coefficient and an input power to the fiber was changed the Q-factor, Eye Height and Threshold will be: a)maximum when a MZ filter used, b)moderate when a FP used and c)minimum when an AO used. Also shown that the BER will be: a)minimum when a MZ filter used, b)moderate when a FP used and c)maximum when an AO used. According to this observations a Mach-Zehnder Filter give a high performance and best results than Fabry–Perot which is moderate and an Acousto-Optic which is a lowest one.

5.2 Recommendations

There are many types of optical tunable filters can be used to compensate the attenuations and it required to evaluate their performance. In this thesis Fabry–Perot, Mach-Zehnder and Acousto-Optic Filters is evaluated, therefore it's recommended to consider other types such as Michelson optical filter and Grating-based optical filter in the future research.

Bibliography

[1] C. A. Brackett, "Dense wavelength division multiplexing networks: Principles and applications," *IEEE Journal on Selected Areas in Communications*, vol. 8, no. 6, pp. 948–964, 1990.

[2] N. Olsson, J. Hegarty, R. Logan, L. Johnson, K. Walker, L. Cohen, B. Kasper, and J. Campbell, "68.3 km transmission with 1.37 tbit km/s capacity using wavelength division multiplexing of ten single-frequency lasers at 1.5 μm," *Electronics Letters*, vol. 21, no. 3, pp. 105–106, 1985.

[3] P. J. Winzer, D. T. Neilson, and A. R. Chraplyvy, "Fiber-optic transmission and networking: the previous 20 and the next 20 years," *Optics express*, vol. 26, no. 18, pp. 24 190–24 239, 2018.

[4] T. G. Ulmer, M. C. Gross, K. M. Patel, J. T. Simmons, P. W. Juodawlkis, B. Wasbburn, W. S. Astar, A. J. SpringThorpe, R. P. Kenan, C. M. Verber *et al.*, "160-gb/s optically time-division multiplexed link with all-optical demultiplexing," *Journal of lightwave technology*, vol. 18, no. 12, pp. 1964–1977, 2000.

[5] M. Saruwatari, "All-optical signal processing for terabit/second optical transmission," *IEEE Journal of Selected Topics in Quantum Electronics*, vol. 6, no. 6, pp. 1363–1374, 2000.

[6] R. Gross and R. Olshansky, "Multichannel coherent fsk experiments using subcarrier multiplexing techniques," *Journal of lightwave technology*, vol. 8, no. 3, pp. 406–415, 1990.

[7] R. L. Peterson, R. E. Ziemer, and D. E. Borth, *Introduction to spread-spectrum communications.* Prentice hall New Jersey, 1995, vol. 995.

[8] G. P. Agrawal, *Fiber-optic communication systems.* John Wiley & Sons, 2012, vol. 222.

[9] J. Stone and L. Stulz, “Pigtailed high-finesse tunable fibre fabry-perot interferometers with large, medium and small free spectral ranges,” *Electronics letters*, vol. 23, no. 15, pp. 781–783, 1987.

[10] M. Iodice, G. Cocorullo, F. Della Corte, and I. Rendina, “Silicon fabry–perot filter for wdm systems channels monitoring,” *Optics Communications*, vol. 183, no. 5-6, pp. 415–418, 2000.

[11] J. Pfeiffer, J. Peerlings, R. Riemenschneider, R. Genovese, M. Aziz, E. Goutain, H. Künzel, W. Görtz, G. Böhm, M. Amann *et al.*, “Inalgaas bulk micromachined tunable fabry–pérot filter for dense wdm systems,” *Materials science in semiconductor processing*, vol. 3, no. 5-6, pp. 409–412, 2000.

[12] Y. Hibino, F. Hanawa, H. Nakagome, M. Ishii, and N. Takato, “High reliability optical splitters composed of silica-based planar lightwave circuits,” *Journal of lightwave technology*, vol. 13, no. 8, pp. 1728–1735, 1995.

[13] G. P. Agrawal and S. Radic, “Phase-shifted fiber bragg gratings and their application for wavelength demultiplexing,” *IEEE photonics technology letters*, vol. 6, no. 8, pp. 995–997, 1994.

[14] F. Bilodeau, K. Hill, B. Malo, D. Johnson, and J. Albert, “High-return-loss narrowband all-fiber bandpass bragg transmission filter,” *IEEE Photonics Technology Letters*, vol. 6, no. 1, pp. 80–82, 1994.

[15] D. A. Smith, R. S. Chakravarthy, Z. Bao, J. E. Baran, J. L. Jackel, A. d’Alessandro, D. J. Fritz, S. Huang, X. Zou, S.-M. Hwang *et al.*, “Evolution of the acousto-optic wavelength routing switch,” *Journal of lightwave technology*, vol. 14, no. 6, pp. 1005–1019, 1996.

[16] S. Ranjan and S. Mandal, “Mathematical modelling of extrinsic fabry-perot interferometer cavity,” in *Microwave and Photonics (ICMAP), 2018 3rd International Conference on.* IEEE, 2018, pp. 1–2.

[17] Y. Zhu, Q. Zhang, G. Liu, X. Luo, and M. Han, “Fabry–perot sensor using cascaded chirped fiber bragg gratings with opposite chirp directions,” *IEEE Photonics Technology Letters*, vol. 30, no. 16, pp. 1431–1434, 2018.

[18] X. Wang, Z. Li, J. Lin, W. Wang, Y. Tian, and Y. Pang, "The characteristics in the sensitivity of microfiber fabry-perot interferometric transducers," in *IOP Conference Series: Earth and Environmental Science*, vol. 111, no. 1. IOP Publishing, 2018, p. 012013.

[19] D. Kacik, I. Martincek, and N. Tarjanyi, "Enhanced sensitivity of polydimethylsiloxane fabry-perot interferometer temperature sensor," in *2018 ELEKTRO*. IEEE, 2018, pp. 1–4.

[20] J. Yang, F. Xu, S. Yao, and S. Liu, "A high directivity fabry-perot antenna based on metamaterial substrate," in *2018 IEEE MTT-S International Wireless Symposium (IWS)*. IEEE, 2018, pp. 1–3.

[21] Q. Deng, L. Liu, R. Zhang, X. Li, J. Michel, and Z. Zhou, "Athermal and flat-topped silicon mach-zehnder filters," *Optics express*, vol. 24, no. 26, pp. 29 577–29 582, 2016.

[22] A. Ovvyan, N. Gruhler, S. Ferrari, and W. Pernice, "Cascaded mach–zehnder interferometer tunable filters," *Journal of Optics*, vol. 18, no. 6, p. 064011, 2016.

[23] J. Ward, S. Valle, C. Pannell, and N. Johnson, "Acousto-optic tunable filters (aotfs) optimised for operation in the 2-4μm region," in *Journal of Physics: Conference Series*, vol. 619, no. 1. IOP Publishing, 2015, p. 012054.

[24] P. Wang and Z. Zhang, "Double-filtering method based on two acousto-optic tunable filters for hyperspectral imaging application," *Optics express*, vol. 24, no. 9, pp. 9888–9895, 2016.

[25] G. Ramírez-Meléndez, M. Bello-Jiménez, O. Pottiez, and M. Andrés, "Improved all-fiber acousto-optic tunable bandpass filter," *IEEE Photonics Technology Letters*, vol. 29, no. 12, pp. 1015–1018, 2017.

[26] J. M. Senior and M. Y. Jamro, *Optical fiber communications: principles and practice*. Pearson Education, 2009.